Sedimentological Lithofacies, Internal Architecture and Evolution of Deep Marine Fans of the Tithonian Angel Formation, Northwestern Dampier Sub-basin, North West Shelf, Australia

Kerrie Elise Deller B.Sc (Hons)

Australian School of Petroleum
The University of Adelaide

This thesis is submitted in fulfilment of the requirements for the degree of Doctor of Philosophy in the Faculty of Science, The University of Adelaide

1 General Introduction

1.1 Project

This research project examines the sedimentological processes, internal architecture and depositional evolution of the deep marine Tithonian component of the Angel Formation located within the Dampier Sub-basin on the North West Shelf of Australia. It was accomplished using lithofacies classifications and the establishment of an architectural element scheme of differing scales in combination with wireline logs, biostratigraphic sections, seismic reflection/acoustic impedance data and applicable outcrop, modern and subsurface analogues.

1.2 Rationale

Approximately 74 billion barrels of oil equivalent total resources had been discovered in deep water from 18 basins on six continents by the end of 2002. Many of these discoveries have been made in frontier regions that include the Gulf of Mexico, Brazil and West Africa (Weimer and Slatt, 2004). Where deepwater exploration in largely untested frontier basins plays a significant role in future success, continued exploration and improvement in field development within proven basins is just as important, especially within mature Mesozoic basins located along the western margin of Australia.

The Dampier Sub-basin located on the North West Shelf (Figures 1-1 and 1-2) represents one of Australia's most mature basins where exploration has been steadily continuous since the 1970's. It contains 149 hydrocarbon fields with combined reserves of 34tcf of gas, 1037mmbbls of condensate and 633mmbbls of oil within fluvio-deltaic and deep marine reservoirs (Longley *et al.,* 2002). It is home to the Angel, Legendre, Cossack, Wanaea, Lambert, Hermes, Exeter and Mutineer fields (Figures 1-3 and 1-4), which exist within the deep marine Angel Formation (Figures 3-4 and 3-5).

Increasing exploration maturity within the basin is leading to a greater emphasis on optimizing development and production of pre-existing fields and on stratigraphic traps as exploratory targets (Allen *et al.,* 2006). Hydrocarbon recovery factors from fields can vary due to differing reservoir architecture. A sound understanding of lithofacies relationships along with reservoir geometry and quality is crucial for exploring and exploiting these deposits efficiently.

Exploring and exploiting fields within the Dampier Sub-basin proves difficult as the architectural elements which control the behaviour of a field are below the resolution of conventional seismic data. The quality of seismic data for the region is poor, a complexity that is caused primarily by the inverted half graben nature of the basin, especially along its western margin with the Rankin Platform. When seismic data fails to resolve the internal architecture and stratigraphic relationships of a particular sedimentary sequence, other available and higher resolution datasets such as core, wireline and palynology can be used effectively as an alternative.

Subsurface development and outcrop mapping from regions such as the Tanqua Karoo in South Africa (Ven Der Werff and Johnson, 2003; Wild *et al.,* 2005), the Ross Formation in Ireland (Elliot, 2000) and the Brushy Canyon Formation, West Texas (Gardner and Borer, 2000) have shown that standard sheet sandstone systems similar to the Angel Formation exhibit more complicated internal architecture than previously understood. This research aims to examine the differing levels of internal architecture within the Tithonian succession of the Angel Formation at a sub-seismic level. The results obtained from this research will assist future exploration and development both within the Dampier Sub-basin and within other basins containing similar structural and depositional styles.

1.3 Objectives

This project has seven objectives. They are:

- devise appropriate core lithofacies scheme based on eleven wells and interpret depositional processes that are responsible for them;
- devise applicable lithofacies associations;
- examine differing scales of architectural elements and their stratigraphic relationships;
- devise applicable lateral and downslope models addressing autocyclic and allocyclic patterns;
- analyse architecture and fan evolution in five field regions that reside within proximal, medial and distal settings;
- investigate non-stratigraphic variables that can affect reservoir architecture such as post-depositional deformation, and;
- discuss implications and their relationship to future exploration and development.

1.4 Regional Setting

The Dampier Sub-basin is encompassed by the greater Carnarvon basin located on the North West Shelf of Australia (Figure 1-1).

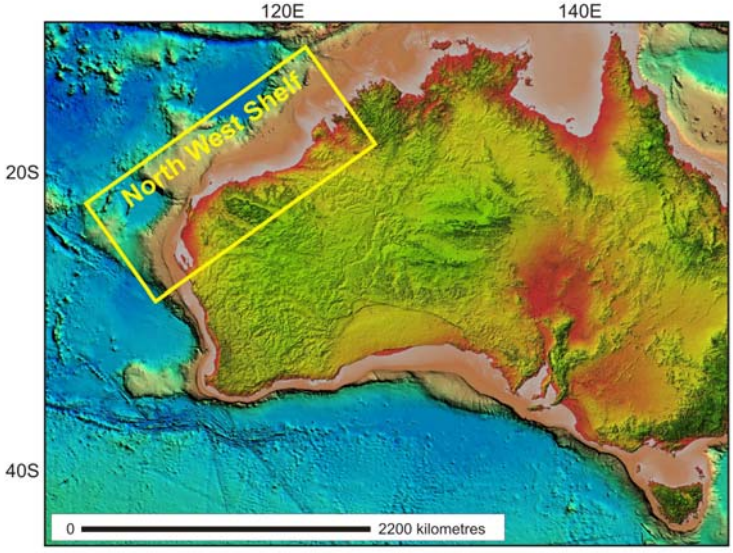

Figure 1-1: Map of the Australian continent highlighting the North West Shelf of Australia (Bathymetry from Geoscience Australia, 2003).

The Dampier Sub-basin is an east-northeast trending basin located west of the Lambert Shelf and east of the Rankin Trend (Newman, 1994) (Figure 1-2). The Beagle Sub-basin, located to the north of the Dampier Sub-basin, is a north-northeast trending basin located in a structurally complex junction between the offshore Canning Basin, a Palaeozoic basement hinge at the Lambert shelf and the northern Dampier Sub-basin (Blevin *et al.,* 1994).

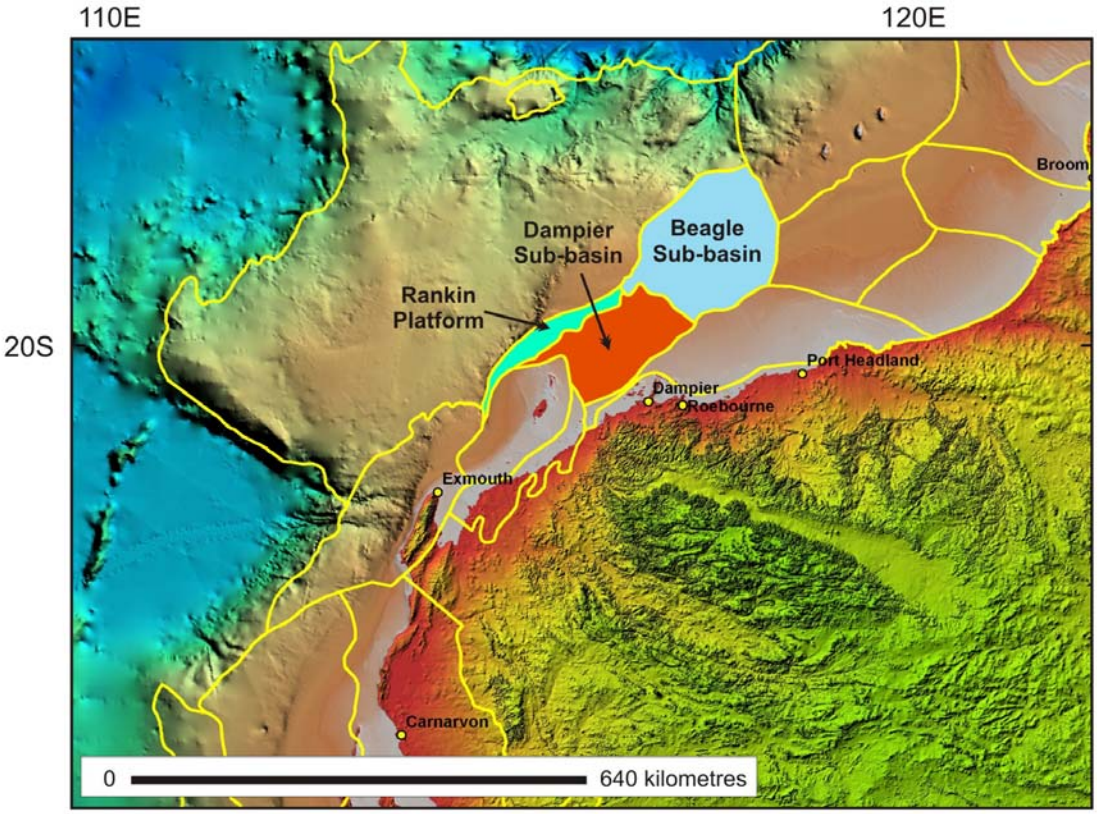

Figure 1-2: Location of the Rankin Platform, Beagle and Dampier Sub-basins within the greater Carnarvon Basin (Bathymetry from Geoscience Australia, 2003).

The project region encompasses the north-western margin of the Dampier Sub-basin with part of the southern Beagle Sub-basin. It is bordered to the southwest by the southern Dampier Sub-basin, to the west by the Rankin Trend, to the north by the central Beagle Sub-basin and to the east and southeast by the Lewis Trough and Enderby Terrace. This region covers an area of 19,000km^2 (Figure 1-3).

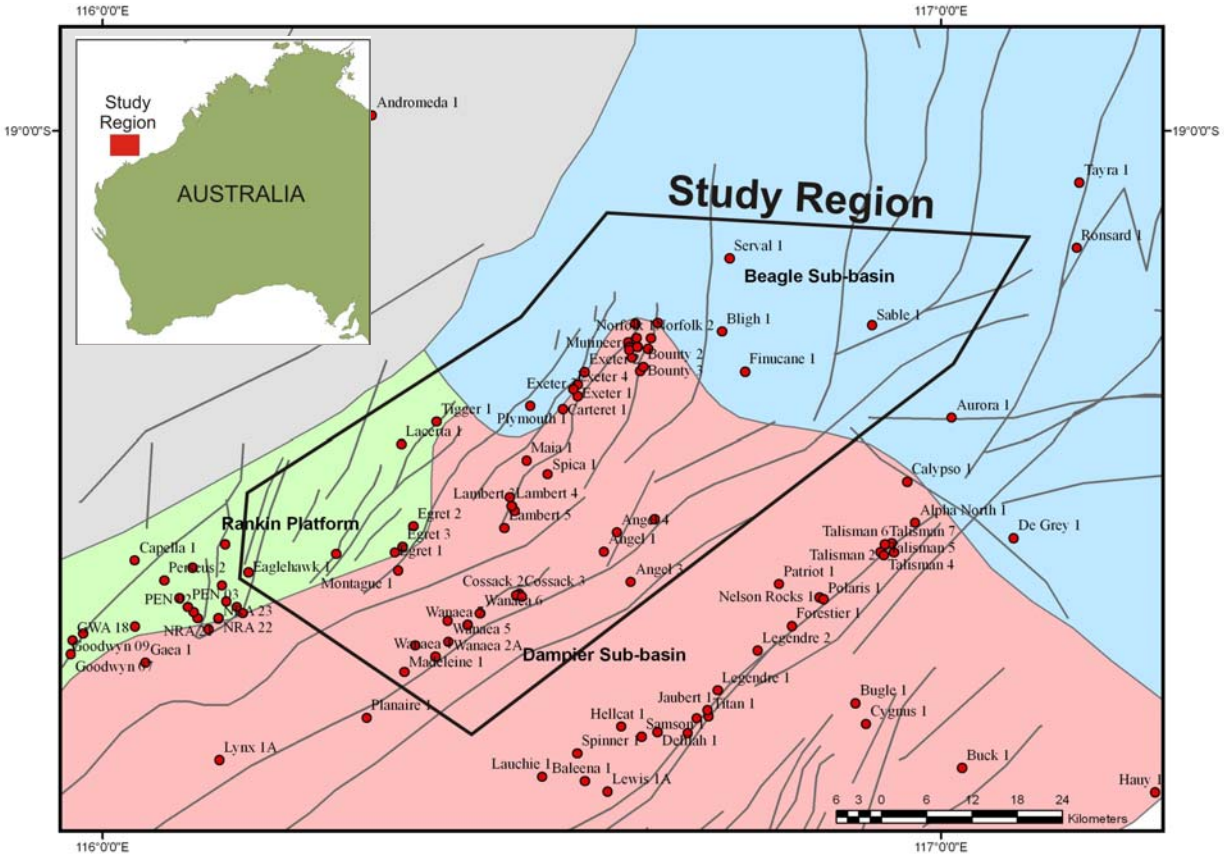

Figure 1-3: Region of study that encompasses the Dampier Sub-basin, Beagle Sub-basin and the Rankin Platform.

1.5 Previous Basin Research

The Dampier Sub-basin has been extensively researched over the past 30 years. Previous research has covered the following.

i. Basin structure and tectonics. Tectonics of the Dampier Sub-basin and the North West Shelf in general was initially researched by Veenstra (1985) and Veevers (1988). Others have included Ballie *et al.,* (1994), Hill (1994), Westphal and Aigner (1997), Gartrell (2000), and Jablonski and Saitta (2004). Newman (1994) and Stein (1994) investigated the structural styles of the Rankin Trend system. Blevin *et al.,* (1994) examined the Mesozoic structural development of the Beagle Sub-basin. Cathro and Karner (2006) recently researched the early Cretaceous to Tertiary inversion history across the Dampier Sub-basin.

ii. Stratigraphy and sedimentology. The stratigraphy and sedimentology of the Dampier Sub-basin has been researched by Barber (1994a and 1994b), Wulff and Barber (1994), Miller (1996), Miller and Smith (1996), Jablonski (1997) and Westphal and Aigner (1997). Heavy mineral distributions were researched by Dibona and Scott (1990) in an attempt to utilise them for stratigraphic analysis. In comparison, little research has been conducted on the sedimentology and stratigraphy of the Mesozoic successions of the Beagle Sub-basin. Blevin

et al., (1994) and Stephenson *et al.,* (1998) investigated the Mesozoic palaeogeography of this sub-basin.

iii. Field scale exploration and development. Individual field studies within the Dampier Sub-basin have been completed on the Wanaea and Cossack fields by Di Toro (1994 and 1995) and Bint (1991), the Lambert field by Kingsley *et al.,* (1998) and the Mutineer and Exeter fields by Auld and Redfern (2003).

Larger scale basin studies incorporating the entire Carnarvon Basin and North West Shelf have been completed by Hocking (1988, 1992) and Longley *et al.,* (2002).

1.6 Regional Exploration History

The initial discovery of hydrocarbons on the North West Shelf of Australia occurred in 1953 with the drilling of Rough Range-1 situated in the northern Carnarvon basin near the town of Exmouth (Johnstone, 1979; Malcolm *et al.,* 1991) (Figure 1-2).

Hydrocarbons were first encountered in the Dampier Sub-basin in 1968 with Legendre-1 (Barber, 1994a) (Table 1-1 and Figure 1-4). Although it was considered to be a relatively small field with only 6.7 metres of net pay (Vincent and Tilbury, 1988), this initial success led to a major boost in exploration activity during the 1970's, leading to the discovery of numerous gas fields including those along the Rankin Platform (Barber, 1994a). An increase in drilling activity in the 1980's led to the discovery of the Talisman, Wanaea and Cossack fields (Ellis, 1988; Bint, 1991) (Table 1-1). Later exploration efforts have focused upon drilling deeper syn-rift objectives below the Muderong Shale regional seal within the Lewis Trough (Lauchie-1 and Baleena-1). Lauchie-1 intersected stacked sandstone packages ranging from Oxfordian to Valanginian in age (Barber, 1994a).

The Mutineer and Exeter fields were discovered in the late 1990's and early 2000's (Table 1-1). They rest within the junction which divides the Dampier from the Beagle Sub-basin (Figure 1-4). Pitcairn-1 produced a hydrocarbon show whilst Mutineer-1B intersected an oil column of 8.2 metres of net pay. This led to the exploration and discovery of an 18 metre net oil column in Exeter-1, located 9km southwest of the Mutineer complex (Auld and Redfern, 2003). The Mutineer and Exeter fields commenced production on the 29th of March 2005 (Santos, 2005).

Exploration in the Beagle Sub-basin yielded poor results in comparison to the Dampier Sub-basin due to the lack of Jurassic syn-rift source rock. Initial exploration was undertaken in 1965 with 13 wells drilled between 1971 and 1983. The initial range of wells tested a variety of plays including uplifted Jurassic and Triassic blocks, Triassic and Jurassic anticlines and fault-controlled structures down dip of the main basin border fault (Blevin *et al.,* 1994). Most other wells were unsuccessful. Nebo-1 drilled in 1993 became the Beagle Sub-basin's first and only hydrocarbon discovery (Figure 1-4). Unfortunately, it was declared uneconomical (Blevin *et al.,* 1994).

The petroleum system chart for the Dampier Sub-basin is highlighted in Figure 1-5.

Table 1-1: A summary of key hydrocarbon fields located within the Dampier Sub-basin. D represents a developed field, UD represents an undeveloped field.

Field	Discovered		Trapping Mechanism	Reservoir	Stage	Predominate Hydrocarbon
	Well	Date				
Legendre	Legendre-1	1968	Faulted anticline	Tithonian Angel sandstone	D	Oil
Angel	Angel-1	1972	Faulted anticline	Tithonian Angel sandstone	D	Gas and Condensate
Eaglehawk	Eaglehawk-1	1972	Faulted Triassic high	Triassic Mungaroo	UD	Oil
North Rankin	North Rankin-1	1972	Tilted fault blocks overlain with angular unconformity and seal	Triassic Mungaroo	D	Gas and Condensate
Egret	Egret-1	1973	Faulted anticline along edge of Triassic/Early Jurassic tilted fault block	Tithonian Angel sandstone	UD	Oil
Lambert and Hermes	Lambert-1	1974	SW-NE elongated faulted anticline	Tithonian Angel sandstone	D	Oil and Gas
Talisman	Talisman-1	1984	Faulted anticline	Berriasian Angel Sandstone	UD	Oil
Wanaea	Wanaea-1	1989	Faulted anticline along the Madeline Trend	Tithonian Angel sandstone	D	Oil, Gas and Condensate
Cossack	Cossack-1	1990	Faulted anticline	Tithonian Angel sandstone	D	Oil and Gas
Mutineer	Mutineer-1B	1998	N-S trending anticline	Tithonian Angel sandstone	D	Oil
Exeter	Exeter-1	2002	Faulted anticline	Tithonian Angel sandstone	D	Oil

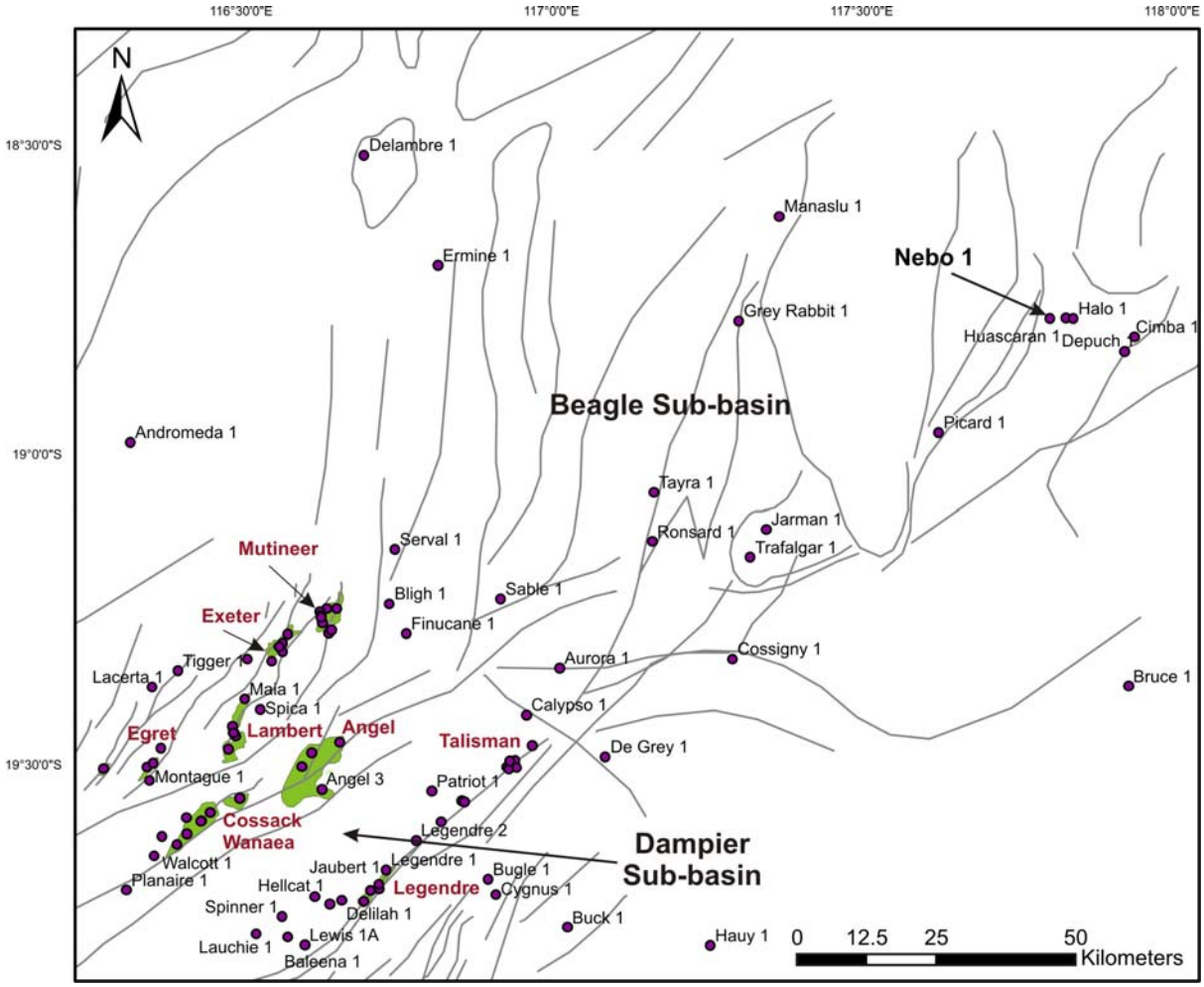

Figure 1-4: Location of major fields and wells across the Dampier and Beagle Sub-basins. The Mutineer and Exeter fields rest on the border between the two sub-basins.

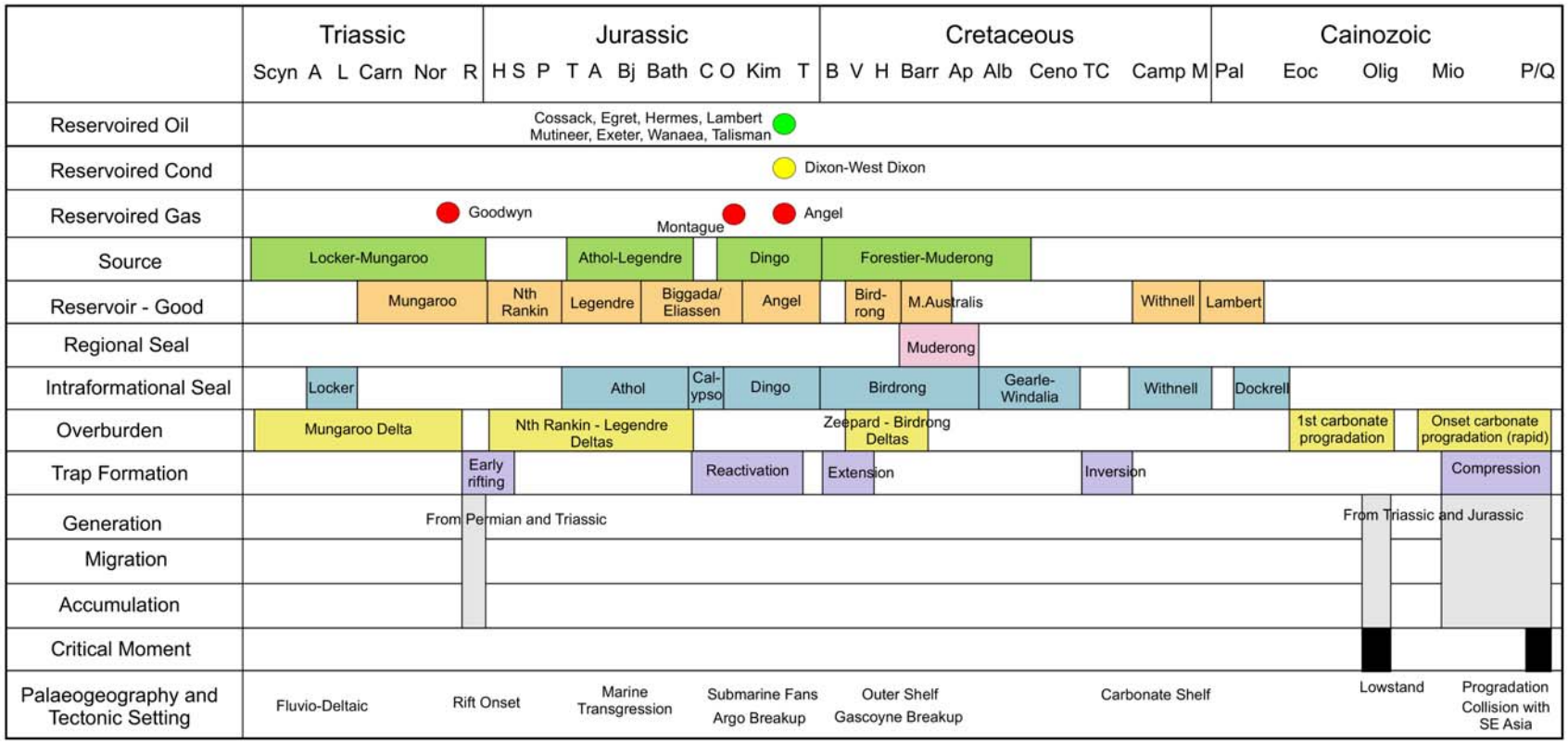

Figure 1-5: Petroleum system chart representing the stratigraphic, structural and petroleum history of the Dampier Sub-basin (adapted from Geoscience Australia, 2008).

2 Deep Marine Processes, Depositional Models and Project Terminology

2.1 Deep Marine Depositional Systems

Deep marine depositional environments occur seaward of the continental break on the continental slope, rise and basin (Figure 2-1) (Cameron *et al.,* 2000). A slope environment extends from the shelf break to the base-of-slope which then grades into an adjoining basin floor region. Slopes typically display gradients of 2° to 5° but can range from between 1° for a mud-rich slope and 10° for a limestone shelf and escarpment environment (Schlager and Camber, 1986).

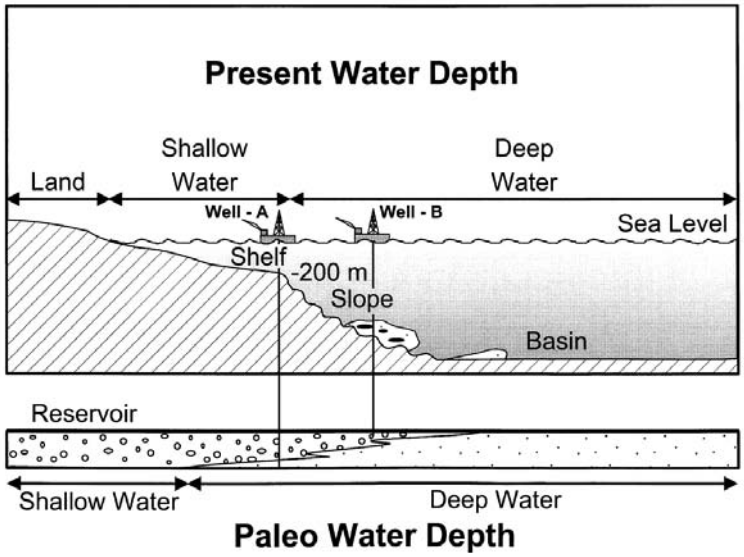

Figure 2-1: A bathyal deep marine environment occurs seaward of the continental shelf break. Gravity flows exist on the slope and basin floor setting (Shanmugam, 2000).

2.2 Deep Marine Processes and Classifications

Resedimentation processes allow large volumes of sediment to be transported into deepwater environments from shallow water settings (Stow *et al.,* 1996). Bottom currents and sediment-gravity processes such as slides, slumps, debris flows and turbidity currents are the dominant deepwater transportation mechanisms (Shanmugam, 2000).

Understanding the depositional processes of sediment gravity flows is a critical prerequisite for explaining and predicting dispersal patterns and sediment architecture in a deep marine basin. The classic Bouma sequence (Bouma, 1962), interpreted to represent a waning turbidity current deposit, is the most widely well-known concept for the deposition of sediments in the deep marine realm. It has been established through research that deep marine sandstones and their related sedimentological structures can be deposited through a variety of different processes (Lowe, 1982; Shanmugam and Moiola, 1995; Kneller and Branney, 1995; Mulder and Alexander, 2001; Talling *et al.,* 2004) and not just from waning turbidity flow events as suggested by Bouma (1962).

A largely discussed aspect of deep marine sandstone deposition is the existence of sandstone with little grading and internal structure. Researchers have recognised these sandstone successions in cores and outcrops (Stow and Johansson, 2000) with many attempting to put forward process and stratigraphic models to explain their existence (Shanmugam *et al.,* 1995, Pratson *et al.,* 2000). Some models suggest that structureless sandstones are deposited through en-masse freezing typical of a cohesive debris flow (Shanmugam, 1996, Mulder and Alexander, 2001). Others suggest they are deposited through the aggradational deposition of high density turbidity currents (Kneller and Branney, 1995), or through surging (Lowe, 1982).

Depositional processes that deposit sandstones with little internal structure and grading are difficult to interpret. It is important when dealing with these types of deposits that the distinction is made between those formed by turbulent processes and those formed by debritic processes (Mulder and Alexander, 2001). The classic hypothesis for dominantly unstructured and ungraded sandstones is the high-density turbidity current model of Lowe (1982). It has been argued by some that the model it is not strongly supported by field and experimental observations (Baas, 2004). Shanmugam (1996) challenged the high-density turbidity current model with another hypothesis termed the “sandy debris flow”. Mulder and Alexander (2001) introduced hyperconcentrated and density concentrated flows in an attempt to clarify the sedimentological problem.

The processes which govern deposition of unstructured and ungraded sandstones continue to remain unclear. It is uncertain whether any of the above concepts hold entirely true and what the implications would be for a typical geologist studying a sandstone body deposited by one type or another (Baas, 2004). It has been stated by many researchers that poor sorting, lack of internal stratification and inverse grading are not criteria for recognizing en-masse freezing of a sand-rich debris flow body (Hiscott *et al.,* 1997; Baas, 2004).

Literature research for this study has identified and classified the different classes of gravity flows into several categories (Table 2-1). These are:

- strongly cohesive debris flows;
- weakly cohesive debris flows;
- stratified flows;
- low density turbidity flows, and;
- non-cohesive debris flows.

Table 2-1: Varieties of gravity flows from literature.

Category	Sub-category	Description of flow processes and resultant deposit
Strongly Cohesive Debris Flows	Debris Flows (Mulder and Alexander, 2001)	Strongly cohesive debris flows are moving masses of rock clasts, clays and water containing high concentrations of cohesive material (Stow *et al.,* 1996). They display non-Newtonian Bingham plastic rheology. They flow only when the yield strength is exceeded (Pickering *et al.,* 1989). Once shear stresses can no longer overcome the internal shear strength, the flow freezes, preserving its poorly sorted texture (Stow *et al.,* 1996; Shanmugam, 2000). The dominant sediment support mechanism with strongly cohesive debris flows is matrix strength from interstitial fluids and fine sediments that have finite strength (Middleton and Hampton, 1976; Nardin *et al.,* 1979; Lowe, 1982; Gani, 2004). Cohesive materials hold the primary flow mass together as it travels downslope in a laminar fashion and undergoes continuous deformation (Iverson, 1999). No related turbulence. Flows can be capable of hydroplaning and in some cases, the head of the flow can detach from the rest of the flow body (Mohrig *et al.,* 1998; Ilstad *et al.,* 2004).
	Cohesive Debris Flows (Gani, 2004)	
Weakly Cohesive Debris Flows	Hyperconcentrated flows (Mulder and Alexander, 2001)	A sand-rich low cohesive variation of cohesive debris flows as listed above. A hyperconcentrated flow remains non-Newtonian with a cohesive material percentage as little as 2% by volume if sand is fine and 19% by volume if sand is coarse (Hampton, 1975). The sediment is deposited through frictional freezing. Very little to any grading, visible vertical clast fabrics and dewatering features such as dish and pillar structures can be preserved. Suspension fallout is inconsequential. These deposits are expected to be preserved within very proximal settings. With few cohesive grains within the matrix, transformation to high density turbidity flows is considered rapid and easy (Kneller and Buckee, 2000). Transformation could be triggered by the flow travelling over undulating sea floor topography (Fisher, 1983).
	Non-cohesive debris flows (Gani, 2004)	Similar classification to the above hyperconcentrated flow deposit of Mulder and Alexander (2001) where deposition occurs through freezing of the sediment flow preserving no vertical grading and vertical clast fabrics. The sub-category of non-cohesive debris flow as labelled by Gani (2004) is confusing given that it is suggested that the non-cohesive flows require as little as 2 - 4% cohesive material to remain as a plastic laminar flow.

High Density Turbidity Flows (Continued next page)	High density turbidity current (Postma *et al.,* 1988)	Postma *et al.,* (1988) first suggested the bipartite flow model for rapidly transforming weakly cohesive sand-rich debris flows. The term "high density turbidity current" for this model has been argued in recent times due to the plastic laminar nature of the basal debritic-like base of the flow event.
	Sandy debris flows and related turbulent cloud (Shanmugam, 1996)	Classification based on research from North Sea (Shanmugam *et al.,* 1995). Reclassifies the basal component of the concentrated density flow/dense flow/high density turbidity current of Postma *et al.,* (1988) as being a sandy debris flow. Sandy debris flows display plastic rheology and laminar flow conditions. Sediment support mechanisms include matrix strength and dispersive pressure. A moderate to high sediment concentration exists within the flow and there is a low concentration of cohesive materials. Deposits of sandy debris flows are ungraded with rafted mudstone clasts at the tops of the beds, can display inverse grading at the base and can have floating coarser sized grains or granules. It can have trailing turbulent clouds similar to the other classifications.
	Concentrated density flows (Mulder and Alexander, 2001)	Transformed hyperconcentrated flow where dilution of the flow body is sufficient enough to allow the upper part of the flow to become turbulent, thus making the overall flow stratified. The presence of connected voids between grains allows the hyperconcentrated flow to ingest water, expand, and transform into a concentrated density flow. Rate of water entrapment depends on slope gradient, lateral confinement, flow thickness, water depth and bed roughness. Flow stripping can also separate the turbulent top from the basal flow (Piper and Normark, 1983). Sediment support mechanisms include dispersive pressure and grain on grain interaction. Flows can be erosive and can display structures which include flute clasts and climbing ripples and laminae that are deposited through waning of the upper turbulent flow. Prominent normal vertical grading is more likely to be preserved within the upper part of a concentrated density flow deposit (the turbulent component). The preserved lower bed is considered massive and possibly inversely graded at its base.
	Dense flow (Gani, 2004)	Dense flows are comparable to concentrated density flows of Mulder and Alexander (2001) and sandy debris flows of Shanmugam (1996). They are stratified bi-partite flows that are partly turbulent and partly laminar. The turbulent component increases downslope. This classification is determined on sediment concentration, sediment support mechanisms, flow state (laminar or turbulent) and rheology.

	High density turbidity current (Lowe, 1982) and aggradational turbidity current (Kneller and Branney, 1995)	Thick bedded sandstones displaying stratified tops are interpreted as being products of high-density turbidity currents. A Bouma (1962) Ta division represents deposition where suspended load fallout rates are high enough to suppress tractional transport. The laminated Tb and Tc divisions represent the final flow stages where flow density and velocity are suitably low enough for bed flow development (Lowe, 1982). Laminated Tb and Tc divisions are related to the distance of the sandstone to the source as they are not considered to form in proximal settings, only in distal settings. The model suggested by Lowe (1982) comprises proximal sandy high density turbidity currents which transform downslope into later stage distal low density turbidity currents. Deposits are represented by traction carpets and dewatered suspension divisions. They are normally graded from the base.
Turbulent Flow	Turbidity Flows (Bouma, 1962)	Suspensions of sediment that are sustained by fluid turbulence. Grains are supported within an active turbidity current by the upward component of turbulent fluid motion. Turbidity current deposition generally occurs as sediment settles from suspension. Coarse- and fine-grained particles settle independently during deposition, depending on fall velocities. This produces a fining-up/normal size grading sequence of grain-size with gradual upper contacts (Shanmugam, 1997). The traction carpet at the base of the flow within turbidity currents are near-bed layers where particle support is dominated by grain collisions, while particles in the overlying flow are supported largely by turbulence (Lowe, 1982, Hiscott, 1994, Sohn, 1997). The classic model for medium-grained sand- and mud-dominated turbidites comprises of sharp based, fining upward sandstone beds with a structured sequence of internal laminae and cross bedding (Bouma, 1962; Stow *et al.,* 1996).
Non Cohesive Debris Flows (~0% Cohesive Material)	Hyperconcentrated density flow (grain flow)	Grain flows are interpreted to require slopes near the angle of repose in order for motion to occur. They are mass movements of cohesionless material in which direct grain-to-grain contact and collisions dominate momentum transfer (Bagnold, 1956; Jaeger *et al.,* 1996). Non-cohesive and gravely flows tend to show higher particle concentrations and are dominated by frictional rather than cohesive interactions (Iverson, 1997).

2.3 Deep Marine Sequence Stratigraphy

Sequence stratigraphy is a study of repetitive genetically-related strata within a framework of chronostratigraphic erosional or non depositional surfaces (Van Wagoner *et al.,* 1988). It provides a useful structure for understanding the interplay between accommodation, subsidence and/or uplift and rates of eustatic sea-level change and sediment supply (Pickering *et al.,* 1989). Strata, or sequences, are the primary unit of sequence stratigraphy. Sequences can be separated into systems tracts, which are defined by both their position within a sequence and by the stacking patterns of parasequences that are bounded by maximum flooding surfaces (Van Wagoner *et al.,* 1988).

The deep marine succession within the sequence stratigraphic model of Vail *et al.,* (1977) comprises a lowstand fan and a subsequent lowstand wedge or slope fan (Figure 2-2 and 2-3). The lowstand fan is representative of a basin-floor fan system (Posamentier and Erskine, 1991) which rests upon a Type 1 sequence boundary (Vail, 1987). These systems are fed by sediment produced through the downcutting erosive activity of fluvial systems on the shelf as the environment adjusts to reach the new equilibrium profile instigated by a revision in marine base level (Figure 2-2).

Lowstand wedge or slope fan deposition begins after deposition of the lowstand fan when the relative sea-level commences rising at the shelf edge, resulting in a decreased sand:mud ratio. Lowstand wedge systems comprise slope fan systems that onlap and/or downlap onto either the basin floor fan system or a Type 1 sequence boundary (Vail, 1987) (Figure 2-2 and 2-3). Mass wasting of canyon walls and the upper slope can occur within lowstand wedge systems. The rate of failure, and its related deepwater sediment supply, decreases with time (Posamentier *et al.,* 1991). The transgressive systems tract eventually overlies the late lowstand wedge as the sea level continues to rise.

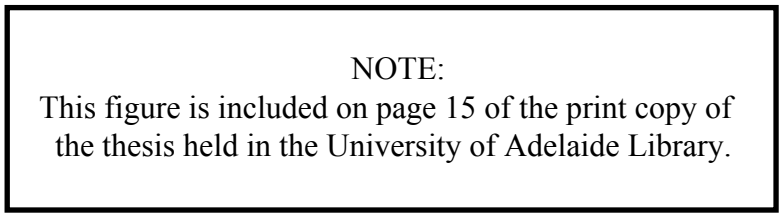

Figure 2-2: Sequence stratigraphic depositional model showing various sequences, surfaces and facies system tracts in linear depth (adapted from Van Wagoner *et al.,* 1988).

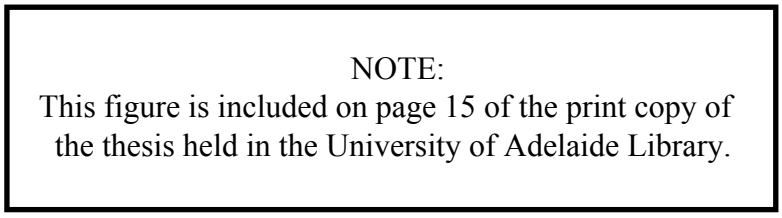

Figure 2-3: Lowstand and slope fan depositional systems from Palaeogene successions of the Central and Northern North Sea (after Armentrout *et al.,* 1993).

2.4 Submarine Fan Facies Models

Submarine fan models have been created in the past in an attempt to improve comprehension of the growth of these depositional systems in the deep marine realm. Early models such as the suprafan model of Normark (1970) (Figure 2-4) and the ancient fan model of Mutti and Ricci Lucchi (as discussed by Mutti and Normark (1987)) (Figure 2-5) were amalgamated to create the classic fan model of Walker (1978) (Figure 2-6).

The Walker model became favoured in hydrocarbon exploration and development by its predictive capabilities (Shanmugam, 2000). Submarine models were further improved by Mutti (1985) who developed three main types of depositional system (Type 1, 2 and 3) based on work conducted in the highly elongate and longitudinally supplied basins of the southern Pyrenees (Figure 2-7). Reading and Richards (1994) reclassified deep marine systems according to the grain-size and the nature of the feeder systems that created them (Reading, 1991; Reading and Richards, 1994). This resulted in the classification of four differing grainsize and three differing supply methods to form in total twelve different depositional models (Figure 2-8, 2-9 and 2-10). These models were widely received resulting in the desertion of the generalised submarine fan model of Walker (1978).

Figure 2-4: The modern submarine model of Normark (1970) based on the modern day Navy Fan located offshore California. It contains a channel complex grading downslope into distributary systems and a suprafan lobe. The term “suprafan” is no longer used in deep marine research.

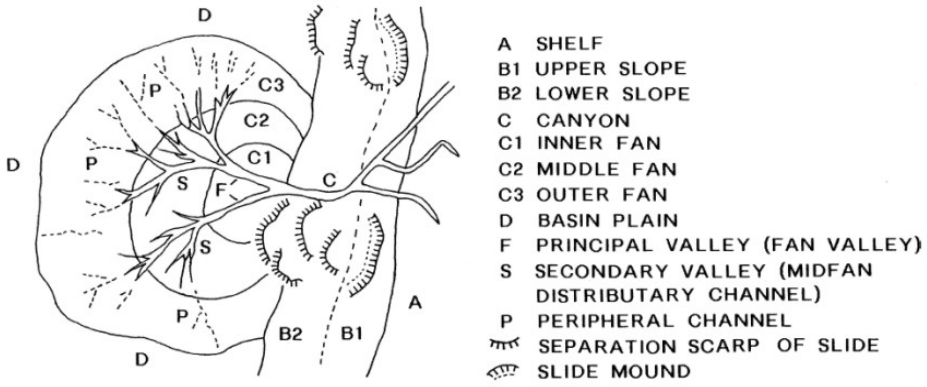

Figure 2-5: The ancient submarine fan model of Mutti and Ricchi Lucchi (1972) (as discussed by Mutti and Normark, 1987). It was based on lithofacies-related outcrop research completed on the Northern Apennines, Italy. It represents a distributary-like fan system.

NOTE:
This figure is included on page 17 of the print copy of the thesis held in the University of Adelaide Library.

Figure 2-6: The submarine fan model of Walker (1978). It was compiled using a mixture of the ancient and modern submarine fan models of Mutti and Ricchi Lucchi (1972) and Normark (1970). It comprises suprafan lobes located at the end of distributary channel systems.

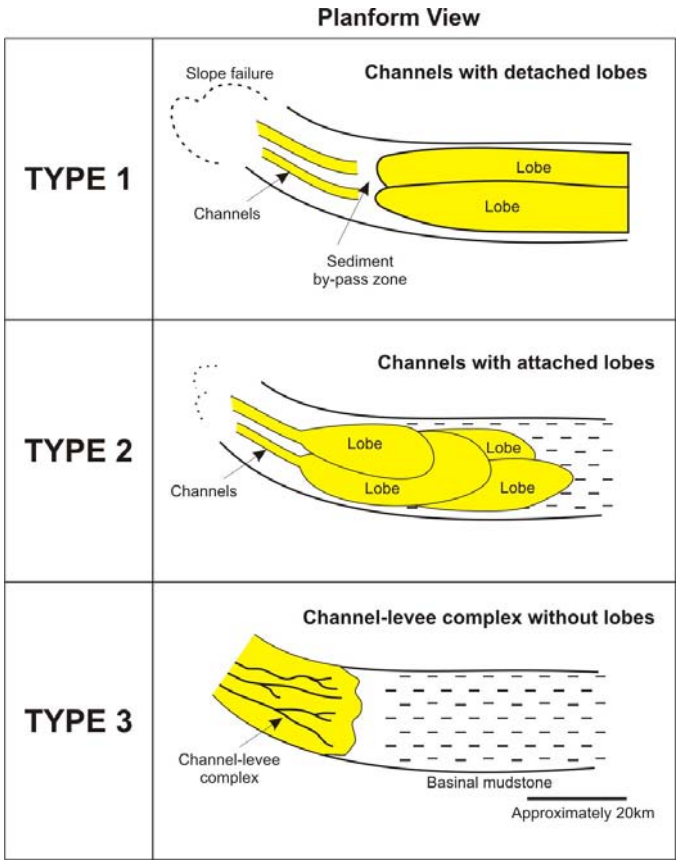

Figure 2-7: Three major depositional systems of Mutti (1985) modelled on the elongated basins of the southern Pyrenees. Type 1 systems comprise extensive unchannelised lobe deposits that are primarily correlated to shelf failures. Type 2 systems comprise channel-lobe systems that grade downslope into lobe deposits. Type 3 systems comprise thin-bedded mudstone-dominated units and sandstone-filled channel-levee systems. The models are based on flow volume variation (Mutti, 1985, Stow *et al.,* 1996).

NOTE:
This figure is included on page 18 of the print copy of the thesis held in the University of Adelaide Library.

Figure 2-8: Slope apron models of Reading and Richards (1994).

Figure 2-9: Submarine fan models of Reading and Richards (1994). They are represented by a single source feeder.

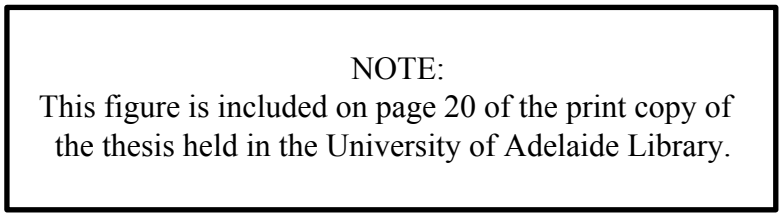

Figure 2-10: Submarine ramp models of Reading and Richards (1994). They are represented by multiple feeder systems.

2.5 Geological Controls on Fan Development

Many variables influence the growth and architectural style of deepwater depositional environments (Figure 2-11). They include:

- sediment supply, accumulation and type;
- tectonic setting, and;
- eustatic or relative sea-level variation.

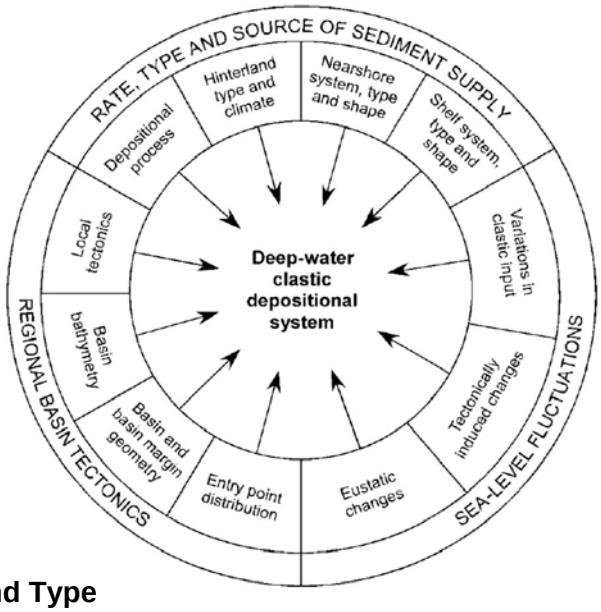

Figure 2-11: Major variables that control the morphology of deep marine depositional systems (after Stow *et al.,* 1996; Richards and Bowman,1998).

2.5.1 Sediment Supply, Accumulation and Type

The geometry and architecture of deepwater deposits are affected by the grainsize and composition of the supplied sediment (Stow *et al.,* 1996). Coarse-grained systems tend to consist of coarse- to medium-sized sands which are supplied by infrequent high velocity and/or high density flows, fed from coarse-grained river systems or longshore drift processes (Pickering *et al.,* 1989). The rate of supply and volume of sediment to a particular region is a crucial variable. Substantial river delta systems such as the Mississippi, Indus and Ganges, can quickly supply large amounts of sediment to the continental shelf. Resedimentation of this sediment downslope of the continental shelf depends on the shelf width and the relative and eustatic sea-level at the time of deposition (Stow *et al.,* 1985).

2.5.2 Tectonic Setting and Basin Geometry

Tectonic setting controls sedimentation by affecting the stress regime of the region, which rules rates of subsidence or uplift in both the source region and the basin region (Stow *et al.,* 1996). Understanding the relationship between tectonism, basin slope tilting and lithofacies geometry leads to the understanding of how gravity-driven processes respond to the deformation of the seafloor bathymetry (Pickering *et al.,* 1989). The interaction of turbidity currents with deformed seafloor topography can result in flow reflection, deflection and separation, which produce complex turbiditic sequences (Haughton, 1994). Denudation of uplifted regions and the quantity of sediment supply, drainage patterns, widths and gradients of the coastal plain and shelf, slope gradients, morphology of the basin receiving the sediment and the position and switching of depocentre are ruled by the local tectonic setting (Stow *et al.,* 1996). Distinctive variables exist for deep marine deposition on active and passive margins (Table 2.2).

Factor	Active Margin	Passive Margin
Eustatic influence	Low to high	High
Tectonic influence	High	Low
Shelf width	Narrow	Wide
Shelf exposure/ sediment availability	Small	Large
Sediment transport	Short distance	Long distance
Fan sediment	Sand-rich	Mud-rich
Fan size	Small (tens of km)	Large (hundreds of km)
Modern example	Navy Fan	Amazon Fan

Table 2-2: Factors affecting fan development on active and passive margins (adapted from Shanmugam *et al.,* 1985).

2.5.3 Relative Sea Level

One of the strongest controlling factors in sequence stratigraphy and the deposition of sediment in the deep marine environment is relative sea-level. As it fluctuates, a whole succession of lowstand fans and wedges can build up in a basin. The degree of relative sea level variation can fluctuate according to duration and amplitude. Five orders have been used to represent the differing magnitudes (Table 2-3):

Sea-level Cycle Magnitude	Duration	Sequence Stratigraphic Unit
First Order	200 to 300 million year cycle	
Second Order	10 to 80 million year cycle	Supersequence
Third Order	1 to 10 million year cycle	Depositional sequence or composite sequence
Fourth Order	100,000 year to 1 million year cycle	Sequence, parasequence or cycle set
Fifth Order	10,000 to 100,000 year cycle	Parasequence or high frequency cycle

Table 2-3: Differing sea-level cycle magnitudes orders (adapted from Pickering *et al.,* 1989). Multiple units of a particular order can exist within the bounds of a higher magnitude set.

The recognition of flooding surfaces indicative of maximum flood conditions can be erroneously interpreted within deep marine settings. Autocyclic mechanisms such as migrational switching and abandonment of fan lobes can produce an environment favourable for the deposition of hemipelagic fines which is irrespective of current relative sea-level (Emery and Myers, 1996) (Figure 2-12). Autocyclicity can affect high resolution architectural scales from frontal splays that develop at the

mouths of distributary channels to the coalescing nature of multiple fan systems. Factors such as the percentage of clay within the source sediments can affect the error on differentiating between autocyclic and allocyclic (maximum flood) siltstones and claystones.

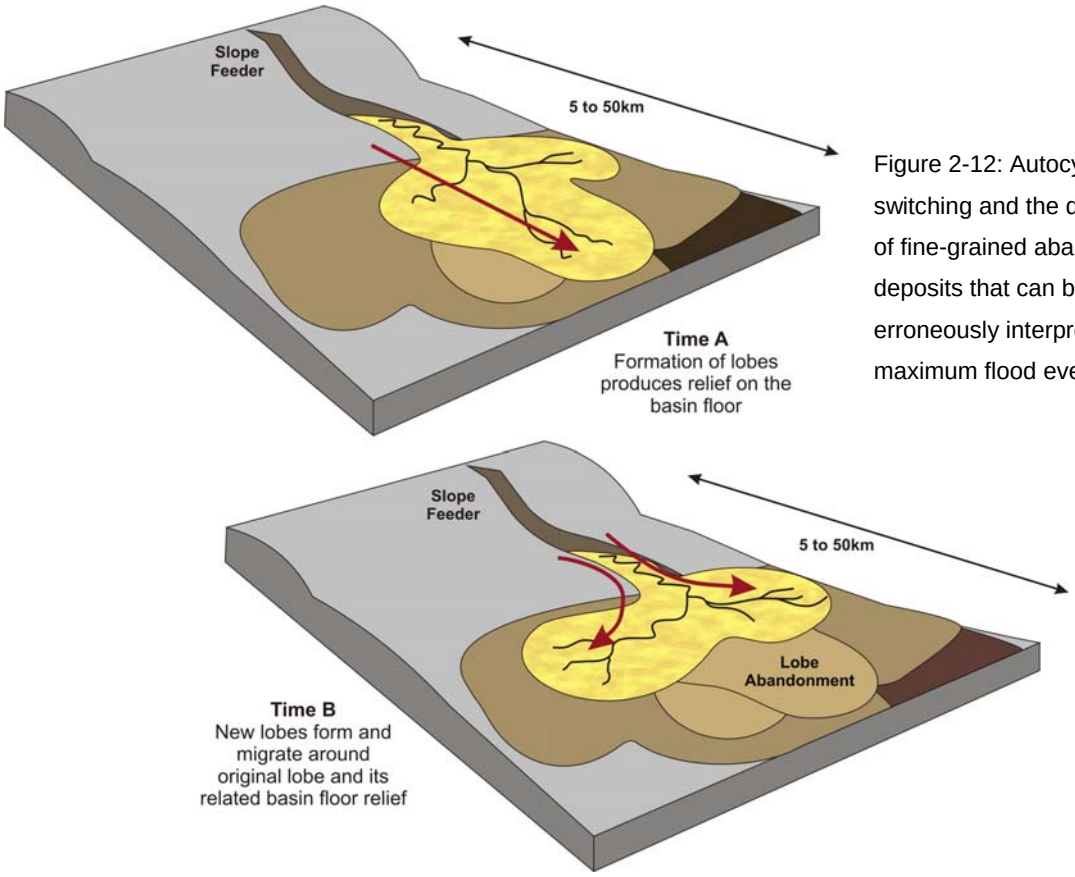

Figure 2-12: Autocyclic lobe switching and the development of fine-grained abandonment deposits that can be erroneously interpreted as a maximum flood event.

2.6 Architectural Elements

Basic components of modern and ancient turbidite systems are those that are easily mapped at outcrop, marine and subsurface scale. Understanding the architecture of submarine fans provides a basis for understanding the reservoir properties of sandstone intervals and their continuity and connectivity (Piper and Normark, 2001). Deepwater deposits comprise architectural elements, defined between bounding surfaces, which can be erosional or conformable. They are the building blocks of submarine fan systems. Pickering *et al.,* (1995) defines the term “architectural element” as the interpretative characterization of a sedimentary feature as defined by its geometry (including orientation), scale and lithofacies. Architectural elements commonly identified within deep marine settings include (Figure 2-13):

- hiatuses, erosional plains, and other bounding surfaces;
- erosional slide and slump scours;
- canyons, troughs, channels and gullies;
- channel-levees and overbank deposits (erosional, depositional and mixed erosive/depositional systems);

- depositional lobes (isolated, clustered, splay);
- irregular mounds (slide, slump and debrite masses);
- contourite drifts;
- sheets and drapes on slopes, basins, fans and drifts, and;
- tectonic features (growth faults, diapers, compressional fault mounds) (Stow and Mayall, 2000).

Each of these listed elements displays its own morphology that has to be considered when investigating the overall depositional architecture of a system (Posamentier and Kolla, 2003). It is important to recognise that deep marine architectural elements exist at a variety of differing scales. Architectural element classifications uncovered in the literature tend to emphasize the larger scaled architecture yet it is the smaller architectural variations on the scale of individual beds or sedimentary lithofacies that are more significant for reservoir characterisation and field development.

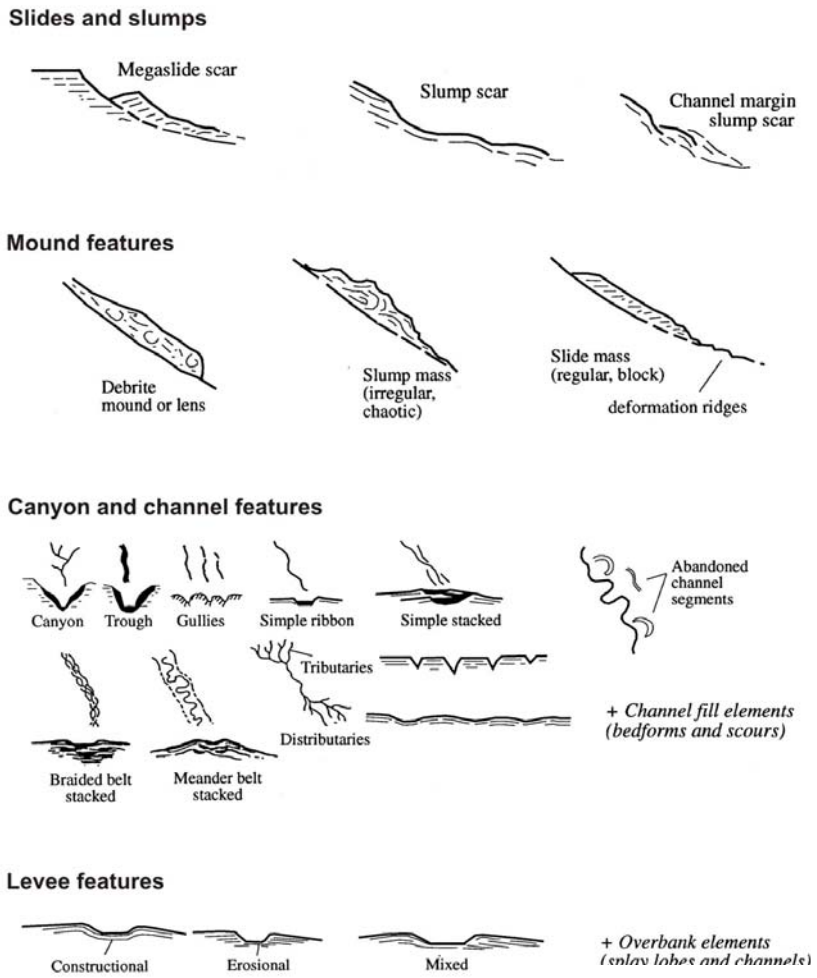

Figure 2-13: Range of architectural elements commonly identified within deep marine settings (adapted from *Stow et al.,* (1996) and Stow and Mayall (2000).

2.7 Project Terminology

An extensive range of terminology is available that can be used when examining deep marine depositional environments. It is imperative that the terminology used within this study is clarified to avoid confusion with pre-existing terminology available from literature.

2.7.1 Deep Marine Element Terminology

Architectural elements can be interpreted at multiple scales of resolution. Depositional element terminology used in this research is listed in Table 2-4 (next page) and represented in Figure 2-14.

Table 2-4: Terminology used in this study.

Term	Description
Depositional distributary channel	Situated within the middle to distal regions of fan lobes. They are formed through the avulsion of channel-levee systems that bifurcate downslope. They are shallow channels with minimal levee construction arranged in a distributive pattern (Posamentier, 2003).
Mixed erosional and depositional channel	Channel system situated within a proximal to mid fan setting. They are comparable to the middle fan region of Mutti and Ricci Lucchi (as discussed by Mutti and Normark, 1987). These systems can stack to form multistorey migrational channel complexes.
Proximal migrational channel complex	Stacked and amalgamated channel systems situated within a proximal region of a fan system. Comparable to fan valleys of Normark (1970) and the inner fan region of Mutti and Ricci Lucchi (as discussed by Mutti and Normark, 1987).
Splay	Unconfined deposition from the mouth of a distributary channel system. Frontal splays are features previously described as a channel termination lobe, lobe or lobeform (Posamentier, 2003). Crevasse splays are features formed through flow stripping and channel avulsion.
Sheet complex	Stacked succession of unchannelised frontal splays.
Proximal and distal abandonment	Relates to both channel and splay elements. When upslope channel avulsion occurs, an abandoned channel would continue to receive low density flows similar to those formed through flow stripping. Proximal abandonment is identified through a high sandstone content and distal abandonment through low sandstone content. This variability in sandstone concentration is directly related to the density-related fallout of grains within a turbulent flow. This philosophy also applies to unconfined splay deposits.
Depositional fan lobe	Represents a compensationally stackable sandstone body comprising a stacked succession of elements (depositional and mixed erosive and depositional channels and splays). It is represented by the suprafan lobe of Normark (1970) and Walker (1978).
Depositional fan	This term applies to a submarine fan system that comprises of multiple compensationally stacked depositional fan lobe units. It is dominantly bound by sequence boundaries and flooding surfaces.

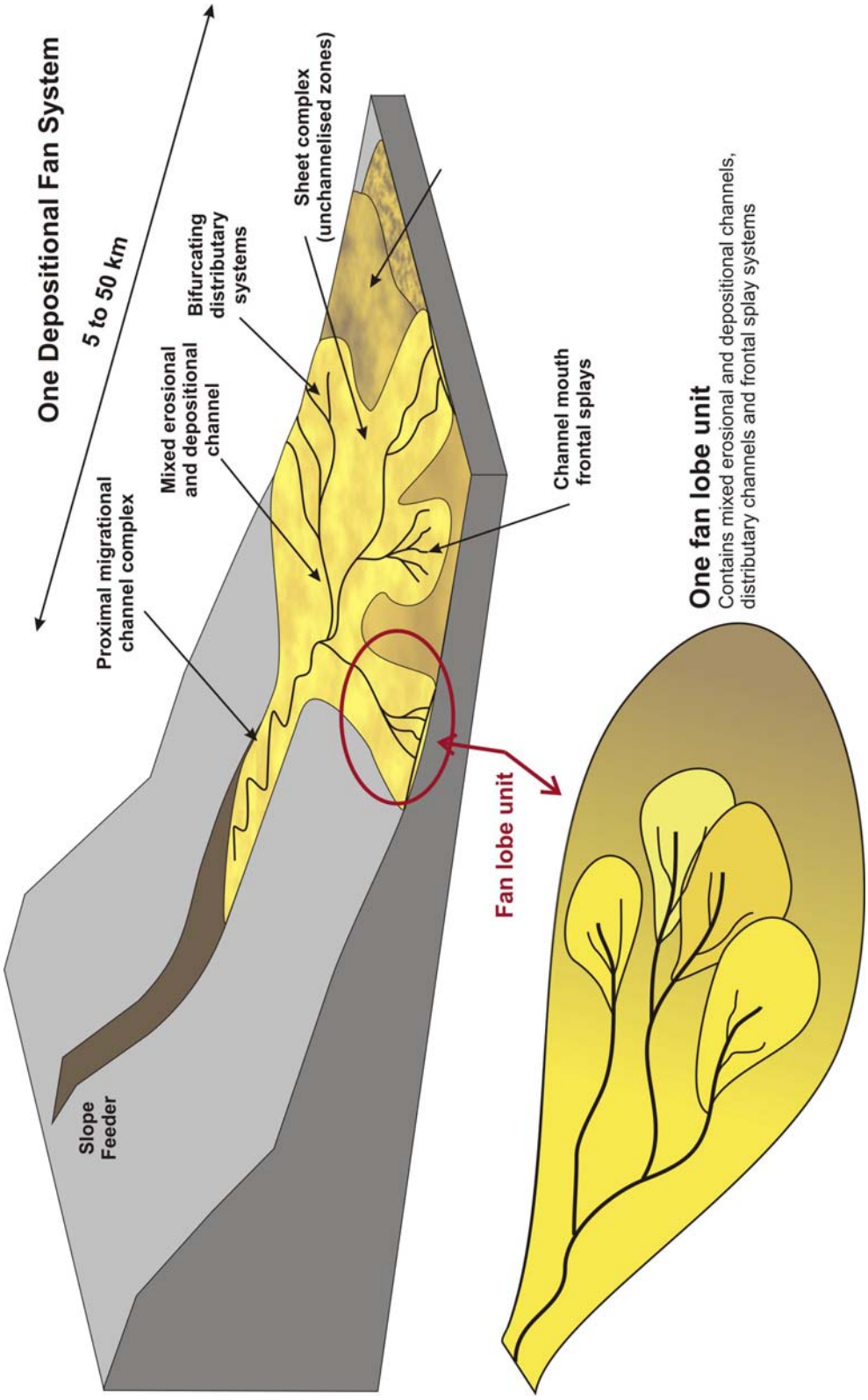

Figure 2-14: Architectural elements used in this study. The fan lobe unit is modelled closely on the latest Pleistocene lobe deposit of Gervais *et al.*, (2006).

2.7.2 Architectural Elements and Stratigraphic Units

The difficulty with the application of the sequence stratigraphic models to high resolution sand-dominated deep marine systems is that a variation in relative sea level may influence the supply of sediment from the shelf to the slope but it may not play a primary role in the formation of many deepwater sequences. Episodes of progradation and retrogradation may be used to define sequences as sequence stratigraphic principle suggests, however, maximum flooding surfaces within the stratigraphic record may not represent regional flooding surfaces that can be used to constrain a valid stratigraphic framework across a study region. They may simply represent autocyclic migration.

Sequence stratigraphy is practical for the analysis of large-scaled and low resolution sequences within deep marine settings. An architectural element based stratigraphic approach is more beneficial for analysing higher resolution sequences where relative sea level variation is not identified nor strongly preserved. This study primarily concentrates on an architectural element stratigraphic framework. Reasoning for this includes:

- the high resolution stratigraphic nature of the study;
- the poor seismic resolution at a high resolution scale, and;
- the sandy nature of the system and lack of regional flooding events.

The architectural element stratigraphic approach for this study is based on a similar approach suggested by Ghosh and Lowe (1993) and Lowe and Ghosh (2004) (Figure 2-15). This approach was first developed for fluvial systems by Miall (1985, 1988). The scheme uses a hierarchy of stratigraphic units and architectural elements where the smallest sub-divisions are first-order elements. This scheme has two parts.

i. Stratigraphic, where each element is defined by their lithology rather than on the basis of bounding surfaces (Ghosh and Lowe, 1993).

ii. Architectural, where each element is characterised by a shape or geometry. It can stack with other elements in a hierarchic fashion to construct successively larger architectural units (Ghosh and Lowe, 1993).

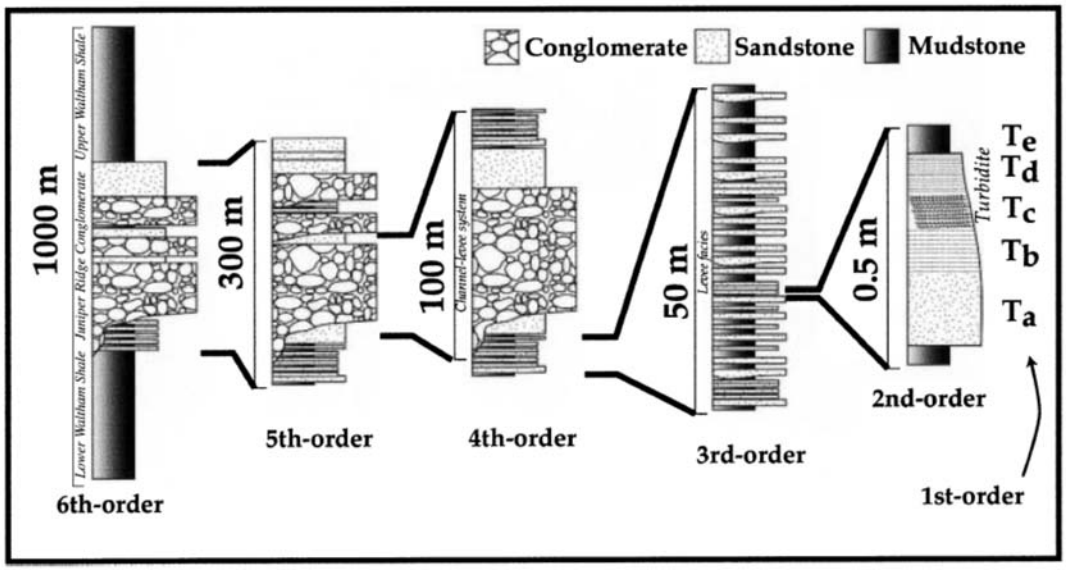

Figure 2-15: Architectural element scheme of Ghosh and Lowe (1993) applied to the facies associations that comprise the architectural elements of the Juniper Ridge Conglomerate.

The architectural element scales classified and used within this study are listed in Table 2.5. Sequence stratigraphic principles are valid for sixth and seventh order elements, however the application of tectonostratigraphic principles (Prosser, 1993) would be recommended as the Middle to Late Jurassic interval of the Dampier Sub-basin experienced a strong rift-related tectonic signature on deposition.

Table 2-5: Architectural element orders classified within this study.

	Architectural Element Order	Description
Autogenic	**First Order**	Deposit of an individual high density turbidity flow event.
	Second Order	Layers of individual flow events.
	Third Order	Depositional associations such as a channel, levee or splay unit.
	Fourth Order	A single storey elementary channel unit.
	Fifth Order	Autocyclic channel and splay complexes that may compensationally stack. They represent a fan lobe unit.
Allogenic	**Sixth Order**	Allocyclically stacked and migrational fifth order channel and splay complexes bounded by maximum flood events. It represents one depositional fan system.
	Seventh Order	Stacked sixth order systems within multiple flooding surfaces. It represents multiple depositional fans within a third order allocyclic sequence stratigraphic unit (1 to 10 million year relative sea level cycle (Section 2.5.3)). It represents the *D. jurassicum* and *P. iehiense* interval within the Dampier Sub-basin.

3 Regional Geology

3.1 Introduction

The evolution of the Dampier and Beagle Sub-basins and their resultant structural and stratigraphic style was fashioned through a relationship between sedimentation and multiple extensional and transpressional tectonic events throughout time (Figure 3-1). This chapter will encompass:

- the modern day structural style;
- the tectonic evolution in relation to multiple continental breakup events along the western margin of Australia, and;
- the stratigraphic and general palaeogeographical development from Triassic through to Early Cretaceous time.

3.2 Present Day Structural Style

The present day structural trend of the Dampier and Beagle Sub-basins comprises elongated northeast-southwest linear depressions in the northern Dampier Sub-basin and inverted north-south oblique rifted blocks in the southern Beagle Sub-basin (Figure 3-1).

The northern Dampier Sub-basin contains two linear synclinal depressions known as the Lewis Trough and Kendrew Terrace (Figure 3-1). They are separated by the anticlinal Madeline Trend (Hocking, 1994) which provided the trapping mechanism for the Wanaea, Cossack and Angel fields (Miller and Smith, 1996). The Legendre Trend towards the southeast is also anticlinal and, along with the Madeleine Trend, was created though a compressive event that inverted basement faults in the Cretaceous (Colwell *et al.,* 1993). The eastern margin of the Dampier Sub-basin comprises rift-related en-echelon fault systems. The western margin is defined by the Rankin Platform, a structural high comprising Triassic to Lower Jurassic sediment (Westphal and Aigner, 1997). The Lewis Trough acted as the main axis for sediment deposition within the region (Hill, 1994) (Figure 3-1 and 3-2).

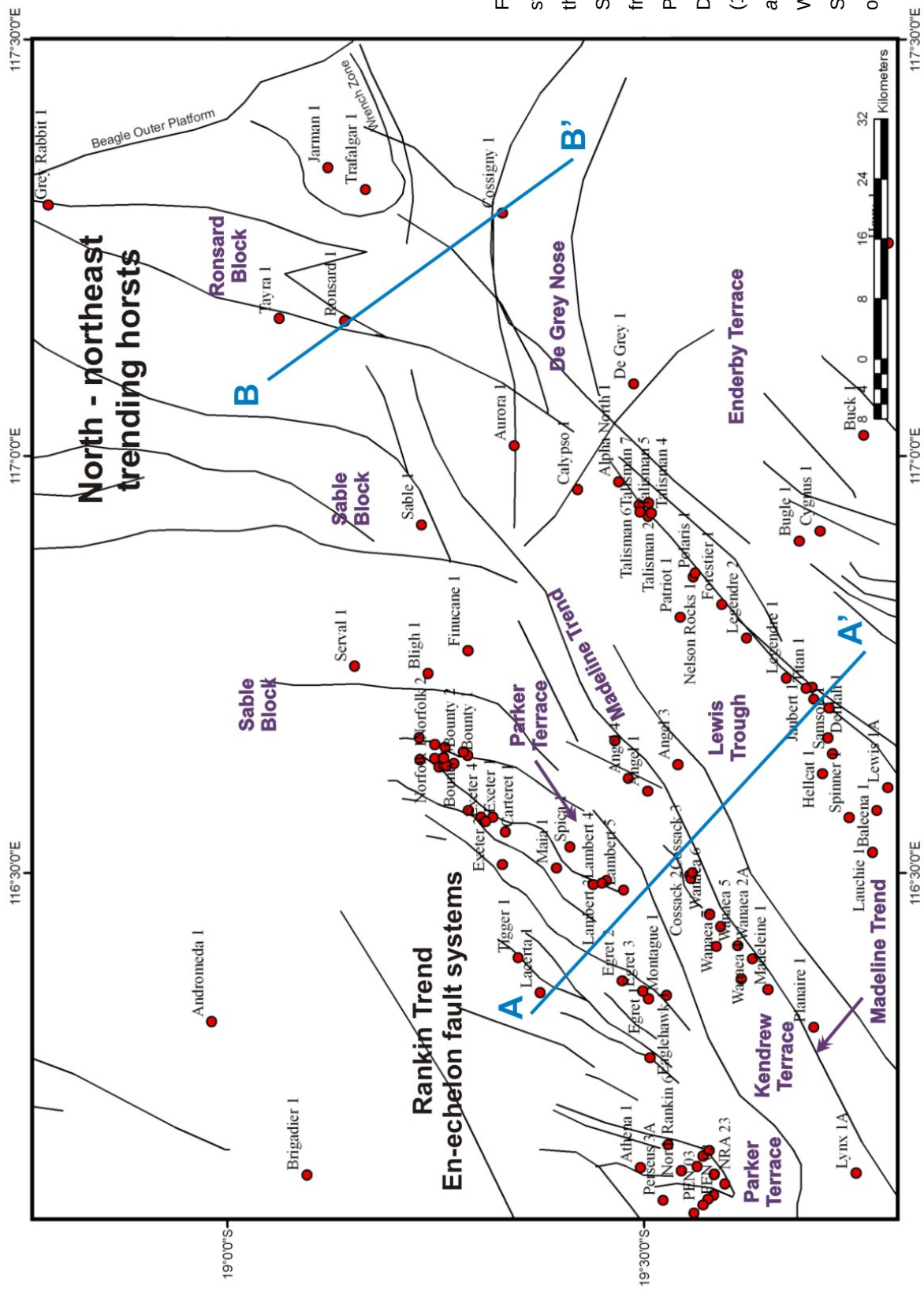

Figure 3-1: Modern structural framework of the Dampier and Beagle Sub-basins (adapted from Woodside Offshore Petroleum (1988), Delfos and Boardman (1994, Stephenson *et al.*, (1998) and Woodside (1999)). Sections A-A' and B-B' on next pages.

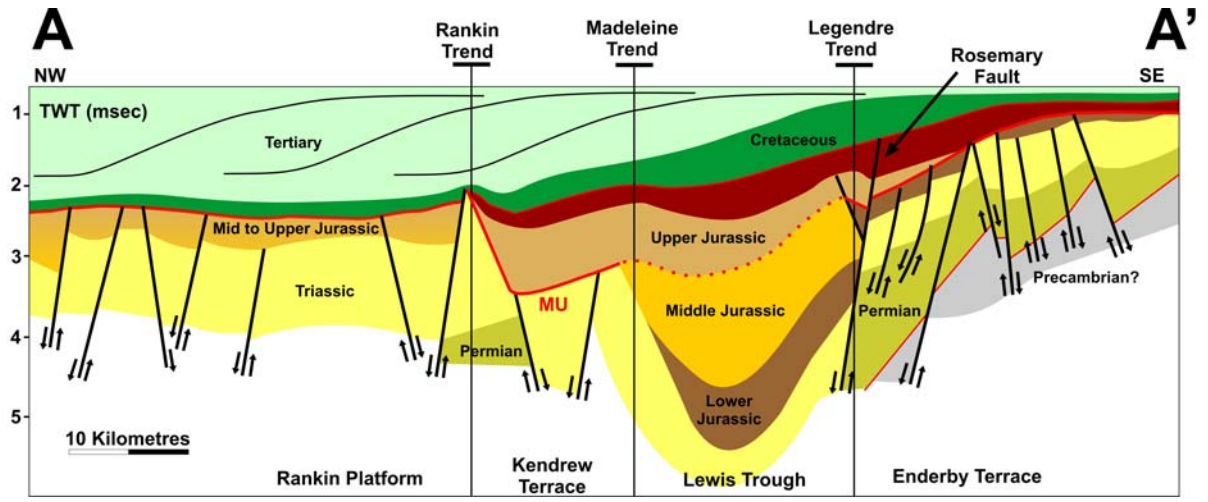

Figure 3-2: Cross-section across the Dampier Sub-basin highlighting rift influenced structure and general stratigraphy (adapted from Veenstra (1985) and Longley *et al.,* (2002). Red lines represent regional unconformities. Refer to Figure 3-1 for line location.

The Madeline and Legendre trends in the Dampier Sub-basin merge northwards into obliquely rifted and uplifted fault blocks of the southern Beagle Sub-basin. These north to northeast trending parallel blocks are separated by structural lows (Blevin *et al.,* 1994). Due to the oblique nature of the blocks, they dip gently towards the north and bifurcate towards the south (Blevin *et al.,* 1994). This northward tilt was introduced during Late Jurassic and Early Cretaceous time through a block rotational movement associated with extension in the Gascoyne region (Pryer *et al.,* 2002) (Section 3.3). Wrenched zones exist between and landward of the faulted blocks. They were created through lateral strike-slip fault motion which transpired prior to the major Callovian breakup event. The oblique blocks were uplifted whilst the wrench zones between them collapsed (Blevin *et al.,* 1994) (Figure 3-3).

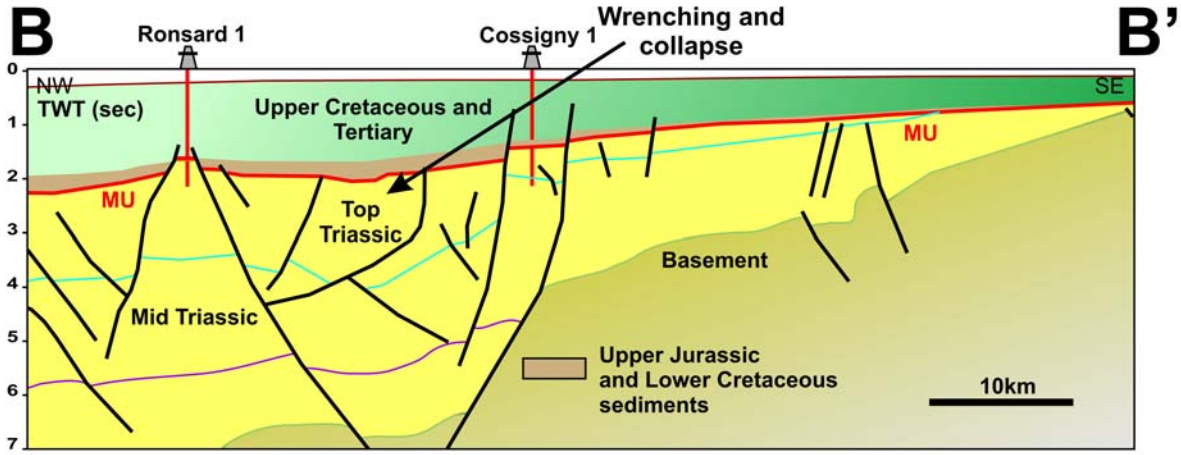

Figure 3-3: A schematic section across the southern Beagle region demonstrating the structural style of the sub-basin. Ronsard-1 is situated on a Triassic stable horst structure. Wrench faulting took place between blocks. Note the thin eroded Jurassic and Cretaceous sediments on top of the horst block (modified from Geoscience Australia, 2005). Refer to Figure 3-1 for line location.

The Rankin Platform (Figure 3-2), which borders the study region to the west, is a faulted and elongated structurally high horst complex of Mesozoic sediments that divides grabens of the Dampier Sub-basin from the broad and faulted trough of the Kangaroo Syncline (Hocking, 1990; Newman,

1994) (Figure 3-2). It is the western peri-platform edge of the Middle to Late Jurassic Dampier failed rift complex. It contains a series of Upper Triassic to Middle Jurassic fault blocks which are truncated by a regional unconformity known as the Main Unconformity (MU) that was created through extension-related uplift (Figure 3-2). It is overlain by post-rift Lower Cretaceous marine shales (Veenstra, 1985). Fault geometries along the platform are characterised by steep faults and unsystematic fault block rotations (Etheridge *et al.,* 1991), which are related to the late Tithonian block rotational event suggested by Pryer *et al.,* (2002).

3.3 Tectonic Evolution of the Beagle and Dampier Sub-basins

The structural history of the Dampier and Beagle Sub-basins is divided into six episodes ranging from Permian to Late Miocene times (Fullerton *et al.,* 1989; Gartrell, 2000; Hill, 1994; Westphal and Aigner, 1997) (Table 3.1). The northern Carnarvon basin is a passive 'failed' rift system that formed through the gradual breakup of eastern Gondwanaland which commenced in the Permo-Triassic and continued through to the Early Cretaceous (Wulff and Barber, 1995).

Table 3-1: Structural history of the Dampier and Beagle Sub-basins.

Structural Event	Regional and Biostratigraphic Pick	Timing	Resultant Structure and Discussion
Permo-Carboniferous Sibumasu Breakup Event	N/A	Commenced Late Carboniferous to Early Permian. Terminated Late Permian	• Northwest – southeast extension • Established the dominant northeast-southwest structural grain of the Dampier Sub-basin (Gartrell, 2000). • Formation of the Lewis Trough (Hill, 1994, Pryer *et al.,* 2002). • Resultant tectonic style interpreted to comprise half grabens bounded by listric faults which were overlain by a new passive margin of Triassic post-rift sediments (Hill, 1994). • Development of Neo-Tethys Ocean by Early Triassic time (Veevers, 1988)
Late Triassic Restructuring Event	N/A	Late Triassic	• Related to transpressional Fitzroy movement in the Canning Basin • Sub-divided Beagle Sub-basin into series of stable north-south trending horst blocks with intervening lows. • Separated the Beagle and Cossigny Troughs from the Lewis Trough (Blevin *et al.,* 1994). • Very little structural influence on the Dampier Sub-basin.

Early Jurassic West Burma Block 1 Breakup Event	TRR (rift onset) Base *R. rhartica* JP1 (Final breakup) *D. prisum*	Rift onset commenced Late Hettangian. Block broke away in the Sinemurian	• Breakup event resulted in thermal subsidence combined with a rifted arch setting in the northern Carnarvon basin (Veevers, 1988, Jablonski and Saitta, 2004). • Resulted in flooding episode across the Beagle Sub-basin (Longley *et al.,* (2002). • The initial rift event which eventually led to the series of breakup events along the North West Shelf (Jablonski, 1997) • Formation of the Lewis Trough and Rankin Trend (Jablonski, 1997)
Callovian West Burma Block 2 Breakup Event	JC (rift onset) Base *W. digitata* JO (Final breakup) Base *W. spectabilis*	Rift onset commenced Callovian Block broke away Oxfordian	• Active extension led to the continental breakup in the Argo Abyssal Plain approximately 500km from the Dampier region (Fullerton *et al.,* 1989). • Extension direction of north-northwest determined from magnetic isochron mapping. Sea floor spreading commenced at 155Ma (Exon and Von Rad, 1994). • Transtensional movement resulted in deepening and broadening of the rift complex towards and across the Rankin Trend, forming the Kendrew and Parker Terraces (Barber, 1994a; Hill, 1994). • Peri-platform regions (Rankin Trend, Orion Eliassen Terrace and Enderby Terrace) all uplifted and eroded. • Beagle Sub-basin did not undergo subsidence like the Dampier due to a differing structural grain. Principal fault movement during the Callovian breakup was strike slip with localized extension. Grabens between horst features were deformed through the formation and collapse of wrench zones. The horst blocks remained undeformed. The pre-existing pre-rift north-south horst block fabric of the Sub-basin did not conform to the NW-SE extensional direction resulting in the failure of the Beagle Sub-basin to subside along with the Dampier Sub-basin (Morley *et al.,* 1990; Nelson *et al.,* 1992; Withjack *et al.,* 2002; Hill, 1994).

Late Jurassic West Burma Block 3 and Block Rotational Event	JK (rift onset) Intra *W. clathrata* JT (Final breakup) Base *C. perforans* and *D. swanense*	Rift onset commenced Kimmeridgian Block broke away early Tithonian Block rotation event Tithonian	• West Burma Block 3 separated from a region outboard of the Bonaparte Basin (Longley *et al.,* 2002; Jablonski and Saitta, 2004). • Fault reorientation and block rotation occurred within the Dampier Sub-basin in relation to the changing extension direction from northwest (the Argo spreading ridge) to west-northwest (the Gascoyne spreading ridge). • Block rotational processes instigated minor uplift and erosion of south facing flanks of the Rankin Platform blocks, resulting in the accumulation of Late Jurassic and Early Cretaceous sediments on the downthrown side of the fault systems (Barber, 1994a; Hill, 1994). • Northward tilting of fault blocks reactivated pre-existing Jurassic transfer structures and localized inversion of footwalls also occurred, creating localized anticlines (Pryer *et al.,* 2002).
Valanginian Greater India Breakup Event	K (rift onset) Base *C. delicata* KV (Final breakup) Base *S. aerolata*	Rift onset commenced Early Cretaceous Block broke away Valanginian	• West-northwest extension resulted in the breakaway of Greater India, resulting in the formation of the Gascoyne and Cuvier abyssal plains during Valanginian time (Fullerton *et al.,* 1989; Gartrell, 2000; Hill, 1994; Westphal and Aigner, 1997). • It eventuated to the passive subsidence of the North West Shelf between Late Cretaceous times to present day (Hill, 1994).
Quaternary Trans-pressional Event	N/A	Middle to Late Miocene	• Transpression brought about by the collision of the Indo-Australian plate with the Banda Arch and Eurasian plate (Keep *et al.,* 2003). • Large scale transpression resulted in strike-slip and inversion along northeast trending faults (Keep *et al.,* 2003). • This event created the main structural closure for the majority of discovered hydrocarbon fields in the northern Carnarvon basin.

3.4 Stratigraphic Evolution

3.4.1 General Stratigraphy of Dampier and Beagle Province

The Dampier and Beagle Sub-basins contain sediments deposited between Early Jurassic pre-rift and Early Cretaceous post-rift time. Preserved Mesozoic successions within the two basins differ considerably due to the structural differences between the Dampier and Beagle Sub-basins in relation to Mesozoic subsidence (Table 3.1) (Figure 3-4 and 3-5).

3.4.2 Stratigraphy and Palaeogeography of the Dampier and Beagle Region

The stratigraphic development of the Triassic to Cretaceous intervals within the Dampier and Beagle Sub-basins is largely controlled by tectonism in association with continental breakup. The standard sequence stratigraphic model of Posamentier and Vail (1988) can not be applied with confidence within these settings as the strength of tectonic signature on the timing and distribution of coarse-grained sediment greatly outweighs that of eustacy. Tectonostratigraphic models are used instead.

Miller (1996) and Miller and Smith (1996) separated the Mesozoic section of the Dampier Sub-basin into five tectonostratigraphic packages. They are the:

- late post-rift package (Early Cretaceous to present day);
- immediate post-rift package (Kimmeridgian to Late Tithonian);
- rift climax package (Early to Late Oxfordian);
- rift initiation package (Callovian to Early Oxfordian), and;
- pre-rift package (Triassic to Middle Jurassic).

Although the succession above indicates that the Mesozoic rift event was considered to be one structural event, it fails to acknowledge the multiple smaller-scaled extensional events that occurred throughout the Mesozoic as the Burma sub-blocks broke apart separately as suggested by Longley *et al.,* (2002). Jablonski (1997) improved the stratigraphic classification for the Mesozoic rift successions taking into consideration the multiple rifting events that occurred as the break-up matured from north to south along the western Australian margin. He recognises multiple syn-rift packages in relation to the multiple rift events (i.e. West Burma Block-1, -2).

Jablonski (1997) applies sequence stratigraphic terminology to improve the understanding of the basin and divides the Mesozoic to Lower Cretaceous succession into “megasequences”. They are the:

- late syn-rift and post rift successions (Berriasian to Valanginian);
- syn-rift 2 megasequence (Oxfordian to Tithonian);
- syn-rift 1 megasequence (Callovian to Oxfordian);
- early syn-rift megasequence (Pliensbachian to Callovian), and;
- active margin megasequence (Triassic to Early Jurassic).

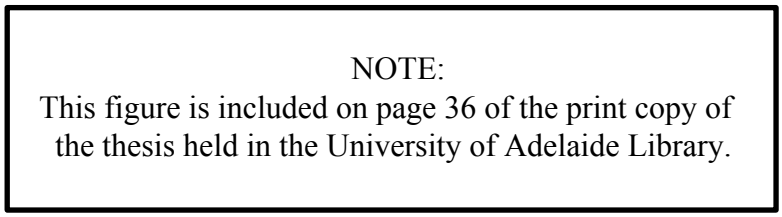

Figure 3-4: Basic stratigraphic chart for the Dampier Sub-basin (modified from Auld and Redfern, 2003). It highlights the depocentre created within the Lewis Trough which, over time, widens laterally with continuous extension resulting in the deposition of sediments on the Kendrew and Parker Terraces to the west.

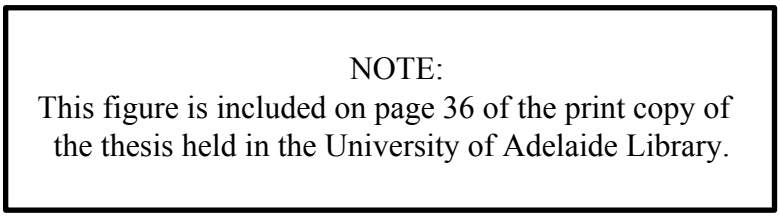

Figure 3-5: Basic stratigraphic chart for the Beagle Sub-basin (modified from Stephenson *et al.,* 1998). A significant component of the Legendre Formation is interpreted to have been removed from the horst blocks in the southern Beagle Sub-basin (Stephenson *et al.,* 1998).

3.4.2.1 Active Margin Megasequence (Triassic to Early Jurassic)

A fluvio-deltaic and nearshore environment existed over the Dampier and Beagle Sub-basins during Late Carnian to Norian time, leading to the deposition of the Mungaroo Formation (Hocking, 1990; Stephenson *et al.,* 1998). Active extension in relation to the Fitzroy movement in the Canning basin was felt within the Beagle region, resulting in the creation of an intrabasinal horst and graben network (Blevin *et al.,* 1994). It was completely filled by fluvial sediments by Hettangian to Pliensbachian time (Longley *et al.,* 2002; Stephenson *et al.,* 1998) (Figure 3-6).

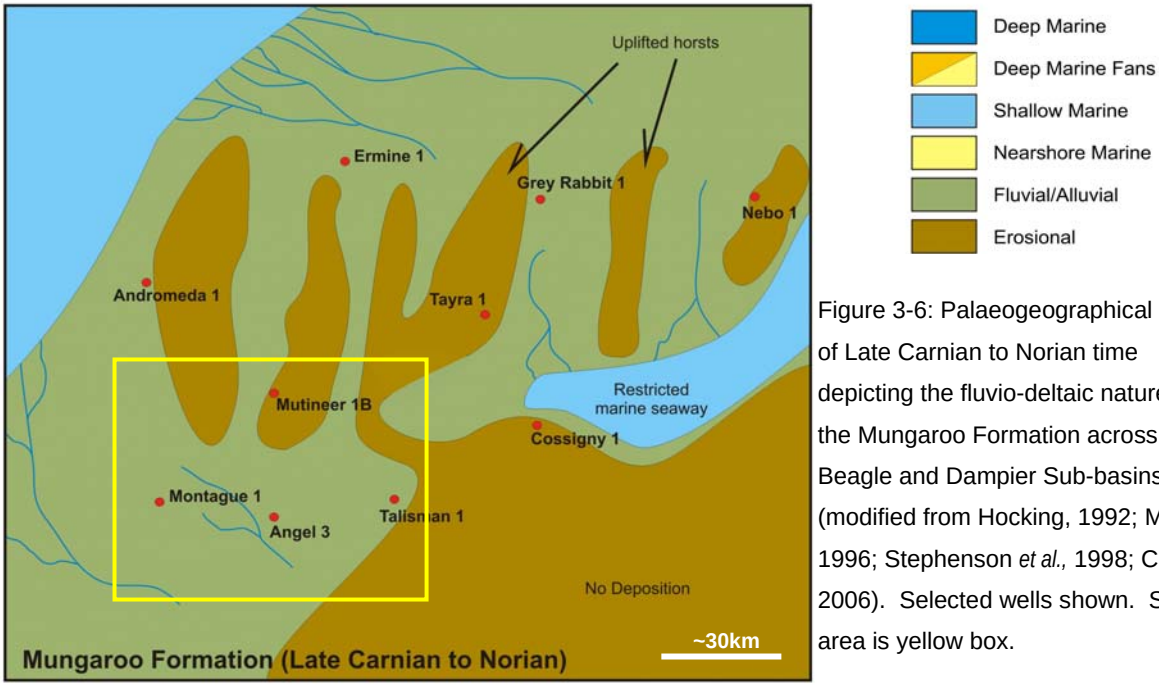

Figure 3-6: Palaeogeographical map of Late Carnian to Norian time depicting the fluvio-deltaic nature of the Mungaroo Formation across the Beagle and Dampier Sub-basins (modified from Hocking, 1992; Miller, 1996; Stephenson *et al.,* 1998; Clark, 2006). Selected wells shown. Study area is yellow box.

Subsidence slowed in the Sinemurian and sedimentation began to outpace the diminishing rate of transgression, resulting in the deposition of the highstand fluvio-deltaic North Rankin Formation across the sub-basins (Santos, 1998). Increased transgression in the Dampier region lead to marine flooding which resulted in the deposition of the Murat Siltstone (Figure 3.7).

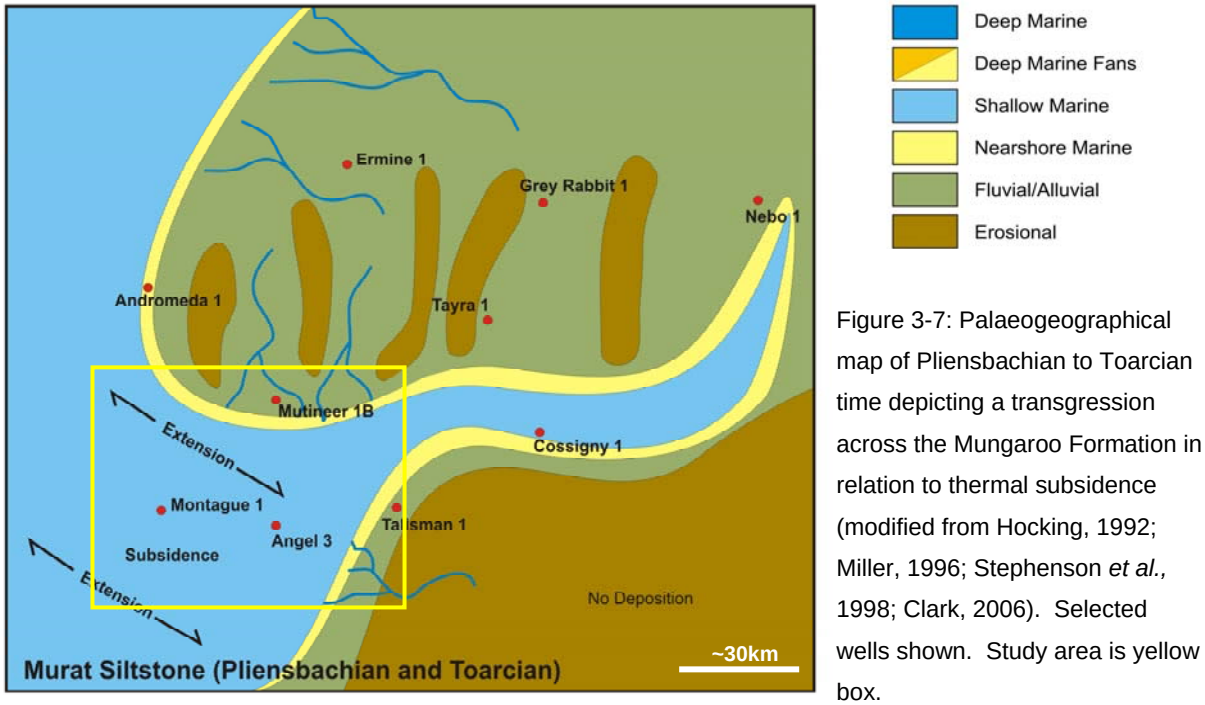

Figure 3-7: Palaeogeographical map of Pliensbachian to Toarcian time depicting a transgression across the Mungaroo Formation in relation to thermal subsidence (modified from Hocking, 1992; Miller, 1996; Stephenson *et al.,* 1998; Clark, 2006). Selected wells shown. Study area is yellow box.

3.4.2.2 Early Syn-rift Megasequence (Pliensbachian to Callovian)

Rifting commenced in Toarcian time and continued into Aalenian time, resulting in further marine incursion across the Beagle Sub-basin and further deepening of the Dampier Sub-basin (Stephenson *et al.,* 1998). The Late Pliensbachian top Murat Siltstone is recognised as a rift-onset unconformity, representing the commencement of large scale faulting along the basin margins in the Dampier region (Barber, 1982; Hocking, 1992; Kopsen and McGann, 1985; Malcolm *et al.,* 1991).

The fine-grained Athol Formation was deposited in the Dampier Sub-basin within a low-energy restricted circulation offshore marine setting (Hocking, 1992). Deposition of the Athol Formation stopped around mid *C. turbatus* (Late Toarcian) in the Dampier region when deltaic progradation of the Legendre Formation began (Hocking, 1992) (Figure 3-8). It was deposited by a line source or multiple point source deltaic depositional system (Santos, 1999).

Transgression was replaced by regression in the Beagle and Dampier region, producing a regional unconformity as the base level changed, resulting in the evolution of delta fronts and commencement of progradation of the Legendre Formation across the Dampier and Rankin Platform (Hocking, 1992).

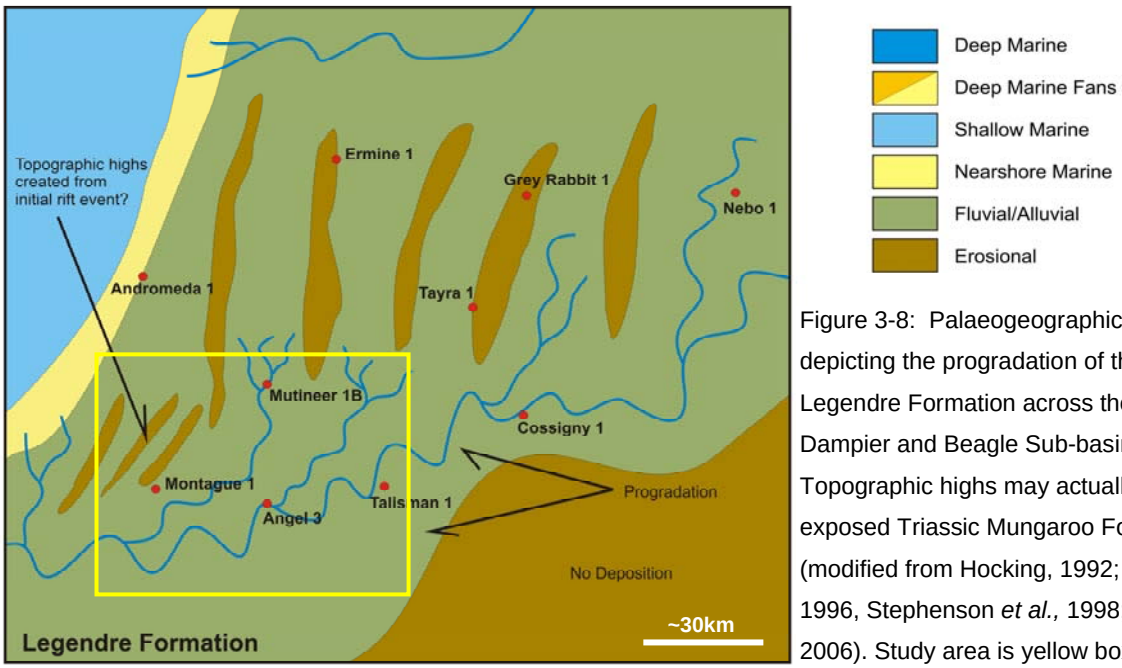

Figure 3-8: Palaeogeographical map depicting the progradation of the Legendre Formation across the Dampier and Beagle Sub-basins. Topographic highs may actually be exposed Triassic Mungaroo Formation (modified from Hocking, 1992; Miller, 1996, Stephenson *et al.,* 1998; Clark, 2006). Study area is yellow box.

Pre-rift transgression commenced during Bajocian to Bathonian time flooding the Legendre Formation towards the south (Hocking, 1992). Within the Beagle and northern Dampier region, the intrabasinal horst blocks remained erosional features surrounded by an upper fluvial plain setting (Stephenson *et al.,* 1998) (Figure 3-8).

Major tectonic features such as the Rankin Trend, Lewis Trough, Cossigny Trough and Rosemary fault systems were established during this early rift event (refer to Figure 3-1 for location of structural elements). The structurally high blocks created from this tectonism define the northwest and southeast margins of the Dampier Sub-basin and were areas of condensed sedimentation during the Early and Middle Jurassic. Infilling of the Lewis Trough and complete progradation of the Legendre Formation occurred across the Dampier and Beagle regions by the end of the Aalenian (Hocking, 1992; Jablonski, 1997) (Figure 3.8).

3.4.2.3 Syn-rift 1 Megasequence (Callovian to Oxfordian)

The early syn-rift package was terminated by the intense phase of rifting which commenced during Late Callovian time in relation to the rift onset of the West Burma Block-2 (Jablonski, 1997; Longley *et al.,* 2002). The breakup and seafloor spreading of the Argo West Burma block commenced around 160Ma, leading to rapid subsidence and transgression over the Lewis Trough (Veevers *et al.,* 1991).

The break off of Argoland resulted in accelerated subsidence, further fault block enhancement, creation of faults sub-parallel to pre-existing faults and flooding of the Legendre Delta. Formation of the Kendrew Trough and Parker Terrace is interpreted to have occurred during this time as the rift depocentre broadened and deepened towards and across the Rankin Trend (Barber, 1994a; Hill, 1994). Peri-platform regions continued uplifting and may have been eroding, however it is not clearly documented whether the Rankin Trend was subaerially exposed during this time.

Legendre Formation sediments initially kept pace with the high rate of subsidence resulting in the deposition of 800 metres of coarse-grained paralic clastic aprons in the Lewis Trough (Barber, 1994a; Miller and Smith, 1996; Wulff and Barber, 1994) (Figure 3-9). Occasional episodes of flooding resulted in the formation of several repetitive parasequence cycles (Barber, 1994a). The intrabasinal highs in the Beagle region were still eroding during this time but formed a range of linear islands surrounded by an inner marine shelf (Stephenson *et al.,* 1998).

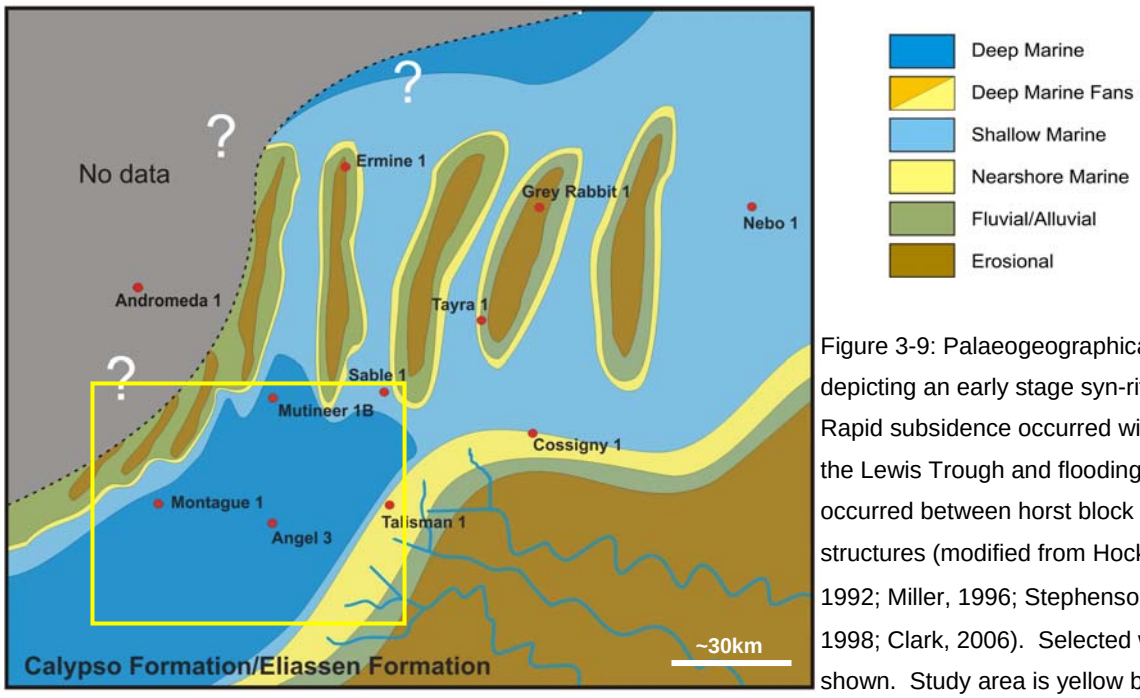

Figure 3-9: Palaeogeographical map depicting an early stage syn-rift. Rapid subsidence occurred within the Lewis Trough and flooding occurred between horst block structures (modified from Hocking, 1992; Miller, 1996; Stephenson *et al.,* 1998; Clark, 2006). Selected wells shown. Study area is yellow box.

3.4.2.4 Syn-rift 2 Megasequence (Oxfordian to Tithonian)

Sediment-filled grabens resulted in isostatic disequilibrium and a compensating rise of the asthenosphere, leading to a major relative sea level lowstand in the region and the formation of an Oxfordian sequence boundary (JO). This lowstand resulted in the initiation of the Main Unconformity (MU) and a period of significant erosion from basinal margins (Rankin Trend and Parker Terrace).

As tectonism continued throughout Oxfordian time, finer grained, low energy marine sediments continued to be deposited in the outer Dampier Sub-basin (Jablonski, 1997). On the eastern margin of the basin, there was a change from paralic marine systems to basin floor fan systems of the Eliassen Formation. They concentrated along the Enderby Terrace and Legendre Trend. This formation is represented by a multiple feeder sand-dominated sequence of coalesced submarine fans which developed in response to fault movement in the eastern region of the sub-basin (Figure 3-10) (Hocking, 1992). The location of the local palaeoshelf was deemed difficult to determine due to significant footwall erosion during this time (Wulff and Barber, 1995).

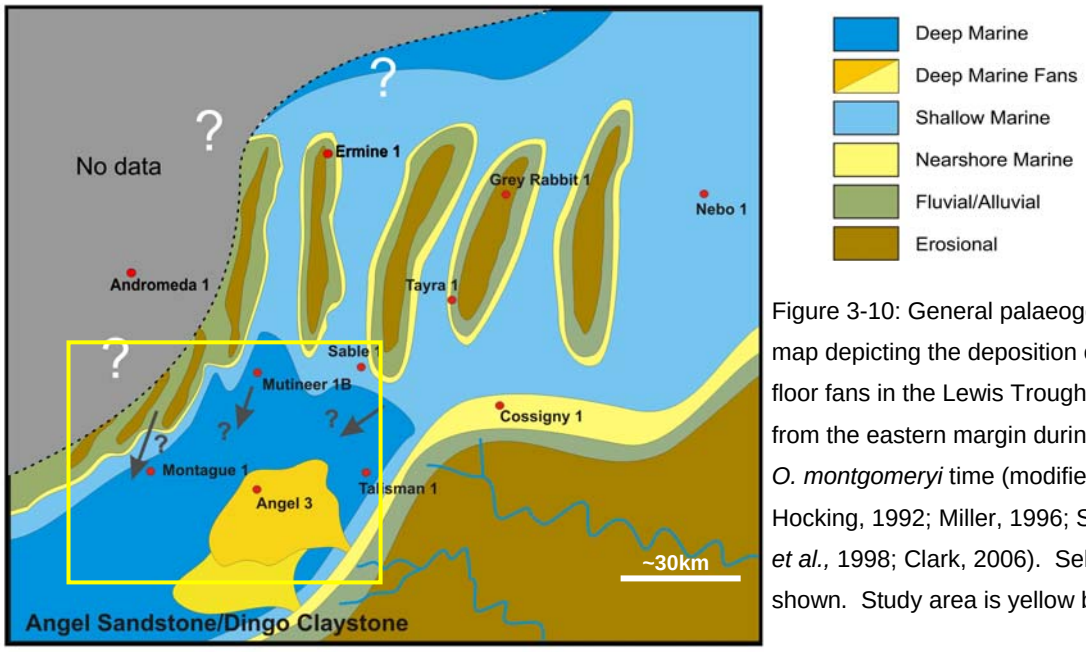

Figure 3-10: General palaeogeographical map depicting the deposition of basin floor fans in the Lewis Trough sourced from the eastern margin during *O. montgomeryi* time (modified from Hocking, 1992; Miller, 1996; Stephenson *et al.,* 1998; Clark, 2006). Selected wells shown. Study area is yellow box.

Large-scale active tectonism and displacement on bounding faults is interpreted to have continued till mid Oxfordian time (144Ma) (Wulff and Barber, 1995). An increase in sediment supply combined with a decrease in total subsidence resulted in the deposition of a gradual shallowing upward succession in the Dampier Sub-basin (Miller and Smith, 1996) and the deposition of Angel sandstones and equivalent Dingo Claystones (Figure 3-11).

The Dingo Claystone was deposited in an open marine low energy environment, which was localised in deep central troughs and their adjacent marine shelves below the wave base (Hocking, 1992). The Angel Formation comprises sandstones with interbedded claystones that have been interpreted to be deposited by high density turbidity currents or mass flows (Miller, 1996). The Kendrew Trough in the Dampier Sub-basin was interpreted to be a main depocentre during this time (Miller and Smith, 1996).

A relative sea level fall during Kimmeridgian time (*W. clathrata*) marked a depositional change with the commencement of the Dingo Claystone in the Dampier Sub-basin. Thick sediments that accumulated on the Eliassen Terrace and on the eastern flank of the Lewis Trough during Oxfordian time have been interpreted to have been subaerially exposed and eroded during Kimmeridgian and Early Tithonian time (Jablonski, 1997). They may have sourced younger Angel sandstone fan systems in the west. Multiple lowstand events have been identified throughout Kimmeridgian and Tithonian time (Wulff and Barber 1995).

Slope aprons and channel-lobe complexes developed along the eastern flank of the sub-basin during this time. They were sourced by both erosion from the Rosemary Fault scarp in the east in addition to the input of terrestrial sediments from the Enderby Platform (Figures 3-1 and 3-2) (Miller and Smith, 1996) (Figure 3-11).

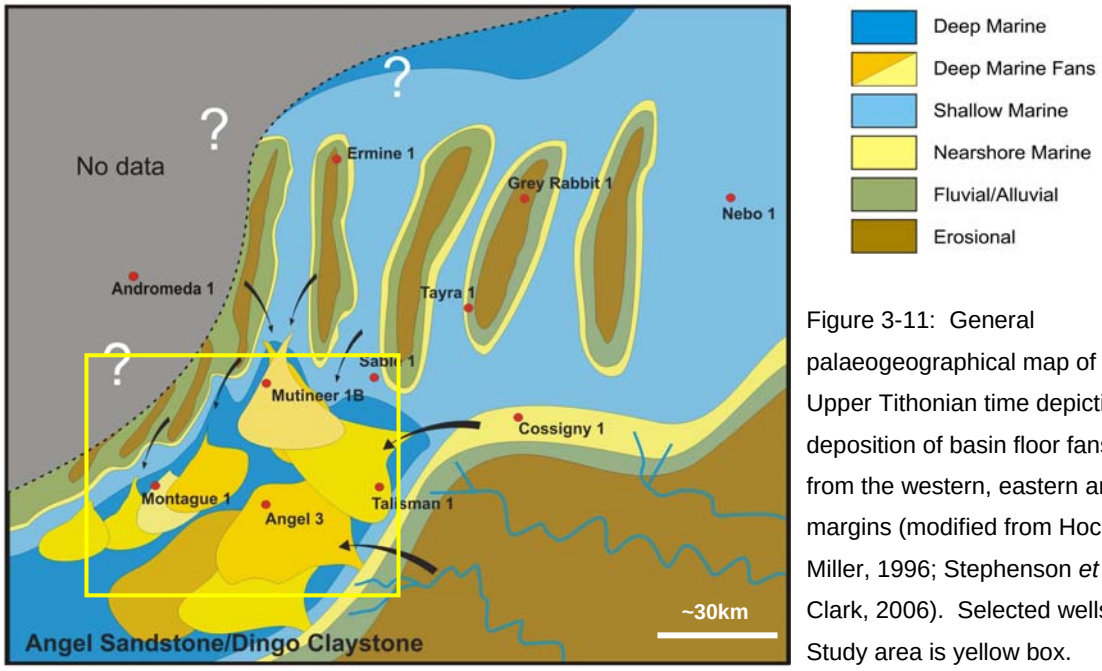

Figure 3-11: General palaeogeographical map of Middle to Upper Tithonian time depicting the deposition of basin floor fans sourced from the western, eastern and northern margins (modified from Hocking, 1992; Miller, 1996; Stephenson *et al.,* 1998; Clark, 2006). Selected wells shown. Study area is yellow box.

The Madeline trend and Kendrew Terrace were dominated by the deposition of the *C. perforans* claystone that is recognised as a significant source rock during very early Tithonian time. Jablonski (1997) interpreted that:

- a lack of sands and the presence of a thick offshore marine claystone during the *O. montgomeryi* biozone indicates that the Rankin Trend was flooded, and;
- a lack of preserved sands from the *C. perforans* to *O. montgomeryi* biozones suggests later exposure and removal of the sediments from the Rankin Trend during relative sea level lowstands.

The onset of Tithonian sand-dominated sedimentation down the Rosemary fault system took place during *C. perforans* time. Fan systems that developed during *C. perforans* to *O. montgomeryi* time were interpreted to be restricted in their lateral extent indicative of a sand-dominated system (Jablonski, 1997).

The predominance of tectonic-related accommodation declined during middle to late Tithonian time, allowing basin floor fans derived from the eastern platform to extend across the Madeleine Trend (Figure 3-11). The Rankin Trend is interpreted to have been exposed through lowstand events (Stein, 1994; Hocking, 1992 and Wulff and Barber, 1994). This trend played a critical role in sand erosion, transport and deposition along a series of footwall-derived scarps and fault transfer zones, resulting in the creation of point sourced, canyon fed mass flow and slope fan deposits adjacent to the platform. These deposits were intersected by Gregory-1, Montague-1, Egret-1, Samson-1, Lauchie-1 and Lambert-1 (Wulff and Barber, 1994) (Figure 3-1 and 3-11). Fault displacement along the Rankin Platform was interpreted to be up to 1500 metres between Kimmeridgian and early Tithonian time (Wulff and Barber, 1994).

A change from fine-grained sedimentation to the deposition of basin floor fans at the base of the *D. jurassicum* biozone correlates to a significant lowstand event (Jablonski, 1997). Basin floor fans became more sand-rich and were interpreted to be deposited through mass flow events that were derived from the Legendre Trend, the south-eastern Beagle Sub-basin and the erosional scarps of the Rankin Trend. These sand-rich units represent the major reservoir section of the Angel Formation that exists within the top *D. jurassicum* and *P. iehiense* biozones. Barber (1994a, 1994b) interpreted this depositional system to be a Type 1 system of Mutti (1985) (Figure 2-7) indicating that unchannelised lobe systems predominantly existed across the sub-basin.

An inner shelf environment existed into Tithonian time in the southern Beagle Sub-basin (Stephenson *et al.,* 1998) (Figure 3-11), which represents the possible existence of a source to sink relationship between this sub-basin and the Dampier Sub-basin. Erosion around the De Grey Nose region in the northeast resulted in the formation of fan deltas building out into the Cossigny Trough (Stephenson *et al.,* 1998). The Talisman region northeast of the Angel gas field received sandy mass flow deposits during *D. jurassicum* time from the eastern source region (Hocking, 1992) (Figure 3-11). The Angel depositional system backstepped towards shelfal regions in regards to transgression throughout Late Tithonian time, especially towards the eastern margin near the Talisman field (Figure 3-11).

3.4.2.5 Late Syn-rift and Post-rift Successions (Berriasian to Valanginian)

A gradual decline of the rifting process and the introduction of gradual thermal subsidence commenced during this time (Jablonski, 1997). Reactivation of the earlier rift zone caused acceleration of Late Tithonian subsidence and the regional Tithonian transgressive event leading to a final submergence of the Rankin Platform. The commencement of Forestier Claystone deposition occurred during the *D. lobispinosum* biozone in the central and western regions of the Dampier Sub-basin. Coeval depositional fans continued to form off the eastern side of the sub-basin around the Talisman field (Jablonski, 1997) (Figure 3-12). Continued subsidence in combination with the transgressive Cretaceous sea lead to the deposition of the Muderong Shale and the later progradation of carbonate-dominated marine systems across the North West Shelf of Australia, which continued up to modern times (Young, 2001).

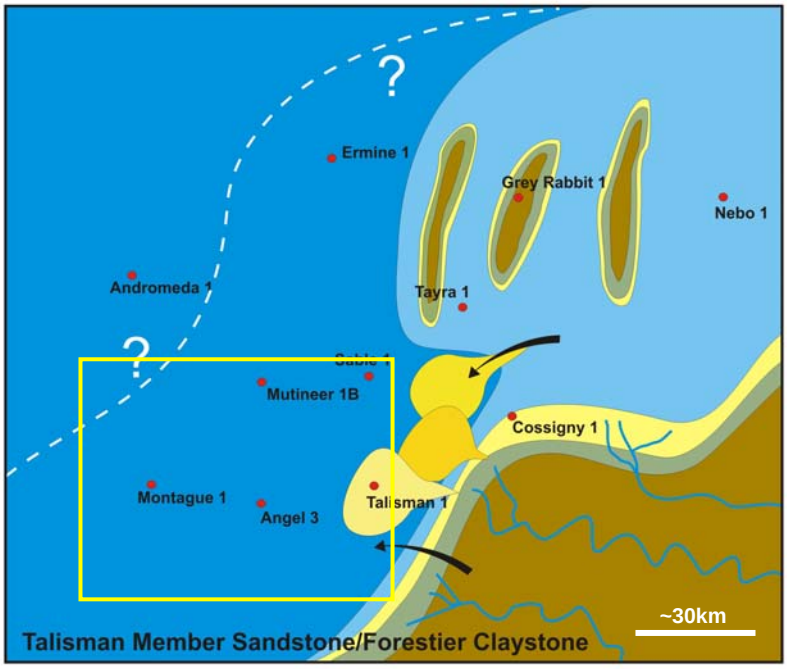

Figure 3-12: General palaeogeographical map depicting the retrogradation of basin floor fans towards the eastern margins (modified from Hocking, 1992; Miller, 1996; Stephenson *et al.,* 1998; Clark, 2006). Selected wells shown. Study area is yellow box.

4 Database and Methodology

4.1 Introduction

The project database contains a collection of cored intervals, well logs, image logs, palynological data and combination two dimensional and three dimensional seismic reflection data of varying vintages. A workflow of the project is represented in Figure 4-1.

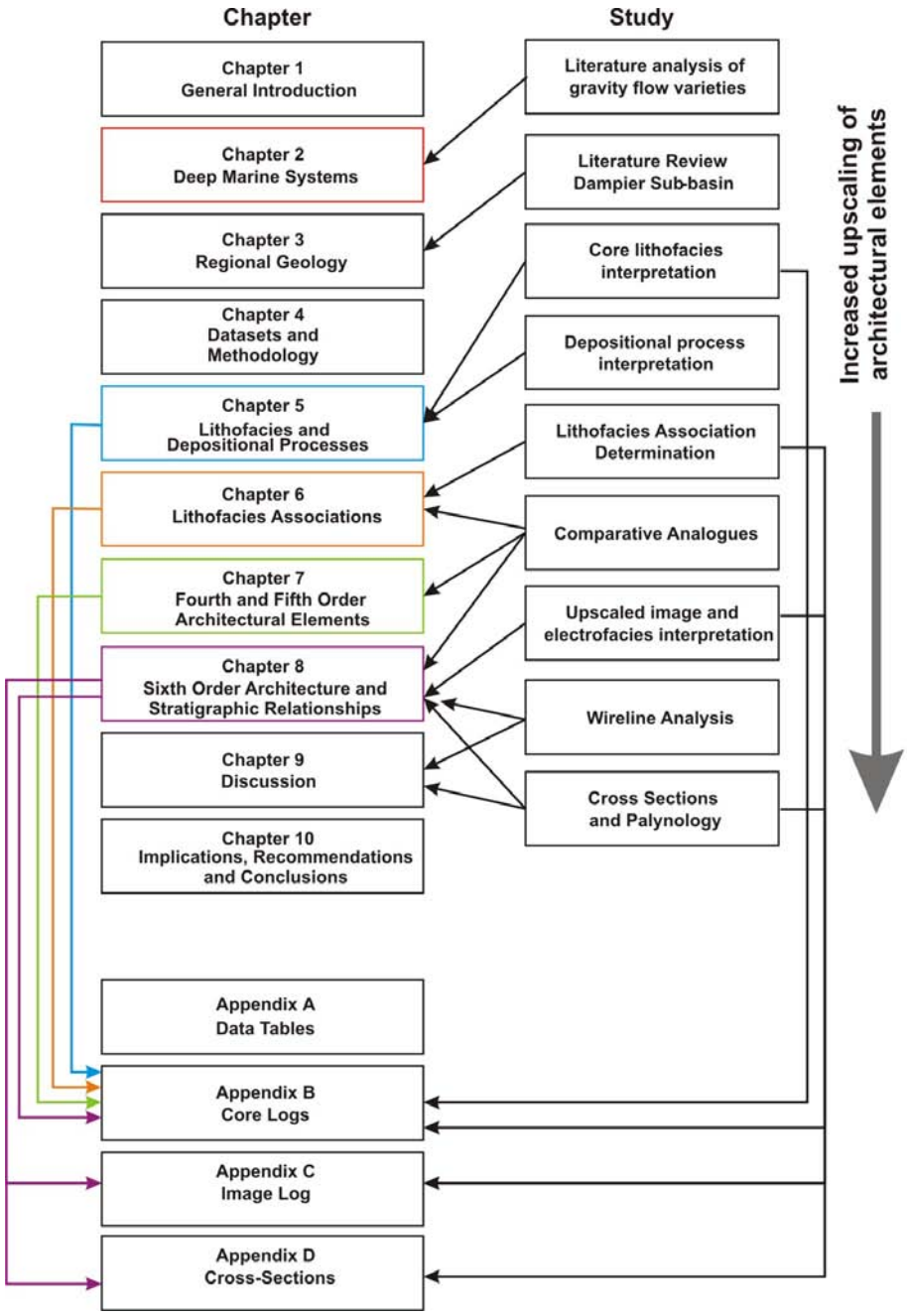

Figure 4-1: Workflow diagram of completed research. It highlights the work completed for the different chapters and how architectural elements are upscaled throughout the study.

4.2 Core Logging and Lithofacies Analysis

Eleven core intervals from the Tithonian Angel Formation were sedimentologically logged for this study. Cores were selected across the western and central regions of the Dampier Sub-basin (Figure 4-2). They totalled a core length of 547 metres (Appendix A). Individual cores came from wells that were drilled in order to discover hydrocarbon in the sub-basin. They were mostly drilled on structural highs identified on seismic. Cores were not available for Late Jurassic intervals in the Beagle Sub-basin. Ditch cuttings were not utilised as they do not preserve structure. A log chart highlighting the zones of core across all wells is represented in Figure 4-3.

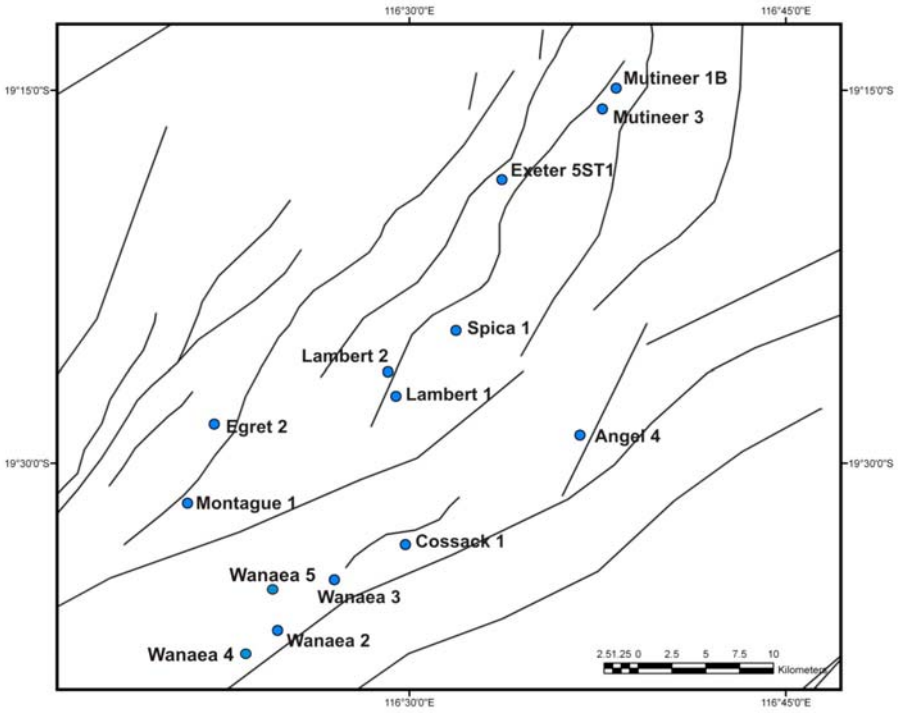

Figure 4-2: Location of viewed and/or interpreted cores. Core depths, thicknesses and recoveries are listed in Appendix A. Lambert-1, Wanaea-4 and -5 was viewed and photographed only.

Core logging was completed at the Western Australian Core Library in Carlisle, Western Australia and at the Santos Core Shed in Port Adelaide, South Australia during May 2005, November 2005, June 2006 and March 2007. Cores were logged at a high resolution centimetre scale of 1:25 allowing detailed logging of smaller scaled features. The logs were drafted in CorelDraw 12 on a template created for this research. The drafted logs are located within Appendix B.

Geological Survey of Western Australia policy states that cores comprising of ¼ or less of the original core volume could not be sampled to ensure future preservation. All cores except Exeter-5ST1 comprised ¼ sized cores hence no petrology work on lithofacies was completed.

The study of lithofacies and their associations was completed on the core to interpret the range of architectural elements present within the depositional system and to infer channelised versus unchannelised relationships.

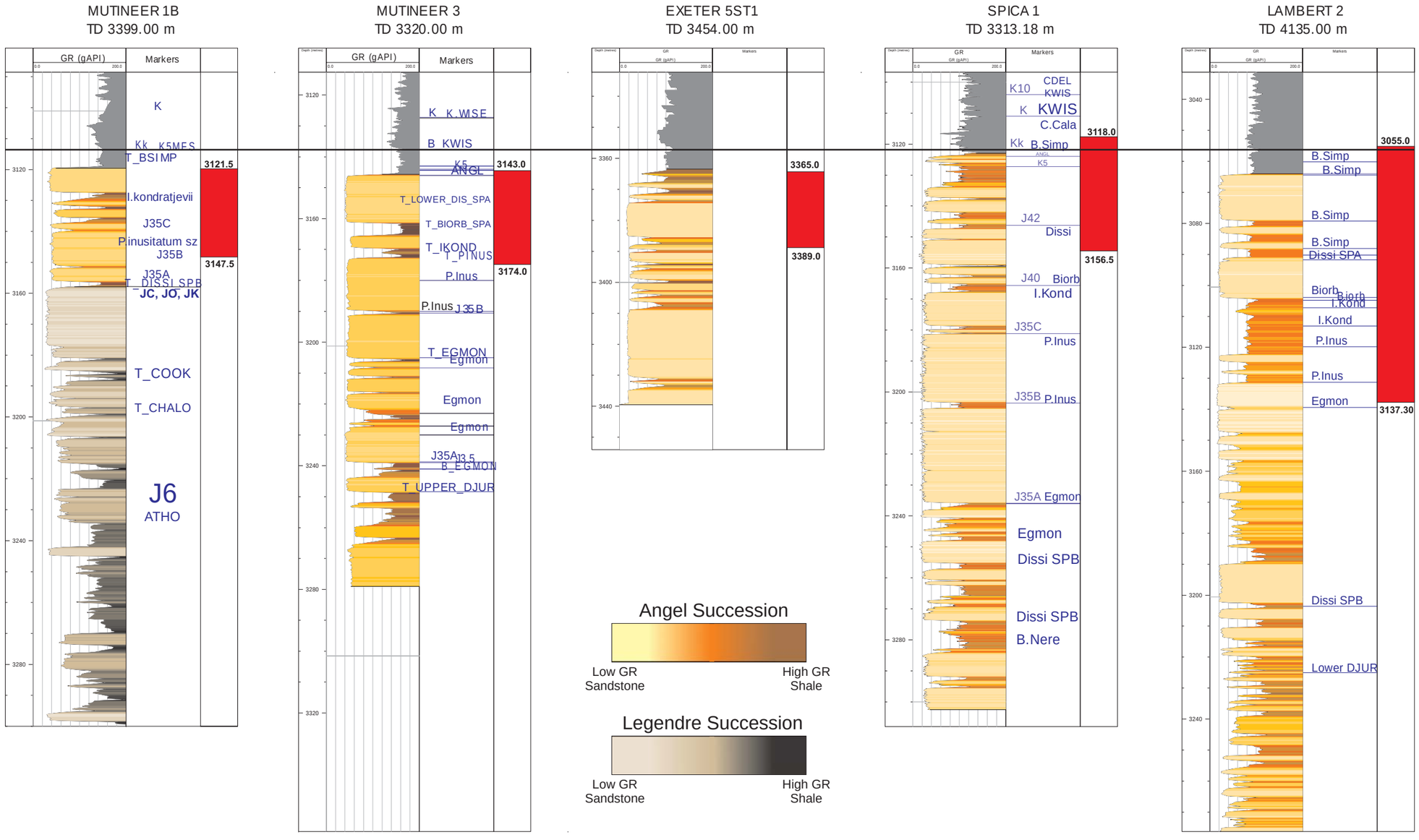

Figure 4-3 (continued next page)

Core intervals of all wells interpreted from western and central Dampier Sub-basin. Intervals represented by red columns. Section datum is the K5 maximum flood surface (K5MFS). Colours shaded based on GR and depth is in metres. Refer to Figure 4.2 for well locations.

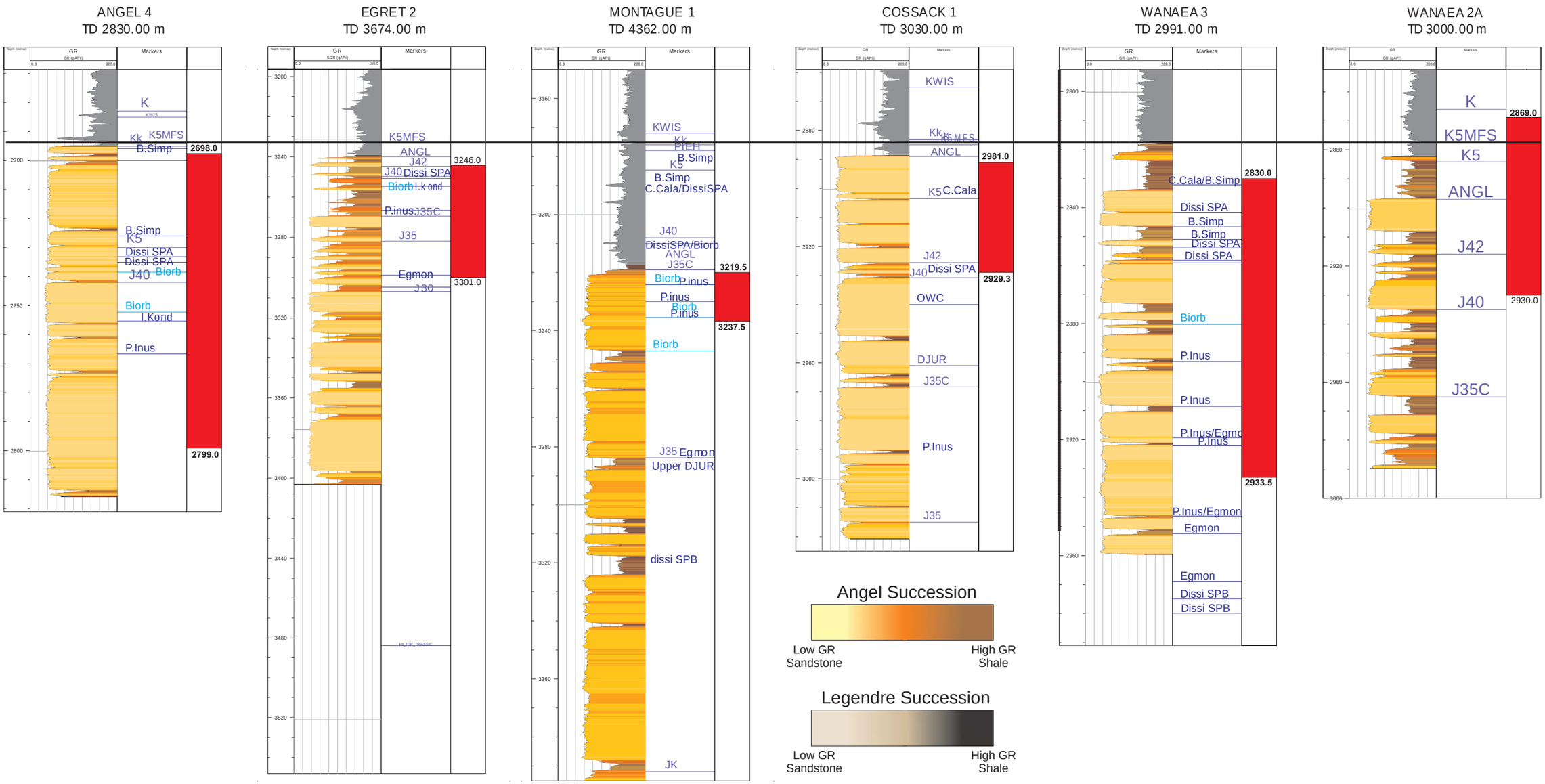

Figure 4-3 (continued from previous page)

4.3 Wireline Log Analysis

This research has concentrated on a database of 88 wells (Appendix A). The wells range in age from 1968 (Legendre-1) to 2005 (Exeter and Mutineer). Some wells were obtained from an original database supplied by Santos to the Australian School of Petroleum. Most were downloaded from the Western Australian Department of Industry and Resources website. A suite of wireline logs accompanies each well (Appendix-A).

All wireline logs were loaded into Geoframe version 4.0.4.2. Well data collected from the Western Australian Department of Industry and Resources website was loaded along with the relevant checkshot, deviation and marker data obtained from well completion reports. Well log data obtained from Santos was received in a project form compatible with Geoframe.

Wireline logs were used primarily to establish a wireline electrofacies classification representative of the reservoir fabric and architecture upscaled from lithofacies analysis. They were correlated with the core intervals. They were used to provide a basis for biostratigraphic interpretations across the basin and for the analysis of fan evolution in differing fields.

The conventional wireline suite was not normalized for this study as it was deemed unnecessary for the following reasons.

i. Good core to wireline correlations.

ii. All the investigated wells exist in the same basin.

iii. Turbiditic sandstones and heterolithics are typically blocky and not strongly variable in log character.

4.4 Image Log Analysis

Detailed sedimentological information can be obtained from image logs by using a sedimentological surface and image facies interpretation based on techniques published by Bourke (1992), Prosser *et al.,* (1999) and Bal *et al.,* (2002). Image log tools sample on average every 0.25 centimetres. This is a significant improvement again on the gamma ray tool where the sample window on the acquisition tool is considered to be around 15 centimetres (Rider, 1996).

Four image logs were available for interpretation from the study region (Mutineer-1B, Pitcairn-1, Bounty-2 and Spica-1). The data was deemed unreliable from Spica-1 (oil based mud), Pitcairn-1 (oil based mud) and Bounty-2 (poorly processed). The image log data from Mutineer-1B was of a high quality. The log was loaded into the JRS Petroleum Research in-house image log interpretation software. Though only one image log (Mutineer-1B) was of interpretative quality, a full surface and image facies classification was created and extrapolated across the log (Appendix C).

The range of sedimentological bedding surfaces classified and interpreted within the Mutineer-1B image log are highlighted in Table 4-1.

Table 4-1: Classification of sedimentological surfaces interpreted in the Mutineer-1B image log.

Code	Surface Description
EB	Erosive boundary
LB	Loaded boundary
PS	Parallel stratification
DL	Dewatered Lamination
WL	Disrupted wavy lamination
RB	Remobilised boundary (post-depositional)
ML	Lamination within siltstone and claystone
SL	Lamination within overlying regional seal siltstone (tectonic tilt)

4.5 Palynology and Biostratigraphy

A well established palynological framework for the Tithonian interval based on dinoflagellate assemblages exists over the Dampier Sub-basin. High resolution biostratigraphic data for the wells was collected from Santos for the Exeter and Mutineer fields and from open file well completion reports and open file palynological reports for other wells which were collected from the Geological Survey of Western Australia. The high resolution palynological information across the Dampier and Beagle Sub-basins ranges from poor to excellent. This study adheres to the updated Jurassic to Early Cretaceous dinocyst zonation chart for the North West Shelf of Australia (Helby *et al.,* 2004) (Figure 4-4).

Thirteen biostratigraphic cross sections were interpreted across the Dampier and southern Beagle Sub-basins in the Geology Office element of Geoframe by using a combination of Basemap, Composite and Cross Section modules (Appendix D). Palynological data was used to assist the interpretation. Palaeogeographical log motif maps for the differing study regions were created in CorelDraw 12 with reference to biostratigraphic sections.

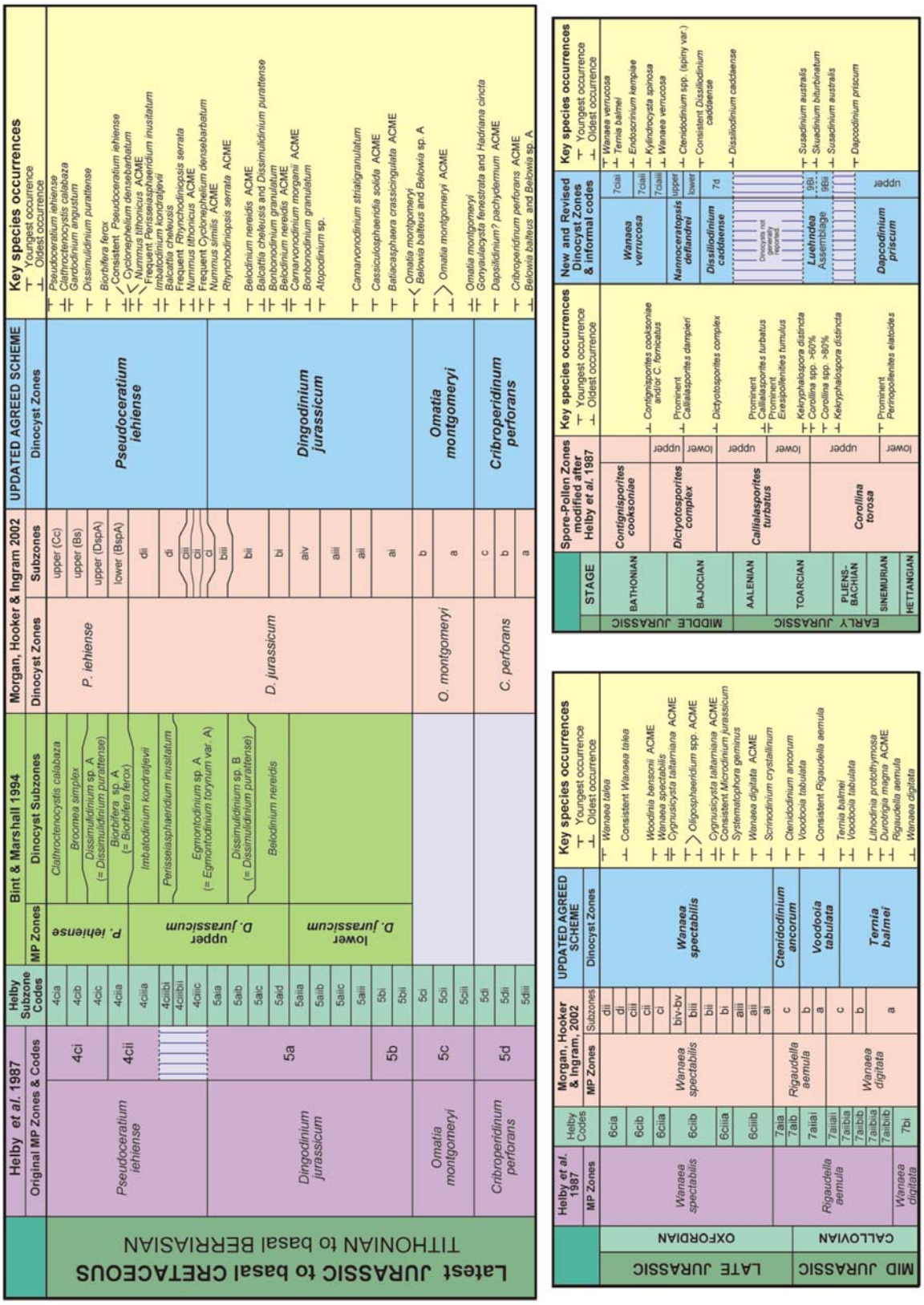

Figure 4-4: Updated dinocyst zonation for Jurassic to Early Cretaceous biozones on the North West Shelf of Australia (adapted from Helby *et al.*, 2004).

4.5.1 Regional Surfaces

A pre-existing classification of regional surfaces available for the Dampier Sub-basin was used for the biostratigraphic and palaeogeographic analyses (Table 4-2).

Table 4-2: Regional surfaces used in this study (modified from Longley *et al.,* 2002). The quoted biozone relates the approximate age of the surface (i.e. JT rests at the base of the *C. perforans* biozone).

Surface	Name	Biozone	Megasequence (Jablonski, 1997)	Event
JP1	Pliensbachian transgressive surface	Intra *D. priscum*	Early syn-rift	West Burma Block 1 separation
JC	Callovian Unconformity	Base *W. digitata*	Syn-rift 1	West Burma Block 2 rift onset
JO	Oxfordian Unconformity	Base *W. spectabilis*	Syn-rift 2	West Burma Block 2 separation
JK	Kimmeridgian Unconformity	Intra *W. clathrata*		West Burma Block 3 rift onset
JT	Tithonian Unconformity	Base *C. perforans*		West Burma Block 3 separation
K5-MFS	Top Tithonian Maximum Flood	Top *B. simplex* to *C. calabaza*	Late Syn-rift and Post-rift	Australia/India rift onset
K	Cretaceous	Base *C. delicata*		
KV	Valanginian Unconformity	Base *S. aerolata*		Australia/India rift breakup

4.5.2 Biostratigraphic Sub-Division

The architectural relationships of the fifth, sixth and seventh order architectural units and related palaeogeography is examined using biostratigraphic and seismic facies techniques on selected seismic and wireline sections (Chapter 8). The Tithonian interval of the Angel Sandstone was separated into a series of biostratigraphic units separated by claystones that are interpreted to represent datums across the region (i.e. Base *Wisemaniae* shale) (Figure 4-4). The claystones are correlatable through the use of palynology. This interpretation considers both autocyclic and allocyclic processes when interpreting claystones that may or may not indicate of flooding events. Each claystone pick may also not exactly correlate to the next claystone pick in a nearby well as removal of sediment through channelisation and erosion is common in deep marine settings. This

biostratigraphic inaccuracy is expected when working a compensationally stacked and coalescing sand-dominated fan system.

The interpreted depositional units used in the study include the (Figure 4-5):

- upper *P. iehiense* system;
- *Dissimulidinium* system;
- *Biorbifera* system;
- upper *P. inusitatum* system;
- lower *P. inusitatum* system;
- upper *D. jurassicum* system;
- lower *D. jurassicum* system, and;
- *O. montgomeryi* and *C. perforans* system.

Figure 4-5: Chart of biostratigraphic units and related palynology (adapted from Santos, 2004).

4.6 Seismic Reflection Data

The seismic reflection datasets represent a range of differing vintages and are found to overlap significantly. Over 105,000 line kilometres of seismic available from multiple surveys of differing vintages across the region of interest (Figure 4-6). The seismic dataset was supplied to The University of Adelaide by Santos.

Seismic reflection surveys not incorporated in this study include the 2003 Demeter 3D and the 2006 CVSN06 Mutineer Exeter 3D M.S.S. The CVSN06 Mutineer Exeter 3D M.S.S will remain confidential until 2012. The Demeter 3D survey became declassified in 2007.

The combined 2D and 3D seismic data was interpreted in the Geoframe seismic module IESX 2D/3D and Basemap module. The dataset was used primarily to map out the early rift basement structure preserved in the Early Jurassic and Triassic sediments. Tectonic structure was deemed essential to map in order to assess if it had control on Tithonian sedimentation. Fault systems were interpreted across the region using primarily a northwest-southeast traverse in line with the direction of Middle Jurassic extension. This traverse angle was interpreted to be the most optimal for the interpretation of structural features along the western and northern margins of the Dampier Sub-basin. The seismic dataset was not used to map high resolution stratigraphic packages due to two reasons.

i. The resolution at two seconds (depth to reservoir zone) is poor and high resolution features can not be mapped confidently over large distances. Only architectures in excess of 30 to 50m thick would be identifiable (Figure 4.7) and in addition to this, due to the sandy nature of the system, poor seismic impedance contrast would exist between sand-dominated channel and splays. Without decent contrast in seismic impedance, differentiating between these features and interpreting them would be impossible.

ii. The structural setting of the north-western Dampier Sub-basin has three structural trends with relays and splays. This includes the oblique nature of the Rankin Platform, the southeast-northwest extensional nature of the central Dampier Sub-basin and the wrenched east-west nature of the Beagle Sub-basin. As there is no one optimal trend for resolving faults of differing trends close to the Rankin platform and Beagle Sub-basin, the data acquired from the region is of a poor quality due to distortion.

The seismic dataset in many cases was used to determine the approximate location of formations on biostratigraphic sections that wells failed to intersect. This was achieved by converting two-way time values to depth mapped from the closest tied well. The checkshot data on some wells required occasional bulk shifting to the seismic dataset due to discrepancies between datasets at the University of Adelaide (seismic dataset in time) and Santos (seismic dataset in depth).

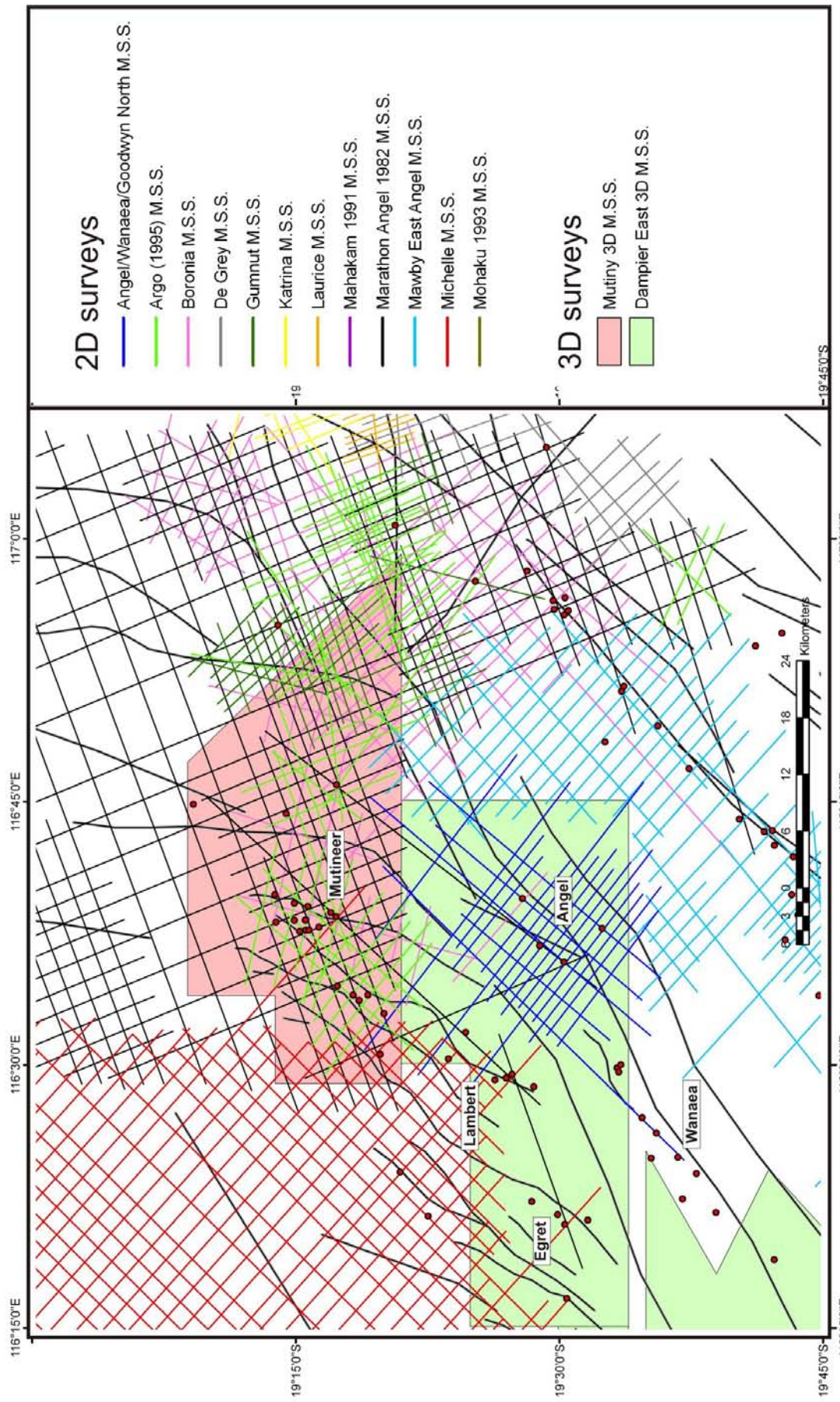

Figure 4-6: Seismic coverage available for this research over the Dampier Sub-basin and southern Beagle Sub-basin region.

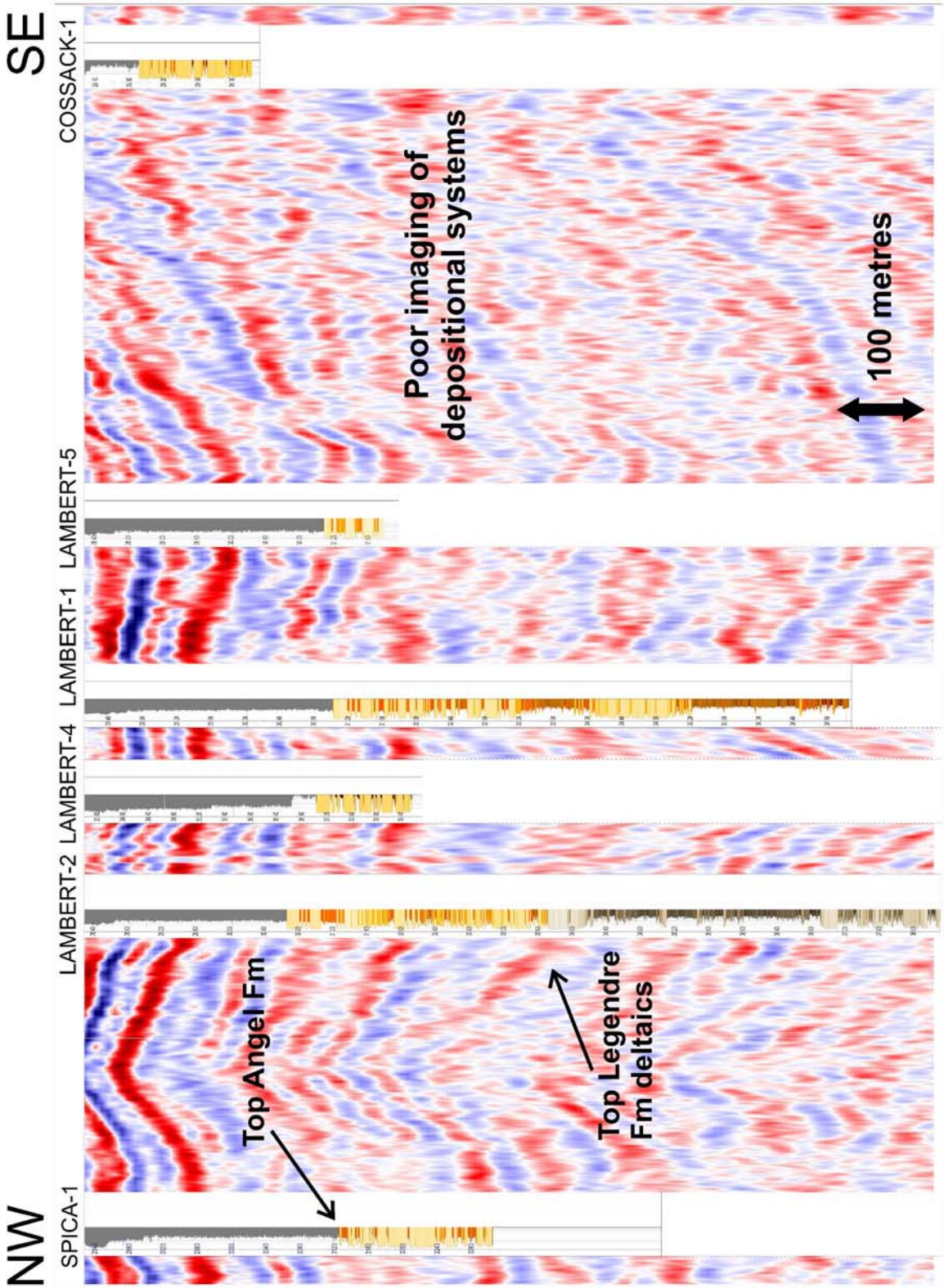

Figure 4-7: Composite seismic line from Spica-1 in the northwest to Cossack-1 in the centre of the basin. This composite line was generated on the Dampier East 3D survey.

5 Sedimentology and Lithofacies Analysis of the Tithonian Angel Formation

5.1 Introduction

The analysis of depositional lithofacies is essential for all subsurface geological studies. The recognition and depositional understanding of sedimentary lithofacies is imperative when determining the architectural uncertainties of a particular formation within a field or basin. A combination of sedimentological surfaces and lithofacies classifications are the architectural building blocks of the Angel deep marine system that can be further used in the determination of lithofacies associations and in the fourth, fifth and sixth order architectural analysis.

5.2 Sedimentological Surfaces

Sedimentological surfaces separate individual or amalgamated deposits of gravity flows. They can be deformed by post-depositional processes. The following varieties of sedimentological surface were identified in core.

i. An erosional surface is represented in core by sharp contact between two differing lithofacies and/or lithologies (Figure 5-1). It could represent bypass of gravity flow events.

ii. A conformable surface is also represented by often a sharp contact between two differing lithofacies and/or lithologies that are parallel to bedding. It represents deposition of gravity flow events with no significant loading occurring.

iii. A loaded surface is often represented in core by a loaded contact between two differing lithofacies and/or lithologies that is parallel to bedding. It represents active loading and deposition of gravity flow events. Flame structures are often observed (Figure 5-2).

iv. An injected surface is represented in core by a disconcordant contact between two differing lithofacies and/or lithologies inclined up to 50 degrees from the primary bedding surface (Figure 5-1). These inclined and bulbous contacts are interpreted to be the result of active fluidisation deforming and inflating the bedding contact. The bulbous nature of the surface can suggest that active injection into the overlying sediments was either close to occurrence or it had occurred laterally in proximity to the cored zone.

These surfaces were used in conjunction with lithofacies classifications discussed within this chapter to build and upscale architectural elements (Chapters 6, 7 and 8).

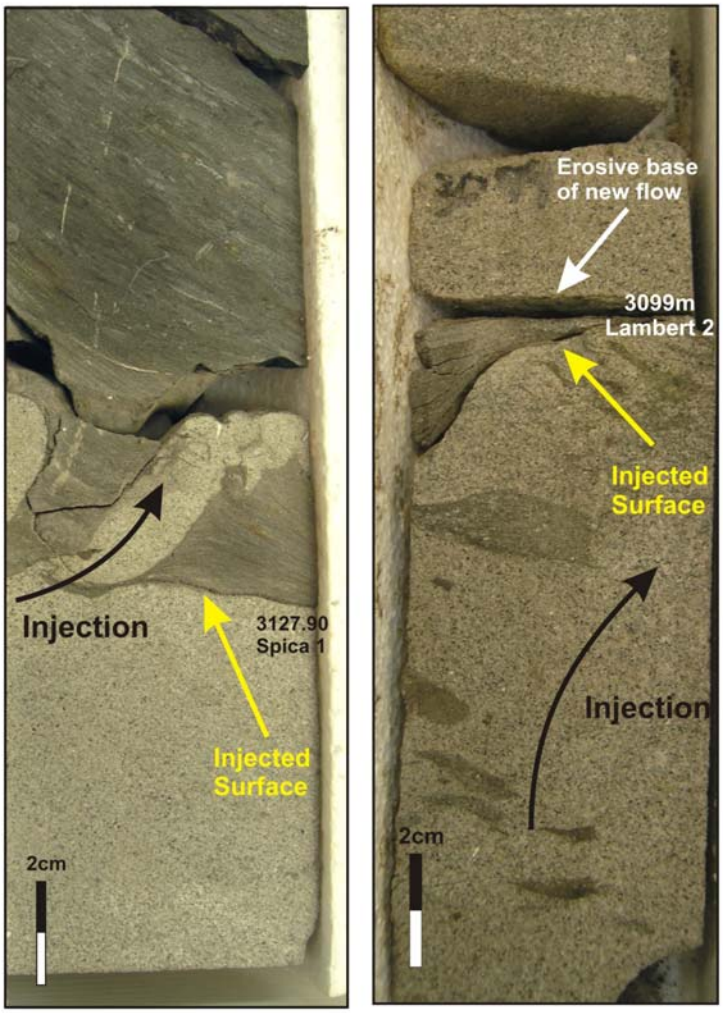

Figure 5-1: Injected and possible erosive surfaces from core (Spica-1 3127.90m and Lambert-2 3099m). Note the disconcordant nature of the upper surface and of the overlying mudstone in Spica-1 where sandstone has been forcibly injected upwards. In Lambert-2, an erosive surface has cut through the top of the injected and clast-bearing unit.

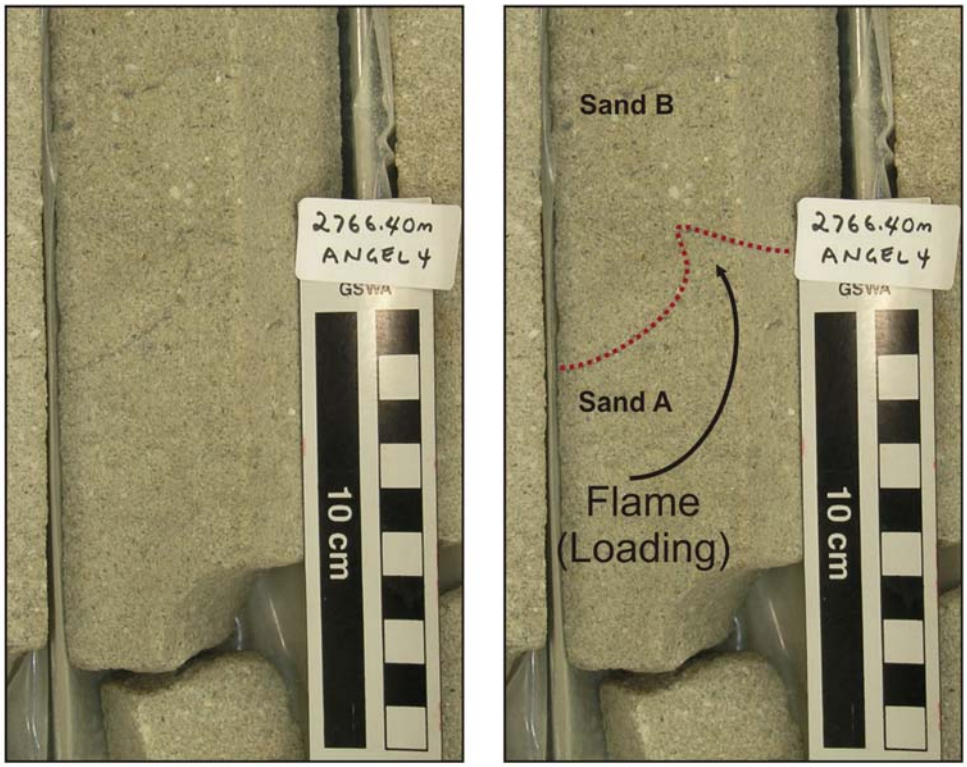

Figure 5-2: A loaded surface interpreted in core (Angel-4 2766.40m) representing an example of high density loading. Sandstone B, which deposited on top of Sandstone A, contains coarser grained material and is interpreted to be denser than Sandstone A, resulting in loading and the formation of a flame structure.

5.3 Lithofacies Classifications

Eleven lithofacies classifications were identified from core to fully represent the assortment of sedimentological processes that were active within the Tithonian deep marine system. They include both primary depositional and secondary remobilized and deformed lithofacies:

Facies A) Homogenous unstructured and parallel stratified sandstone

Facies B) Dish and pipe structured sandstone

Facies C) Clast-dominated sandstone

Facies D) Laminated sandstone

Facies E) Bioturbated heterolithics

Facies F) Structureless to laminated siltstone and mudstone

Facies G) Ptygmatic sandstones

Facies H) Deformed and sheared mudstone breccia

Facies I) Discordant sandstone bodies in sandstones and heterolithics

Facies J) Discordant sandstone bodies in mudstones

Facies K) Contorted sandstone

5.3.1 Homogenous Unstructured and Parallel Stratified Sandstone (Lithofacies A)

5.3.1.1 Description

This lithofacies is represented by intervals of homogenous sandstone that range from being structureless (Figure 5-3) and ungraded to displaying very faint flat to slightly inclined parallel stratification (Figure 5-4). The sandstones range from clear to light or olive grey coloured quartz arenite. Feldspars on average contribute less than 5% of the grain framework (Dubsky, 1999), which represents mineralogical maturity. The grain-size varies from fine- to medium-grained sandstone and the grain shape is typically well rounded to sub-rounded with occasional sub-angularity (Dubsky, 1999). Grain sorting ranges from poorly sorted to well-sorted with an average of moderately sorted (Figure 5-5). Greenish-black pelletal glauconite with concentrations as high as 15 – 20% dominate the accessory mineral index. Other accessory mineral assemblages include zircon, tourmaline, garnet, rutile and red spinel (Dibona and Scott, 1990) (Figure 5-3). Localised detrital clay is present (Dubsky, 1999).

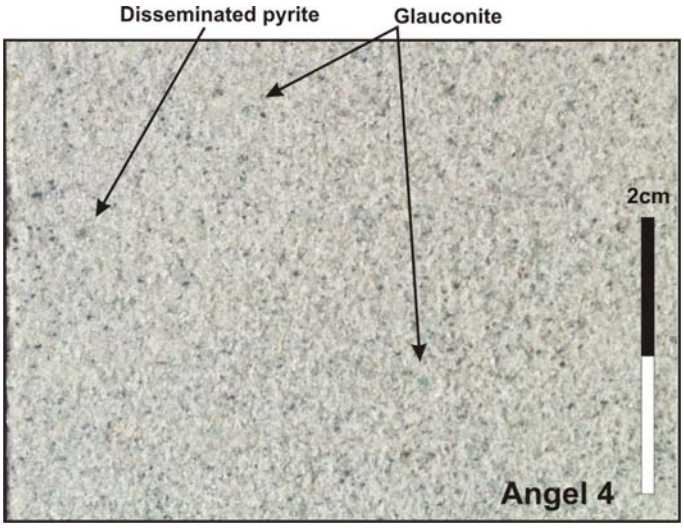

Figure 5-3: Homogenous structureless quartz arenite with visible accessory mineral assemblages that include glauconite and assorted heavy minerals. Patchy disseminated pyrite concentrations are also notable (above).

Figure 5-4: Faint laminae within sandstones from Angel-4 (A) and Mutineer-1B (B). They can encase sandstone units up to 10cm thick and are difficult to identify with the naked eye.

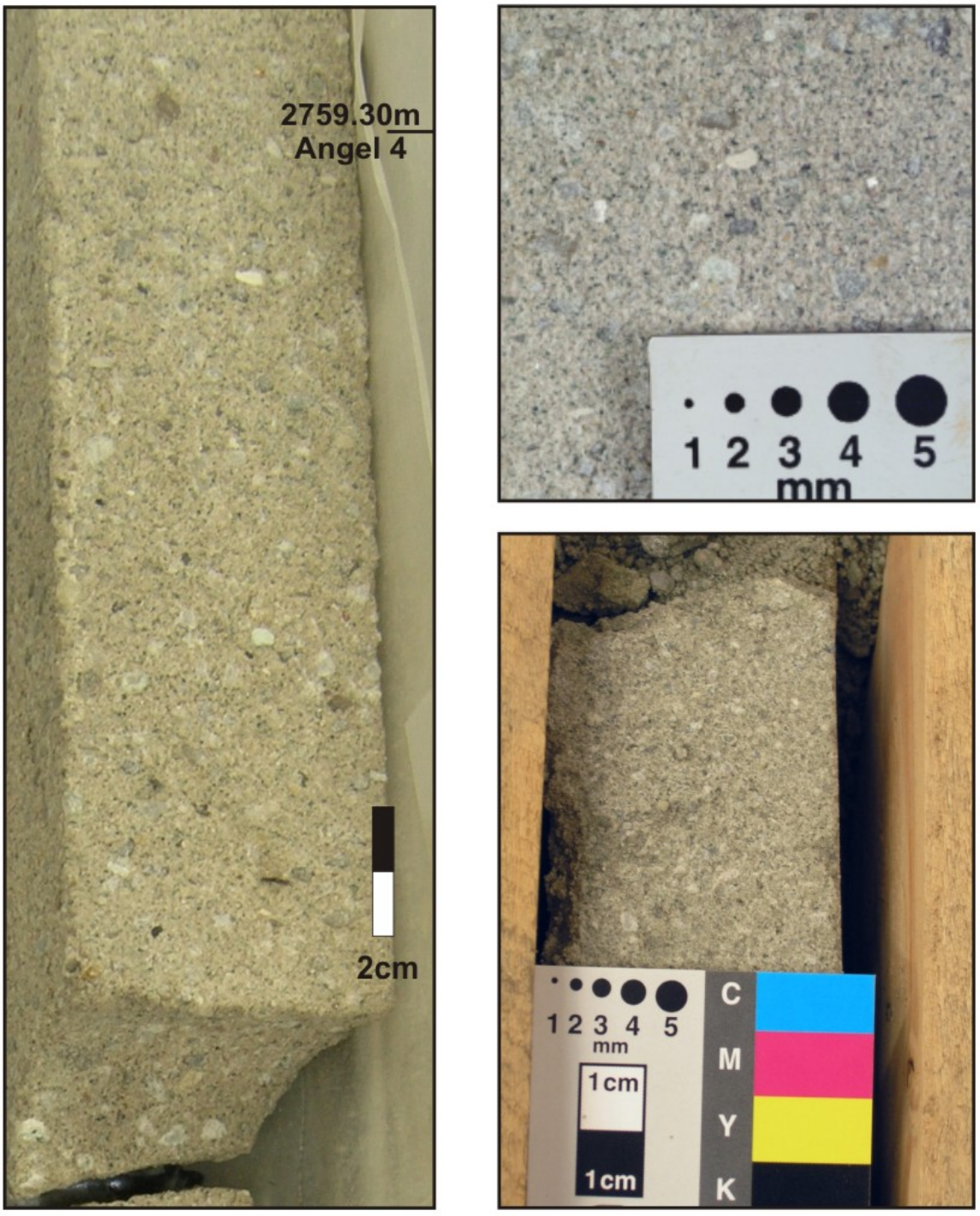

Figure 5-5: Coarse-grained poorly sorted units of Angel-4 (left and top right) and Lambert-1 (bottom right). They comprise of coarse-grained and granule-sized grains of quartz resting within a dominantly medium-grained sandstone matrix. These intervals have only been identified within Angel-4 and Lambert-1. They range from a few centimetres (Mutineer-1B, Mutineer-3, and Montague-1) to approximately one metre in thickness (Angel-4).

Cementation ranges from strongly cemented to completely friable indicating variations in cementation throughout the reservoir (Figure 5-6). Cement varieties include quartz, dolomite, siderite, pyrite (Figure 5.7). Disseminated pyrite cement is produced through the replacement of organic material beneath the sediment-water interface (Woodside, 1996) under euxinic conditions (Brown and Kenig, 2004). Later stage pyrite cementation is often created in conjunction with a palaeo-oil column (Santos, 1999, Ellis, 2006).

Figure 5-6: Friable intervals of core as discovered in Lambert-1 (left) and Montague-1 (right). Interpreting core for sedimentological structure proved practically impossible with core in this condition.

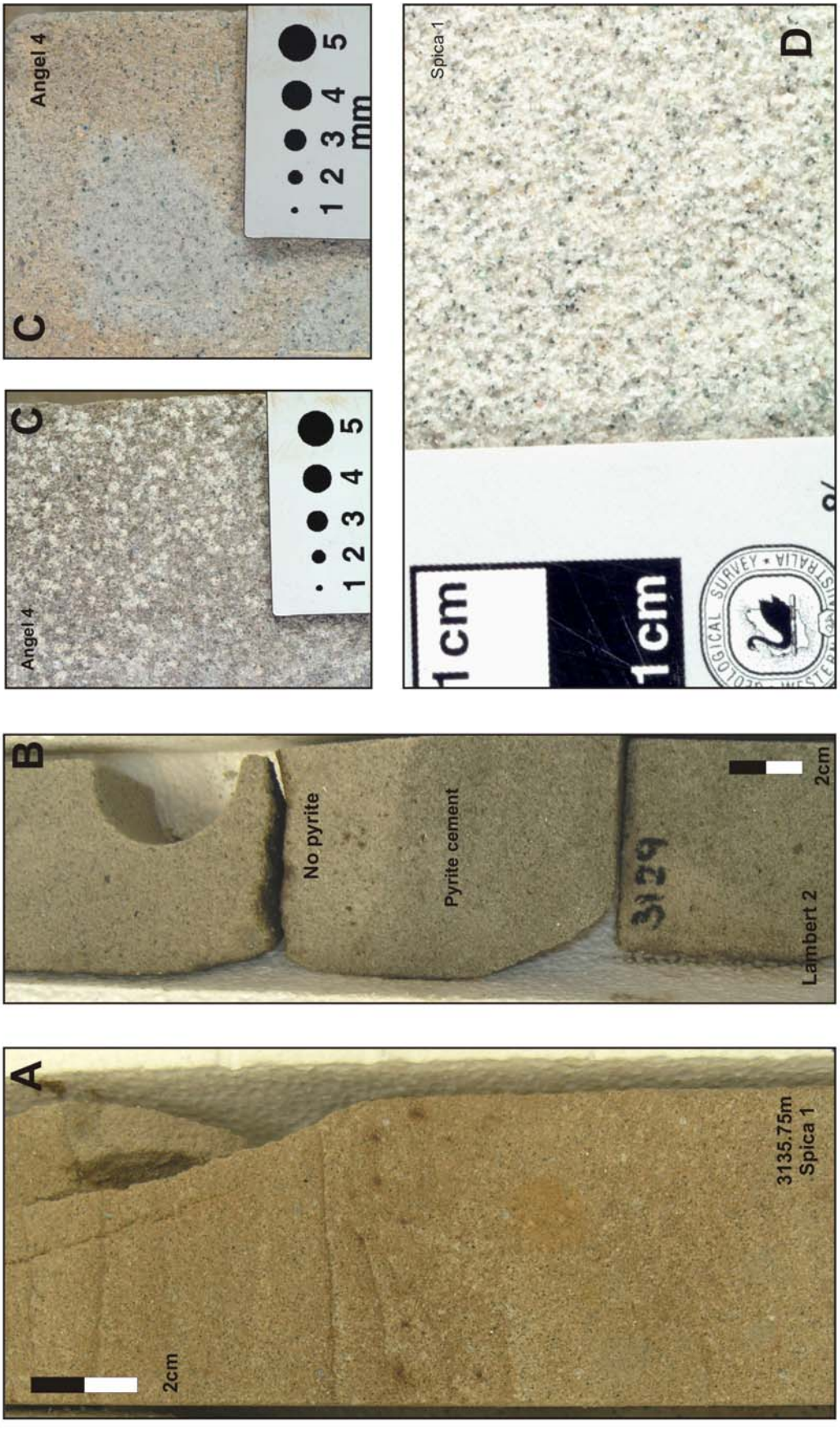

Figure 5-7: Siderite (A), disseminated pyrite (B), dolomite (C) and quartz (D) cementation recognisable within core. The boundaries between cemented and non-cemented successions are often sharp. The examples are from Spica-1 and Lambert-2.

Bioturbation is not common within this lithofacies. Ichnogenera could include *Ophiomorpha*, *Diplocraterion* or *Teichichnus* if a doomed assemblage from shallower water is interpreted (Figure 5-8). Other ichnogenera identified include *Zoophycos* (Figure 5-8). Burrows appear replaced by pyrite. Traces have been identified in Egret-2 and Lambert-2.

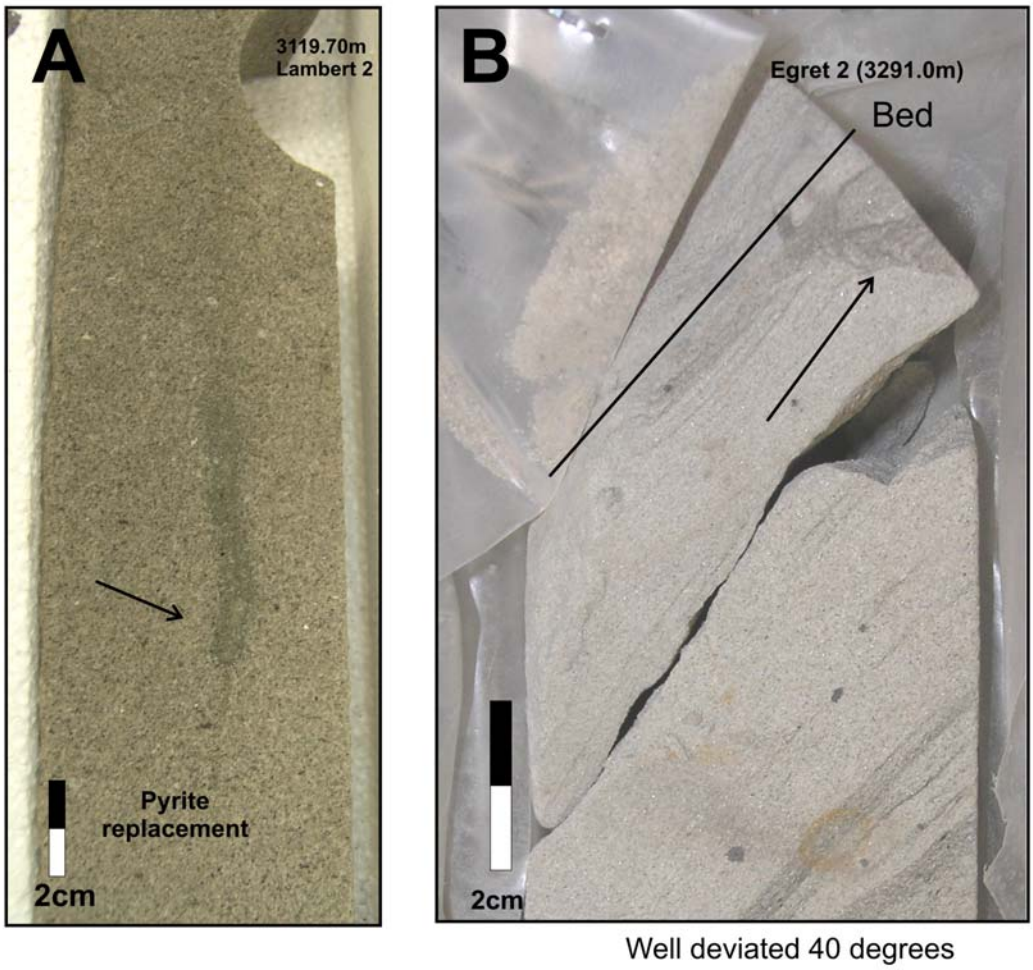

Figure 5-8: Identified examples of bioturbation within sandstone intervals. Figure A to the left could represent doomed *Ophiomorpha* or *Diplocraterion*. The trace in Figure B to the right may represent *Zoophycos*.

The visible parallel laminae are generally a few millimetres thick and appear grey in colour due to a thin layer of pyritic material (Figure 5-4). The thin units of sandstone they encase are generally ungraded to the eye but in rare cases, stepped grain-size variations (Figure 5-9) and vertical normal grading can be recognised (Figure 5-10).

This lithofacies typically forms amalgamated successions up to over 10 metres thick. They commonly vertically grade into dewatered or stratified sandstones of Lithofacies B and D.

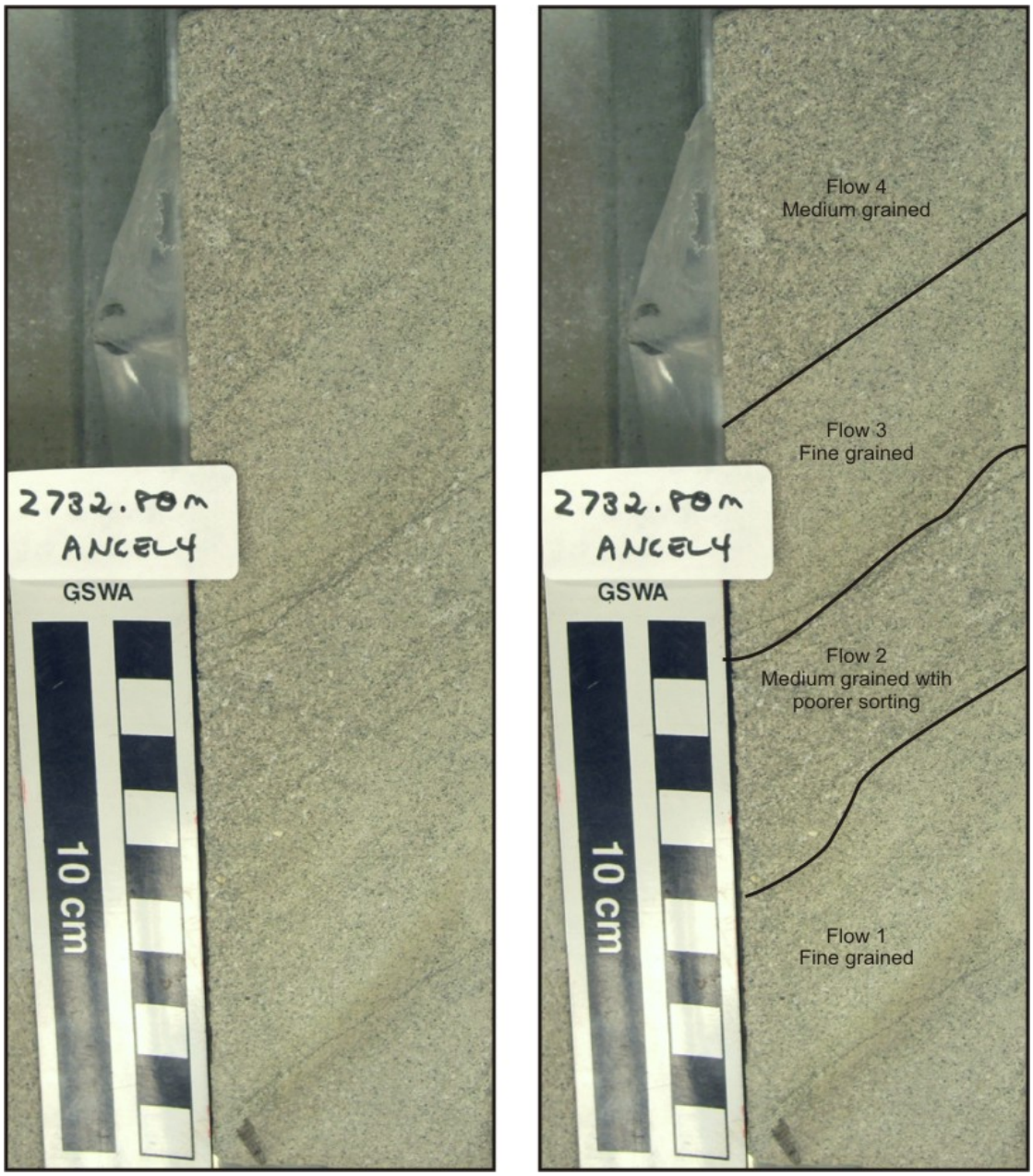

Figure 5-9: Stacked small turbidite events. Stacked 2 – 3 centimetre flow deposits display an overall stepped grainsize and sorting motif. The beds appear inclined and could be caused by injection-related processes (Angel-4 2732.80m).

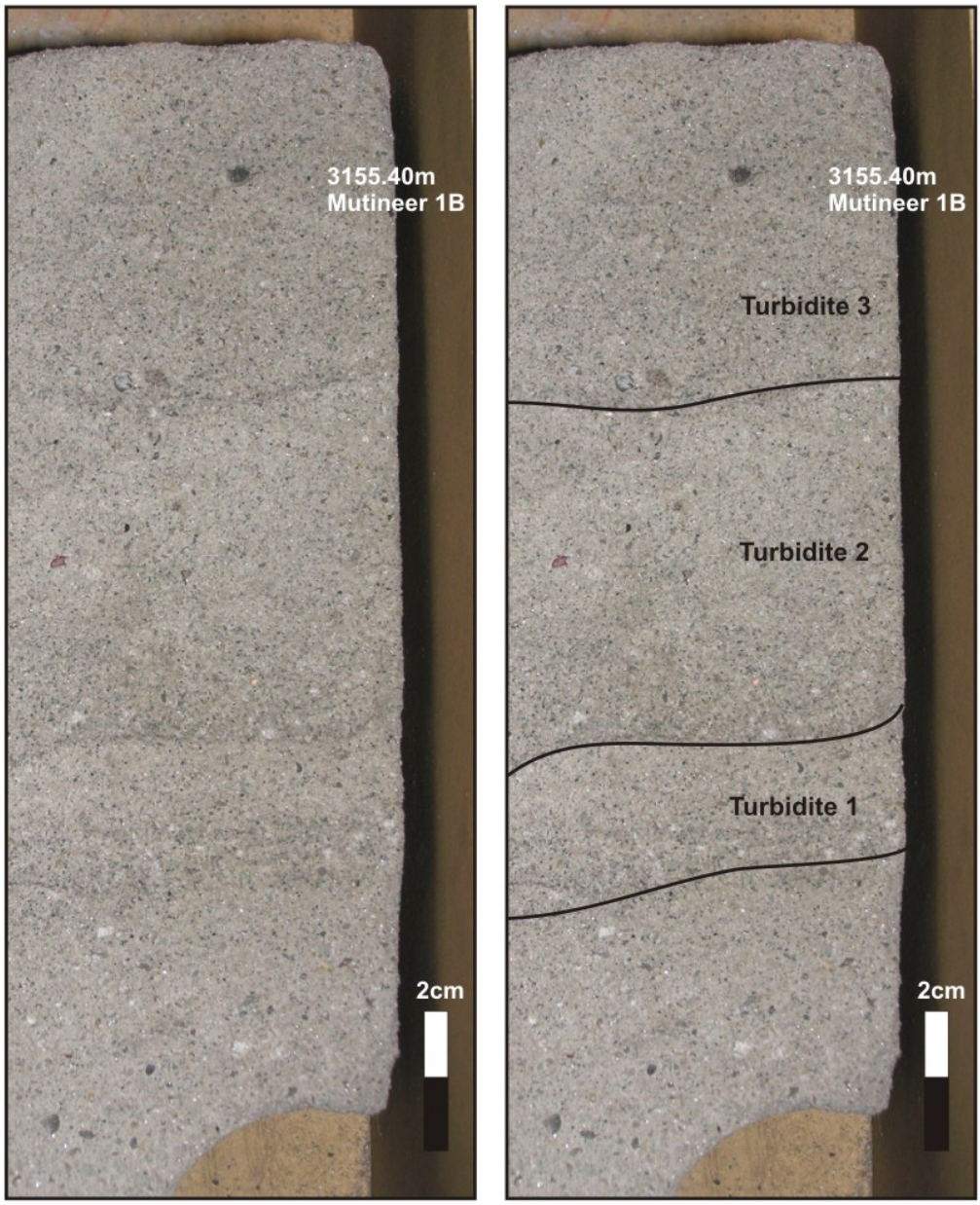

Figure 5-10: Example of stacked small scale turbidity flow events as identified in Mutineer-1B (3155.40m). Note the normally graded packages. This unit could also represent surges within the flow event.

5.3.1.2 Interpretation

The sandstones of Lithofacies A could be described as being deposited through one of three processes.

i. 'En-masse freezing' of a hyperconcentrated or concentrated density flow event situated within a proximal setting (Mulder and Alexander, 2001).

ii. Continuous aggradation of sediment into the basal laminar component of a sand-dominated high density turbidity current (steady or quasi-steady) over time. As the flow event slows and becomes depletive, the flow boundary will migrate upwards within the flow event due to the

high downward flux of grains into the concentrated laminar base and because turbulence is suppressed by the high sediment concentrations that exist close to the bed. Deposition occurs from the base upwards resulting in the gradual aggradation of the deposit (Kneller and Branney, 1995).

iii. Collapse fallout of a high density turbidity current as it loses momentum, becomes unstable and rapidly deposits. This can occur where flows meet a change in slope gradient or a topographic obstruction or where confined flows exit a confined system and expand laterally (Stow and Johansson, 2000).

The rare stepped and normally graded grain-size variations between laminae are best interpreted to represent deposits of small aggradational turbidite events. Each lamination and grainsize variation could represent the boundary between differing depositional events. Tractional features are rare. A poor level of sorting identified in Mutineer-1B (Figure 5-10) suggests that the stacked units represent small stacked turbidites. Another interpretation to this is the process of surging where, within a single aggradational flow event, it can produce a similar structured zone (Lowe, 1982). Surging flows are interpreted to represent an oscillating decline in flow velocity, resulting in repetitions of grading and structured divisions (Lowe, 1982).

Recognised ichnofacies within the sandstones could be interpreted to represent doomed pioneer assemblages that were deposited downslope within flow events sourced from shallower marine settings.

Later stage bedding parallel stylolitization is interpreted to have selectively picked bedding contacts in which to propagate (Figure 5-11). This variety of stylolitization represents bedding plane-normal compression with burial (Baron and Parnell, 2007) and could represent a major source of silica for sandstone cementation.

Flows are interpreted to be voluminous in many cases, resulting in the formation of upright clasts (Lithofacies C). There is only one example that can be interpreted as a sandy debris flow deposit (Angel-4 Figure 5-24) however it is alternatively interpreted as a large and confined stratified flow event rather than a sandy debris flow as suggested by Shanmugam and Moiola (1995).

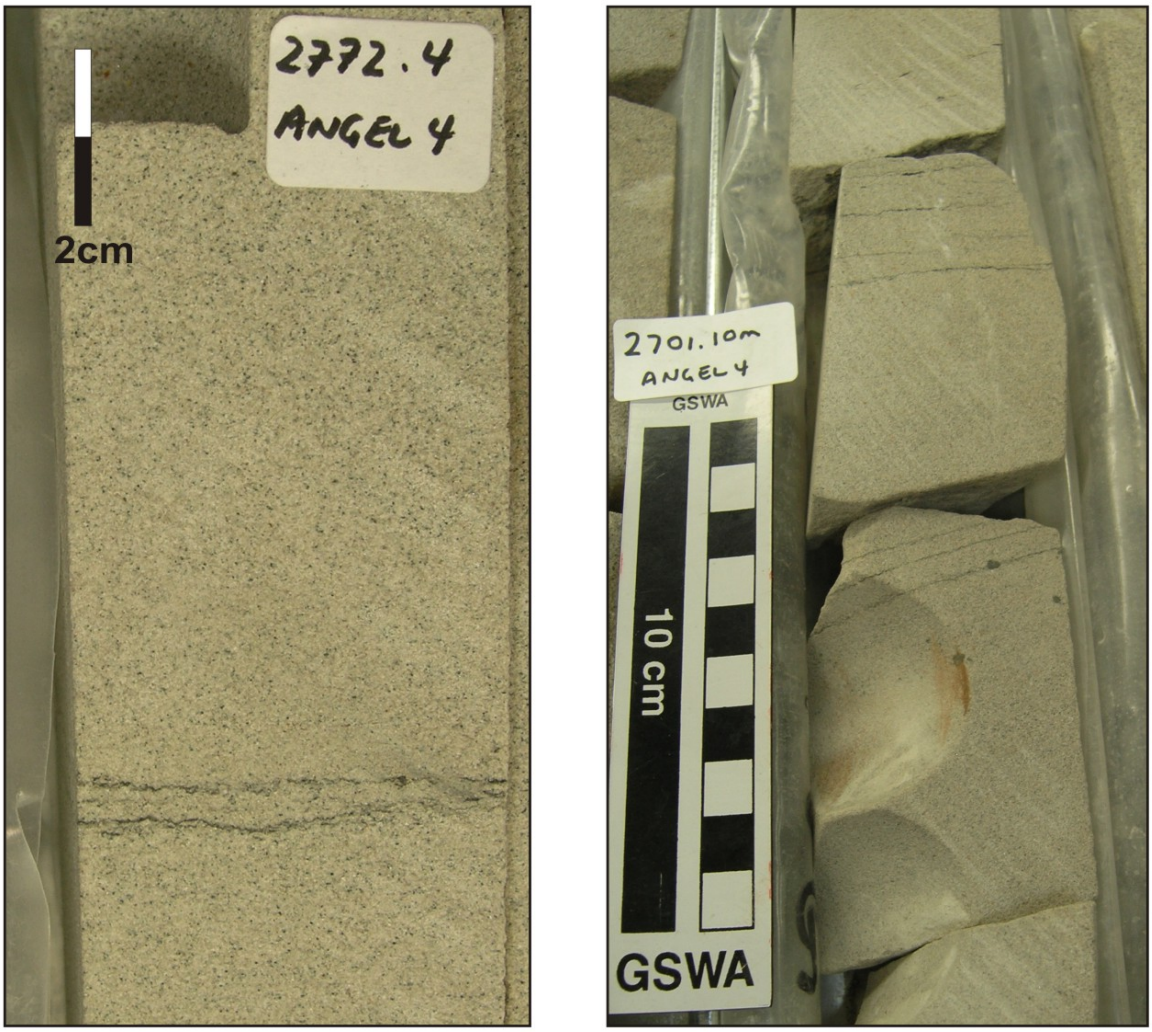

Figure 5-11: Styolite formation in Angel-4. Styolites are visible through concentration of pyritic material. They are interpreted to propagate along bedding surfaces (Baron and Parnell, 2007).

5.3.2 Dish and Pipe Structured Sandstone (Lithofacies B)

5.3.2.1 Description

Dish structures are recognisable by thin dark coloured sub-horizontal to concave upward laminae that rest within a cleaner sandstone backdrop. They are commonly underlain by a very clean sandstone division approximately 1 centimetre thick. Individual dish structures range from being weakly to strongly concave in character (Figure 5-12) and can form successions ranging from 10 centimetres up to up to 8.5 metres thick (Wanaea-2A and 3). Pipe structures, like dish structures, contain cleaner sandstone than the host sandstone. They are lined by dark finer grained argillaceous material that is often pyritised. They are typically vertical to sub-vertical in orientation and can be up to 10 centimetres long (Figure 5-12).

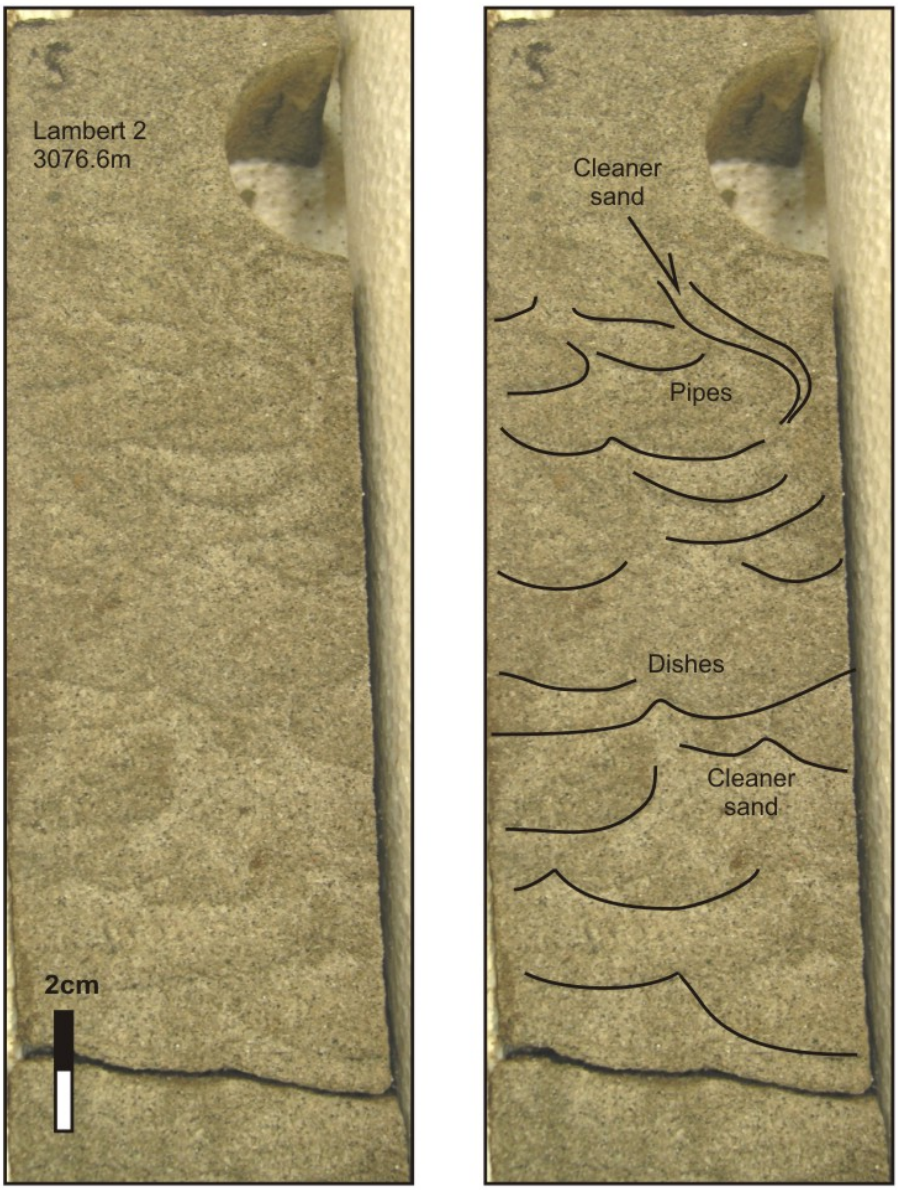

Figure 5-12: Standard example of dish and pipe structures. Dishes comprise of sub-horizontal to concave upward trending laminae overlying cleaner sandstone (fluidised zone). Pipe structures are sub-vertical in orientation and also contain clean fluidised zones.

5.3.2.2 Interpretation

The surfaces that define a dish structure are represented by a planar concentration of interstitial clay which has been pyritised. Laminae are formed when vertically escaping water from rapidly depositing sands encounter a less permeable flow boundary, causing the water to travel laterally until an area of appropriate permeability is located for vertical water escape to continue (Lowe, 1975). The dark lamination is created by fine sediment and low density grains being filtered out and concentrated within the sediment pore spaces of the less permeable flow boundary (Lowe and LoPiccolo, 1974). The clean zone beneath a lamination is interpreted as a horizontal flow path or fluidisation channel (Lowe and LoPiccolo, 1974) (Figures 5-4 and 5-13). The degree of concave shape of a dish structure and the transition from flat laminae to dish structures to pipe structures is interpreted to be related to the amount of water being expelled from underlying sandstone units.

Figure 5-13: Lithofacies B consolidation surface with clear fluidisation channel formation underlying the laminar concentration of intestinal clays and probable organic material (that later becomes pyritised) (A). When the fluid beneath the consolidation surface breaks free, a pipe feature can result (B).

Dish and pipe structures of the Angel Formation are classified as primary structures as they are interpreted to have been created through the stacking and dewatering of rapidly depositing flow events. This is evident as the dish and pipe structures do not cross cut other dish and pipe structures or any other primary structure. The succession of dewatered structures within the Angel Formation is similar to those identified in other similar unstructured and homogenous sandstone bodies that are typically greater than 50 centimetres and over 1 metre thick (Stow and Johansson, 2000).

Depositional patterns are identifiable within the dewatered sandstone successions. A typical succession is represented by sub-horizontal laminae (Lithofacies A) at the base that grade upwards into a succession of dish structures which further grades up to a succession of pipe structures (Figure

5-14). They are classified into categories based on a model derived from Lowe and LoPiccolo (1974) that was improved by Stow and Johansson (2000) (Figure 5-14).

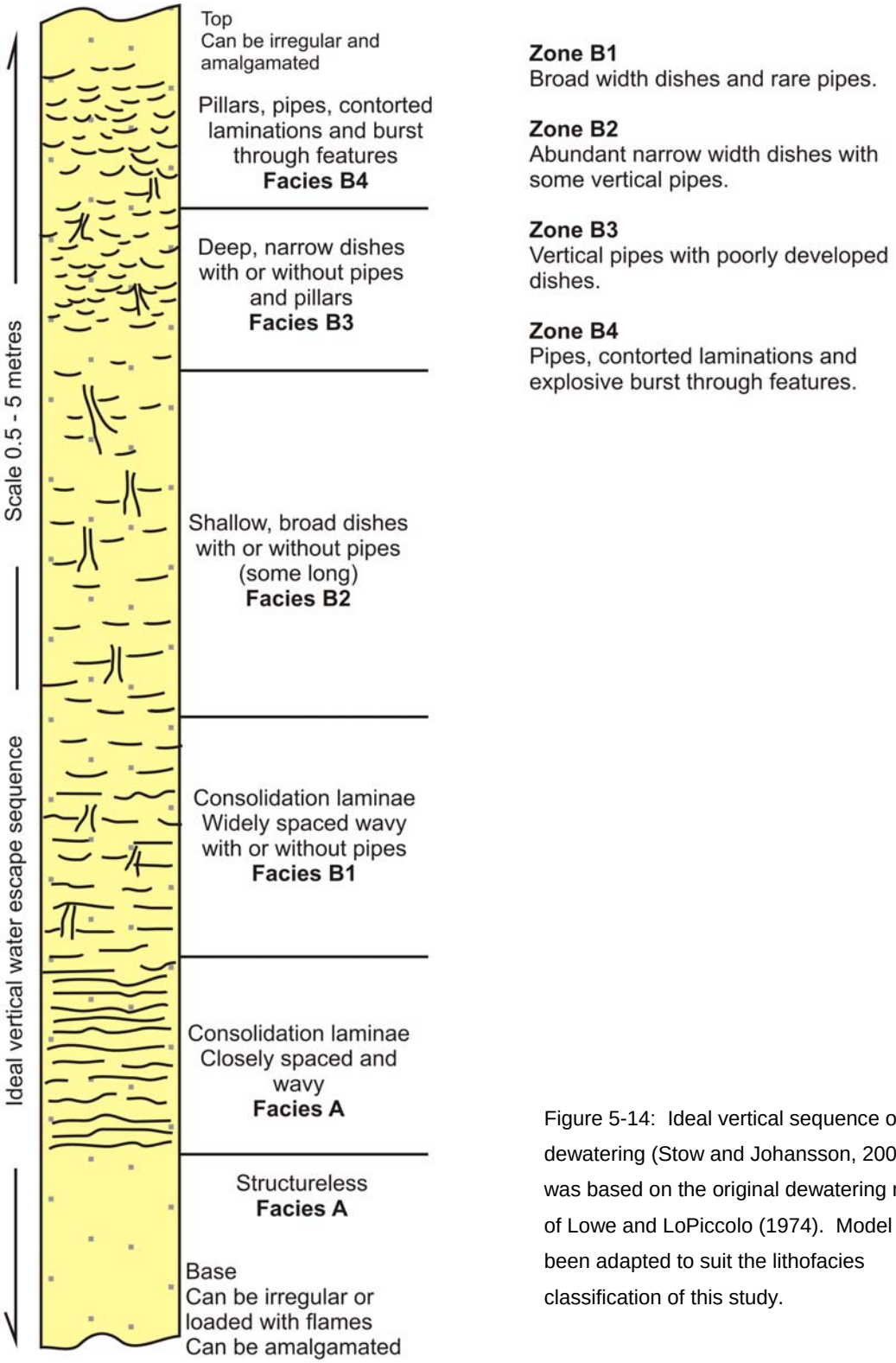

Figure 5-14: Ideal vertical sequence of dewatering (Stow and Johansson, 2000). It was based on the original dewatering model of Lowe and LoPiccolo (1974). Model has been adapted to suit the lithofacies classification of this study.

Examples of dewatered sandstones with visible dish and pipe-structured sandstones are illustrated in Figures 5-15, 5-16, 5-17, 5-18 and 5-19. They can form amalgamated packages with unstructured and faintly structured sandstones of Lithofacies A being overlain by stratified sandstones of Lithofacies D (5-15, 5-16 and 5-17). Post-depositional deformation can destroy these features resulting in fluidised upper contacts and the formation of post-depositional rip down clasts (Lithofacies H) (Section 5.5.2) (Figure 5-19). There is a recognisable relationship between intervals of dewatered sandstone and siderite cementation. This relationship can be simply explained by the presence of organics in the successions.

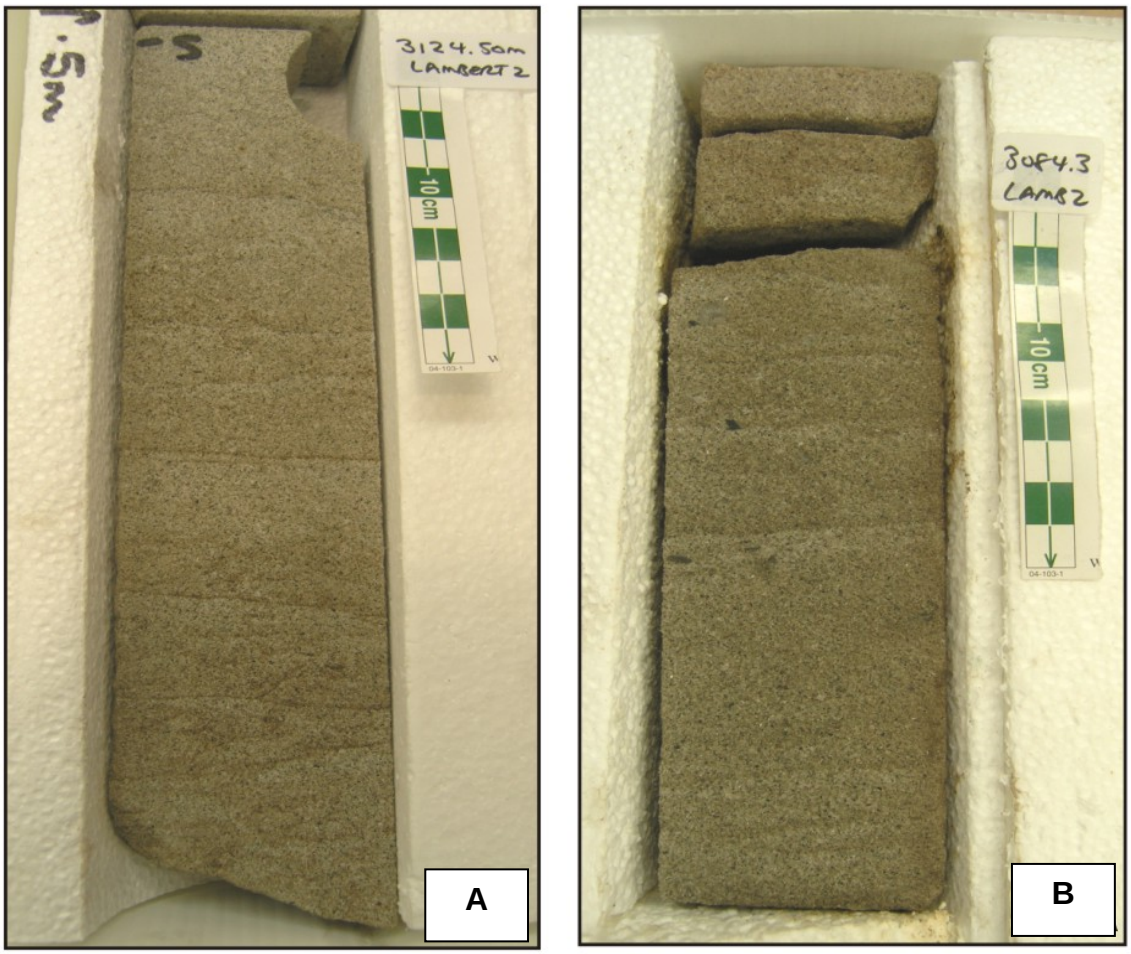

Figure 5-15: Early stage dewatering processes from Lambert-2. Figure A represents early stage consolidation surfaces with clear horizontal fluidisation channel formation (Lithofacies A). Figure B represents Lithofacies B1 grading up to B2 with wavy slightly inclined consolidation surfaces grading upwards to shallow broad dishes.

Figure 5-16 (above): Widely spaced wavy consolidation laminae (Lithofacies B1) grading up to deep narrow dish structures with associated small pillars (Lithofacies B3) from Spica-1.

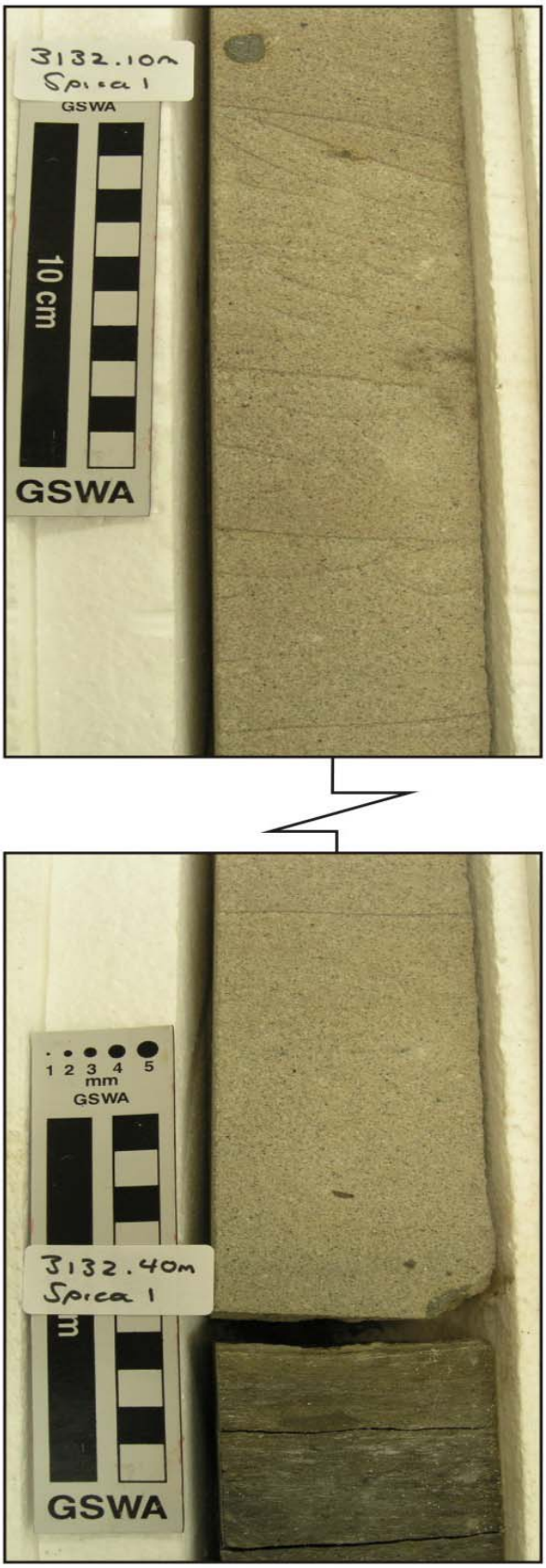

Figure 5-17 (right): Vertical succession from a structureless base (Lithofacies A) through to wavy consolidation laminae and shallow dishes of Lithofacies B1 from Spica-1.

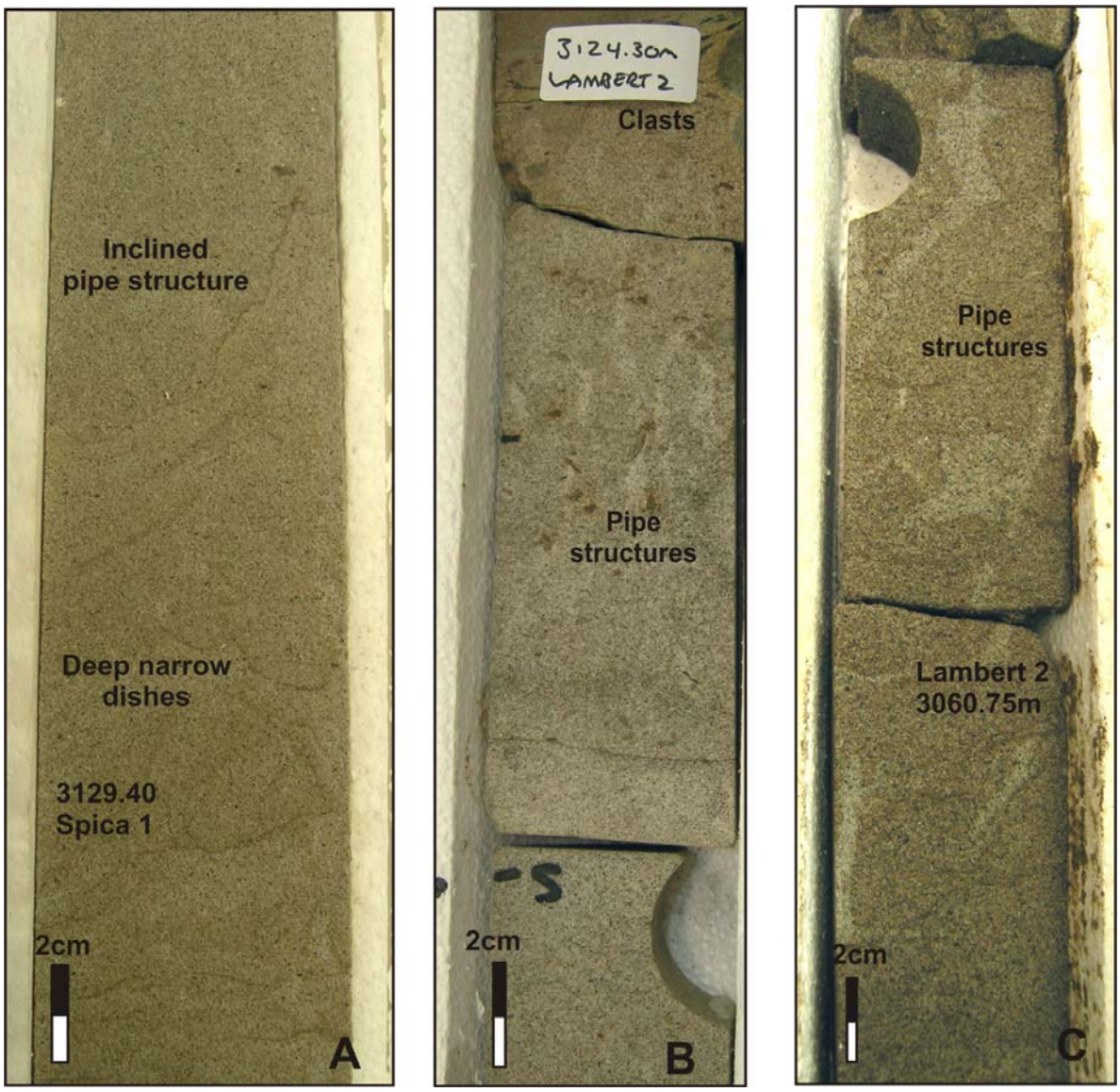

Figure 5-18: Vertical and inclined pipe features within sandstones from Spica-1 and Lambert-2. Figure A represents deep narrow dishes of Lithofacies B3 grading vertically to pipe features of Lithofacies B4. Figure B demonstrates small scale pipe features with visible fluidisation channel formation. They overlie consolidation surfaces of Lithofacies A. Figure C represents larger-scale pipe features with noticeably clean internal fluidised zone.

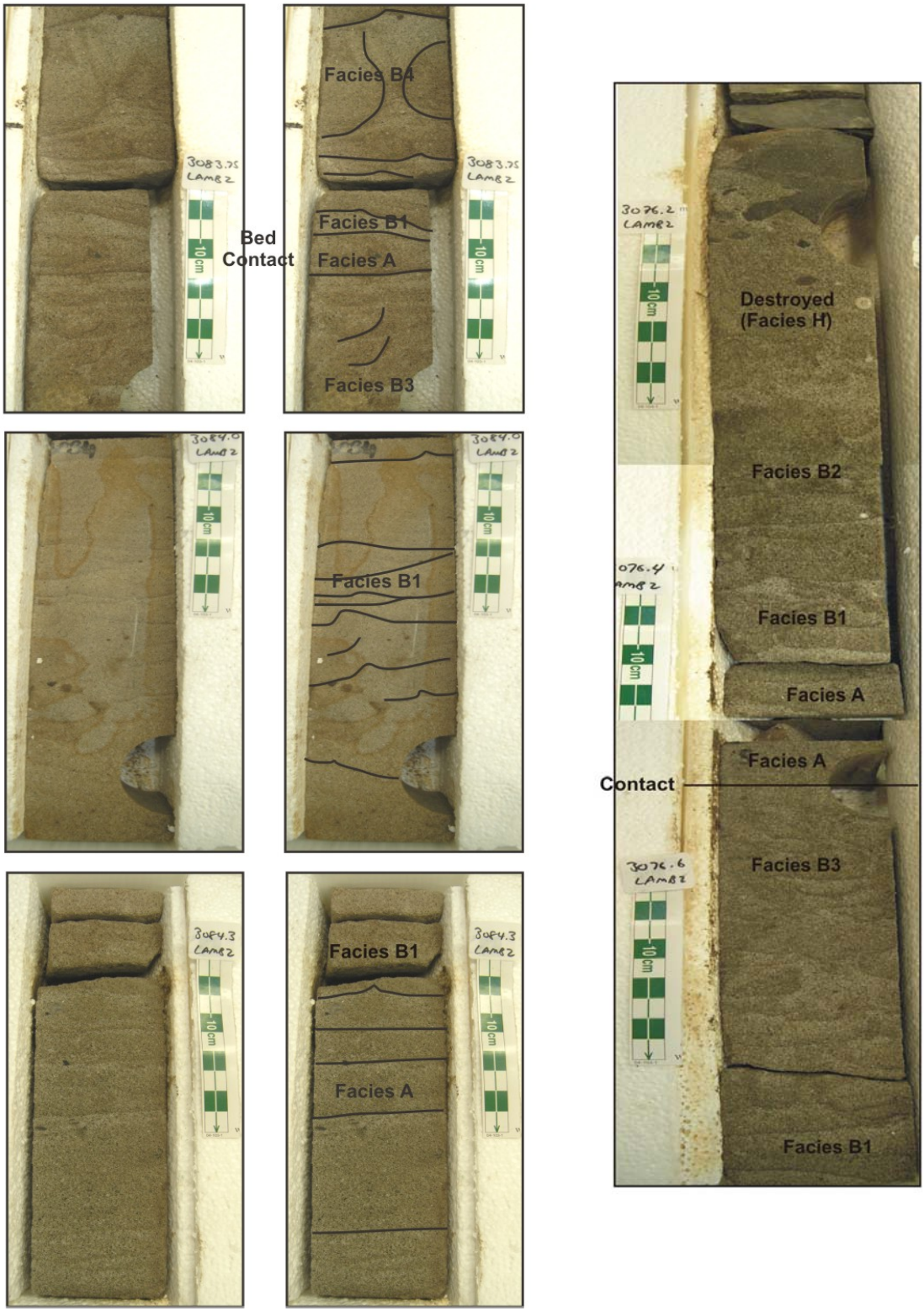

Figure 5-19: Vertical successions of dewatering identified in Lambert-2. They can display in the lower bed (left) a transition from laminae of Lithofacies A through to deep narrow dishes with associated pipe structures of Lithofacies B3. A bedding contact at 3083.80m results in the commencement of a new dewatering succession within the upper bed, complete with a flame feature. On the right, a bedding contact represents the commencement of a new succession. The very top of the second succession has no preserved sedimentological structure. It is interpreted to have been destroyed by post-depositional fluidisation.

5.3.3 Clast-Dominated Sandstone (Lithofacies C)

This lithofacies represents mudstone- and sandstone-dominated clasts that are formed through depositional processes. They differ to the clasts that are formed through post-depositional or linked debritic processes (Lithofacies H).

5.3.3.1 Description

Mudstone- or siltstone-dominated depositional clasts range in size from one to ten centimetres in size and are commonly found with the long axes tending towards flow-parallel and bed-parallel orientations. They are identified within homogeneous unstructured sandstone units of Lithofacies A. They can be found as either single isolated clasts floating at a mid bed position within homogenous sandstones (Angel-4) (Figure 5-20) or can be concentrated along the basal contact of sandstone units (Mutineer-1B and Exeter-5ST1) (Figure 5-21 and 5-22).

Figure 5-20 (left): Isolated mudstone clast identifiable within Lithofacies A. The rounded nature of the clast suggests reworking within the flow body.

Figure 5-21 (right): Small basal ripped up clasts identified in Mutineer-1B. Many have been replaced by pyrite.

5.3.3.2 Interpretation

Depositional clasts are incorporated into a flow event through erosion. Within the flow, the clast can move vertically upwards due to internal shear stresses (Kano and Takeuchi, 1989) and can abrasively corrode and disintegrate over time within the flow (Johansson and Stow, 1995).

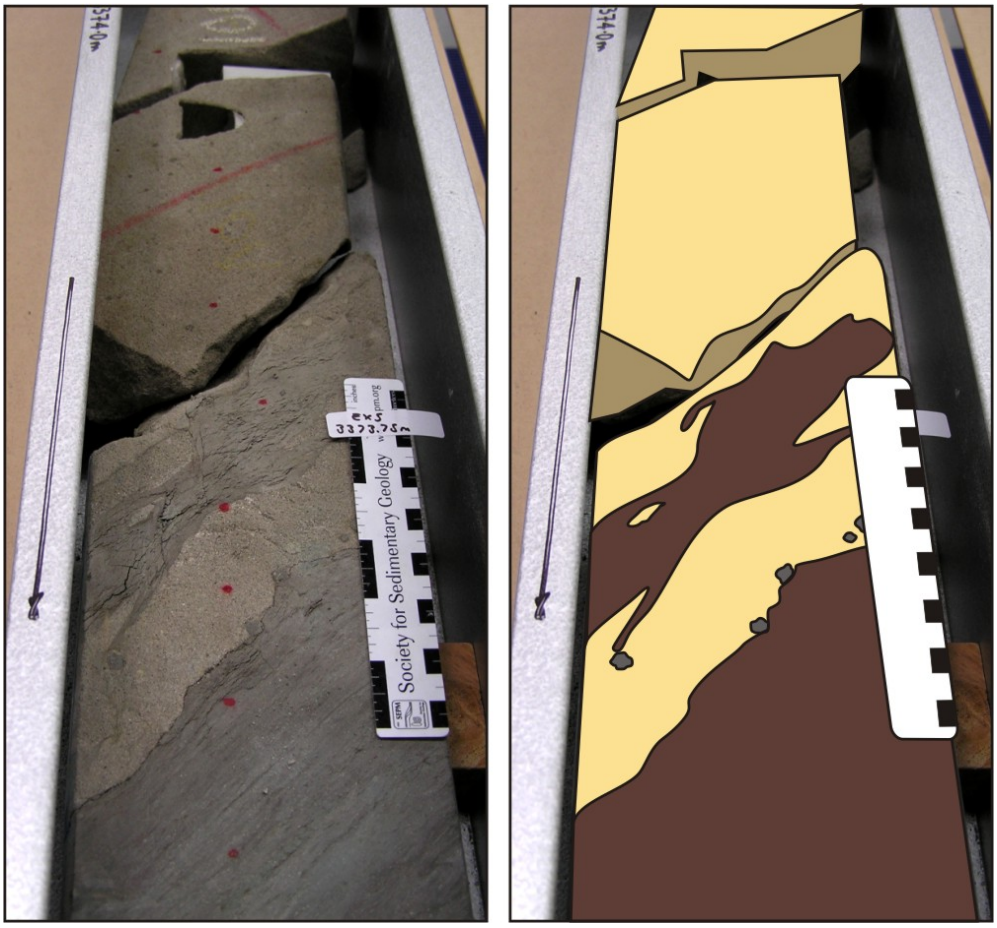

Figure 5-22: Large basal ripped up clast identified in Exeter-5ST1. Note the proximity of the clast to the base of the bed and the composition of the clast in comparison to the underlying claystone.

Multiple proposed mechanisms can explain the existence of isolated single clasts that are suspended in a mid bed position.

i. Mudstone or siltstone clasts are entrained into the flow and emplaced through the gradual aggradation of sediment (Kneller, 1995). This process is described in Lithofacies A.

ii. Clasts are ripped up and are fully incorporated into a basal denser portion of a sand-rich turbulent event. Density differences between the lower density, fluid saturated clasts and the higher density basal sandy layer of the flow would allow the clasts to float upwards through the basal layer. The buoyant upward movement of clasts within the dense basal portion of the current is accompanied by their progressive disaggregation and erosion. This specific position within the bed is thought to be the boundary between the graded Bouma Tb division and the current laminated Bouma Tc division. This division is thought to correspond to the

separation between high and low density flow conditions within the current although field evidence suggests that the clasts lie predominantly between the Bouma Ta and Tb divisions (Johansson and Stow, 1995).

Depositional clasts located along the beds of sandstone units are interpreted to be rafted rip-ups clasts. They are typically sub-angular in shape and can be oriented randomly to sub-parallel to the base of the bed. The host sediment can have a sharp base with scours (Johansson and Stow, 1995). The basal clast recognised in Exeter-5ST1 represents one that has been partially affected by soft sediment deformation (Figure 5-22).

Depositional clasts are not all derived from the erosion of Tithonian aged siltstones and mudstones as some clasts have been derived and worked into Tithonian flow events through the upslope erosion of the Legendre Formation. This is evident from a clast identified within Mutineer-1B that was dated with palynological techniques to Middle Jurassic time (Santos, 1999).

Not all depositional clasts were found to comprise Tithonian-aged siltstone or mudstone. One sandstone clast was identified within Wanaea-3 (2894.8m) (Figure 5-23). Another lithified clast was identified at 2899.90 metres in Angel-4 (Figure 5-24). These clasts are interpreted to have been eroded from canyon regions in a semi-lithified or lithified state.

Small (less than 1 centimetre) isolated thin and sheared mudstone chips are commonly identified throughout Lithofacies A. These clasts are not included in this classification due to their small size and sporadic depositional pattern throughout all sandstones. They are more representative of Lithofacies D (Section 5.4.4).

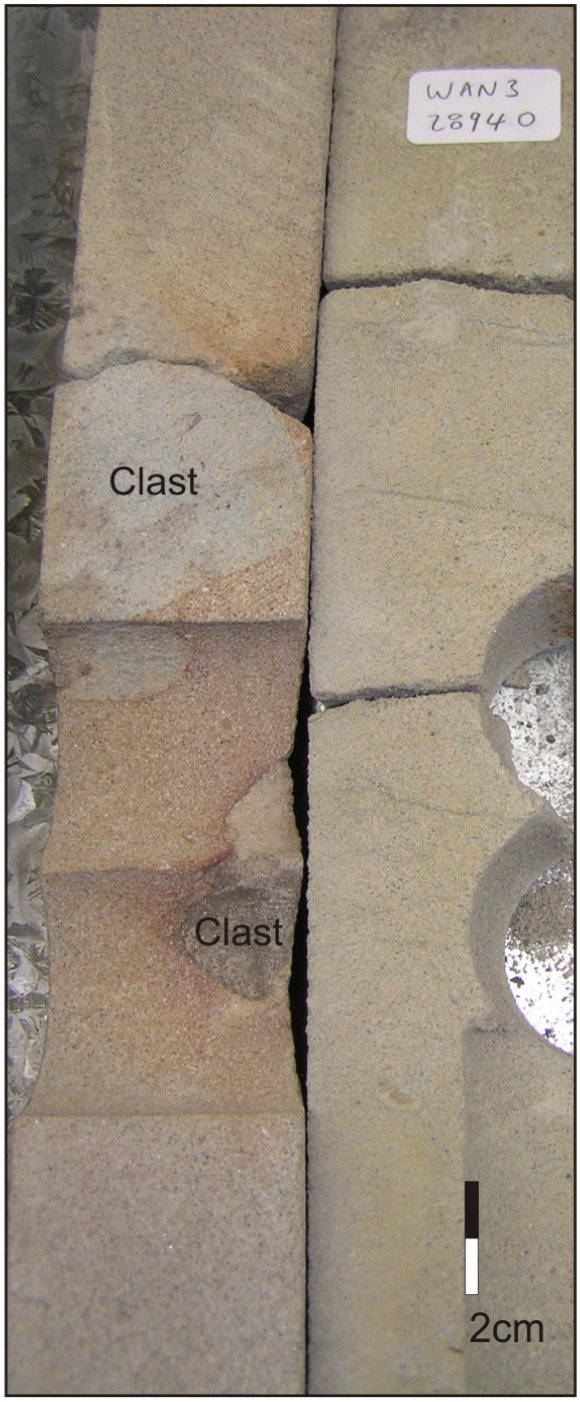

Figure 5-23 (left): Lithified clasts within Wanaea-3. The flow that transported the clasts is interpreted to have been either a large stratified high density turbidity current or sand-dominated weakly cohesive debris flow.

Figure 5-24 (right): Upright lithified clast within Angel-4. Like Wanaea-3 above, the flow body that transported this clast would have almost frozen in place and is comparable to a sandy debrite.

5.3.4 Parallel and Ripple Laminated Sandstone (Lithofacies D)

5.3.4.1 Description

These units comprise sand to silt-dominated well sorted laminated and ripple laminated successions with associated carbonaceous material and mudstone chips. They are identified in all wells. The units were stratigraphically recognised as either resting at the tops of unstructured sandstone units (Lithofacies A) (Figure 5-25, 5-26 and 5-29) or resting upon bioturbated heterolithics (Lithofacies E) (Figure 5-25). Units range from a few centimetres to over three metres in thickness (Egret-2 and Angel-4 (Figure 5-32)).

5.3.4.2 Interpretation

Three varieties of sandstone laminae are present in core. They are interpreted to represent Bouma units Tb, Tc and Td.

i. Sand-dominated parallel laminae (Tb) are those that display parallel laminae within a sand-dominated unit (Figure 5-26).

ii. Disrupted wavy laminae (Tc) are those that display clear cross-bedding and a wavy nature are interpreted to be traction structures that formed within the lower flow regime (Figures 5-25 and 5-28). Climbing ripples are also identified (Figure 5.25).

iii. Fine sand to silt-dominated parallel laminae (Td) are those that display parallel laminae within a very fine sand- to silt-dominated unit (Figure 5-27).

These units are interpreted to have been deposited by traction from sand-rich suspended flows of declining velocity. They can be overlain by younger homogeneous and unstructured sandstones of Lithofacies A with a visible erosive contact (Figure 5-28).

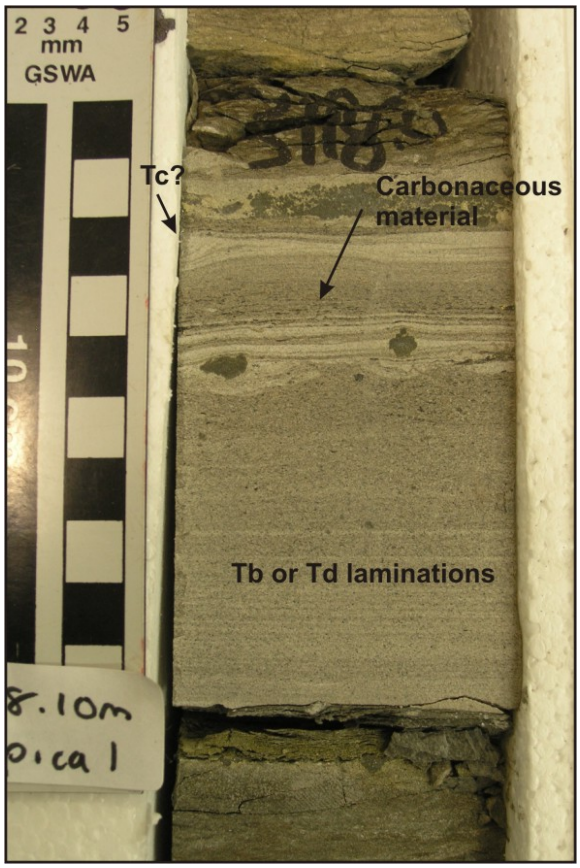

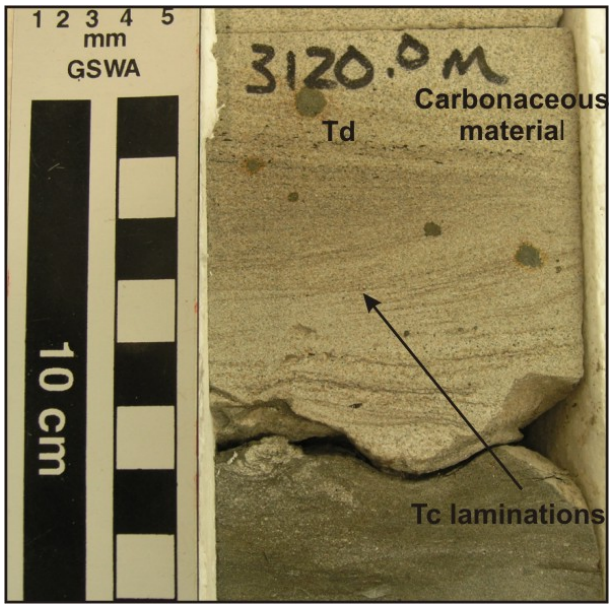

Figure 5-25: Laminated and cross-bedded sandstone from Spica-1 (left and above). No preserved underlying Lithofacies A suggests these are distal turbulent flow deposits. They display Tb, Tc and Td Bouma features.

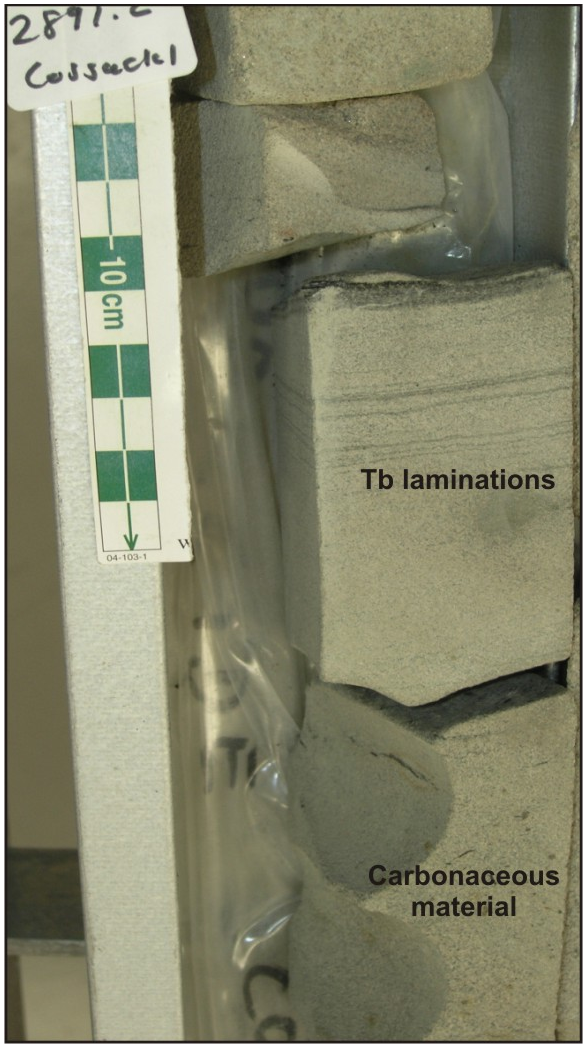

Figure 5-26 (left): Fine-grained normally graded succession displaying Tb parallel laminae from Cossack-1. It overlies a medium grained structureless to faintly parallel stratified sandstone.

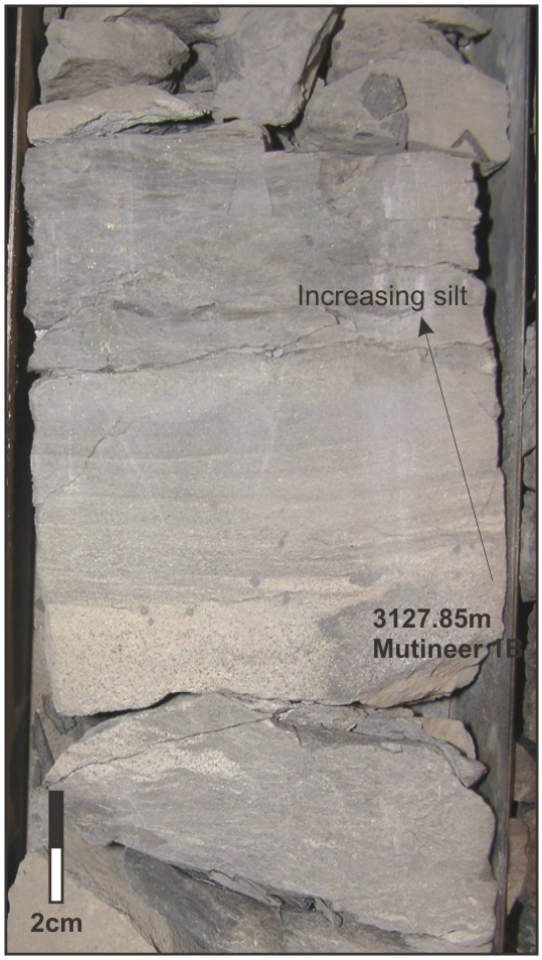

Figure 5-27 (left): Silt-dominated laminated succession (Td) from Mutineer-1B. It overlies a carbonaceous unit.

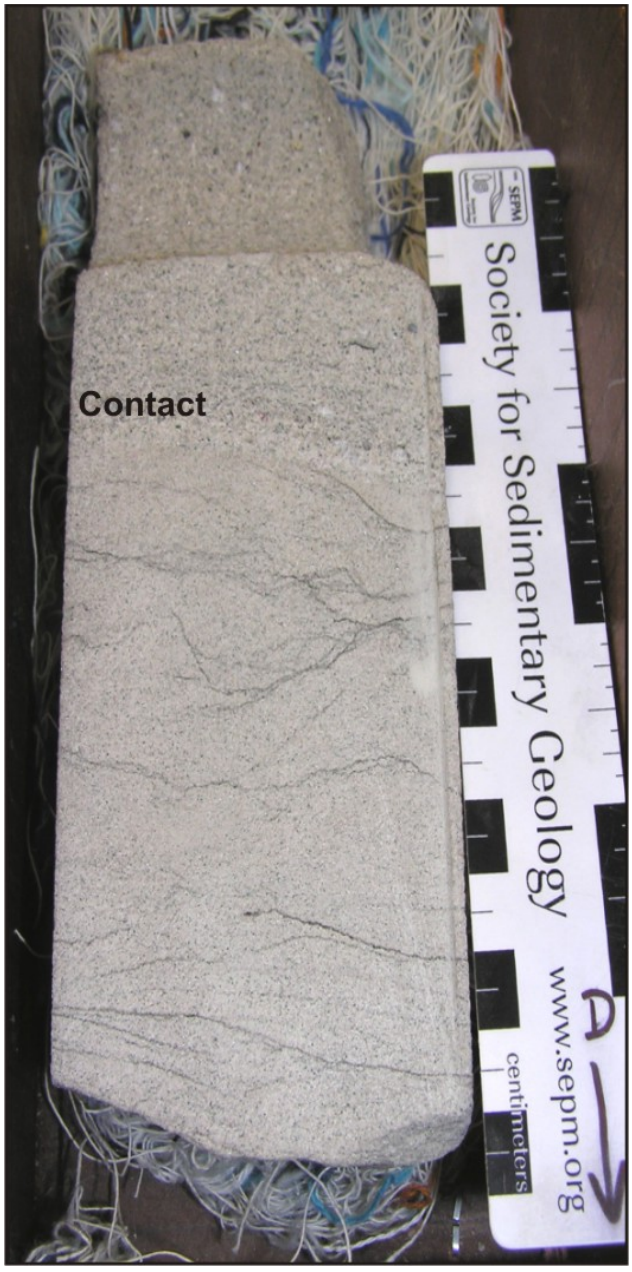

Figure 5-28 (right): Laminated traction deposits underlying an inclined erosive contact in Montague-1. The laminae have been affected by dewatering processes.

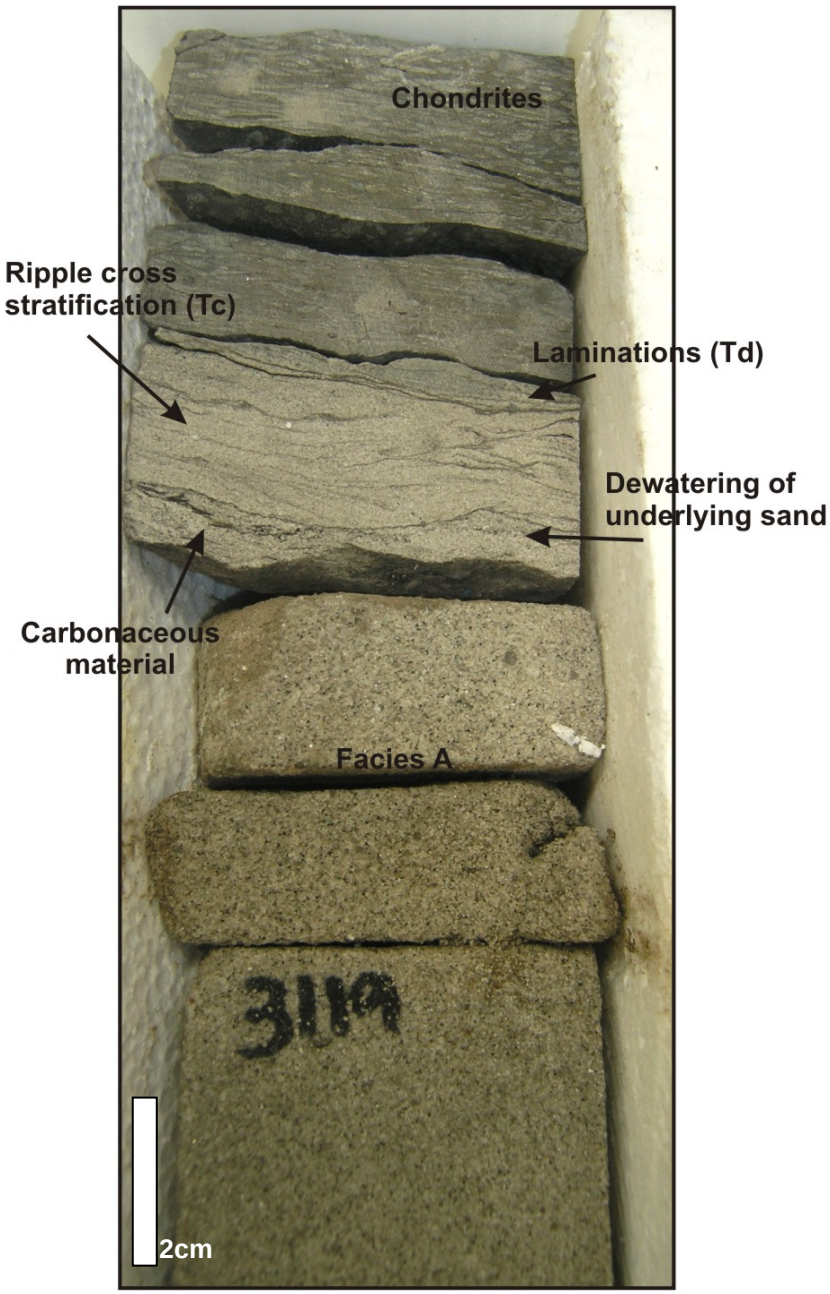

Figure 5-29 (above): Sand-dominated Tc cross stratified and Td laminated zones identified in Lambert-2. Note the very fine carbonaceous material that is present at the base of laminated zone.

Mudstone chips identified within this lithofacies represent clasts that were carried multiple times into the head of the flow event where they were broken down or resuspended into the turbulent cloud to be deposited during general waning flow traction. Carbonaceous material intermixed with the mudstone chips strengthens this interpretation. Carbonaceous material, being of a lower density than mudstone clasts, would have been suspended within the turbulent component of the flow along with the mudstone chips (Figure 5-30). Carbonaceous material can also concentrate to form a bed up to 15 millimetres thick (Wanaea-2A 2894.5m) (Figure 5-31).

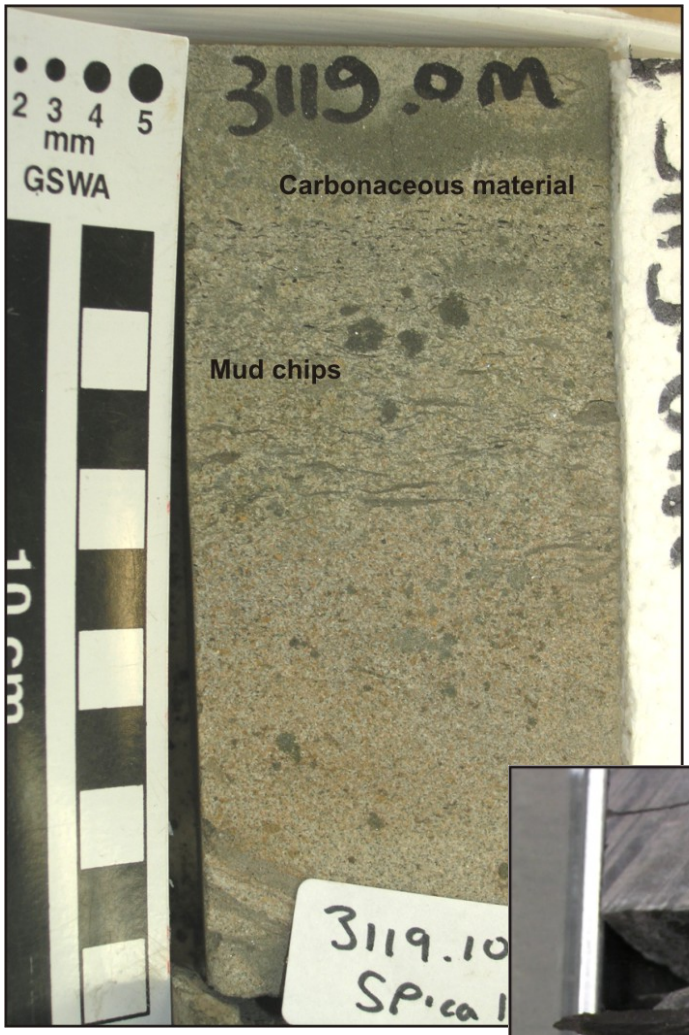

Figure 5-30 (left): Mudstone chips and carbonaceous material from Spica-1. The mudstone chips represent disintegrated mudstone clasts. They could belong to a possible linked debrite.

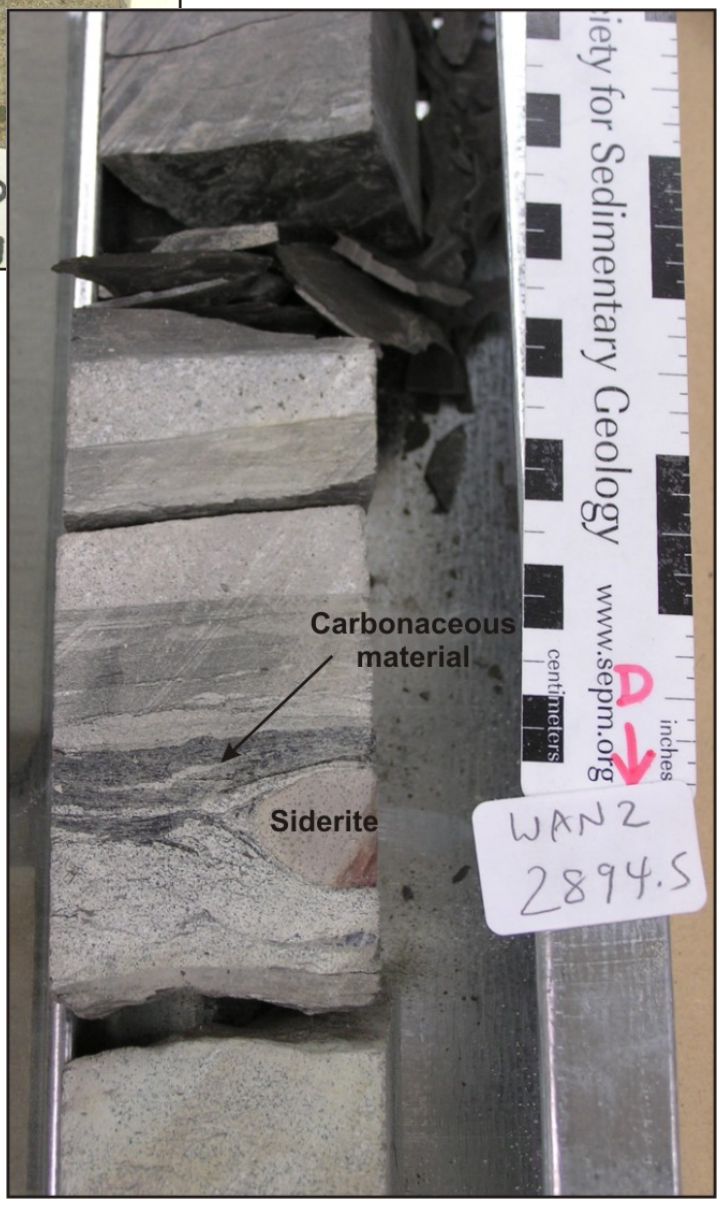

Figure 5-31 (right): Concentrated bed of carbonaceous material along with thin bedded sandstone and siltstone units from Wanaea-2A.

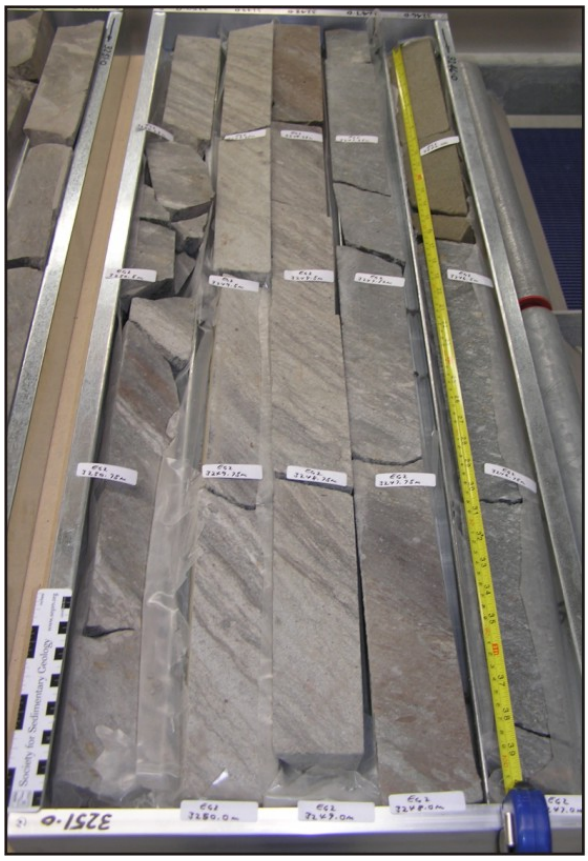

Figure 5-32: Stacked laminated turbiditic deposits identified in Egret-2 (top left and right) and Angel-4 (bottom right). The laminae are wavy in character suggesting a certain degree of traction and dewatering.

Laminated sandstones are not commonly bioturbated, although a possible preserved *Zoophycos* is present within laminated sandstones of Wanaea-2A (2913.5m) (Figure 5-33). This lack of bioturbation could be interpreted as a lack of quiescence between flow events for a strong community of organisms to become established.

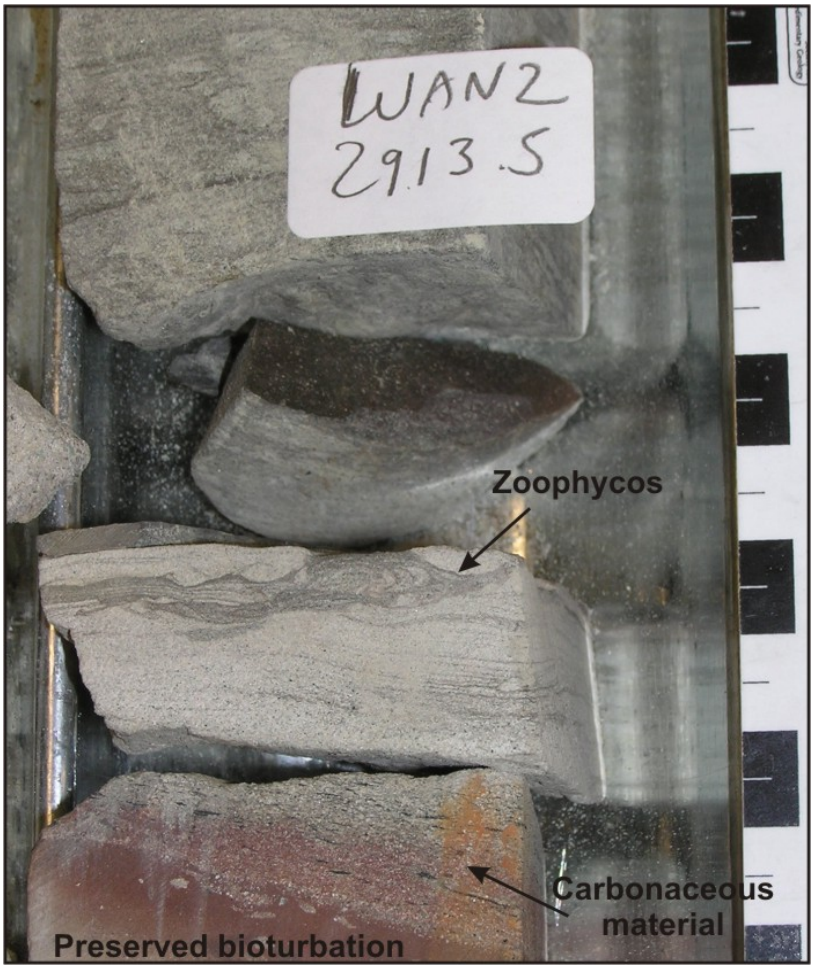

Figure 5-33: *Zoophycos* within laminated sediments in Wanaea-2A. The laminated unit rests upon siderite which was initially bioturbated heterolithics (note the internal preserved bioturbation).

5.3.5 Bioturbated and Laminated Heterolithics (Lithofacies E)

5.3.5.1 Description

Heterolithic deposits exist in most wells and form successions up to ten metres thick. They contain between 10% and 70% very fine-grained sandstone. They are commonly interbedded with coarse- to medium-grained siltstone. Unbioturbated heterolithics are rare and grade abruptly into bioturbated heterolithics.

The degree of bioturbation can range from 0 to 90%. *Cruziana*, *Zoophycos* and *Nereites* ichnofacies dominate, which is expected of a shallow and deep marine depositional setting. Identified ichnogenera include *Terebellina* (Figure 5-34), *Planolites* (Figure 5-35), *Chondrites* (Figure 5-36), *Helminthopsis* and *Helminthoida* (Figure 5-37) and *Zoophycos* (Figure 5-38). Siderite cementation can preserve their uncompacted burrow shape (Figure 5-39).

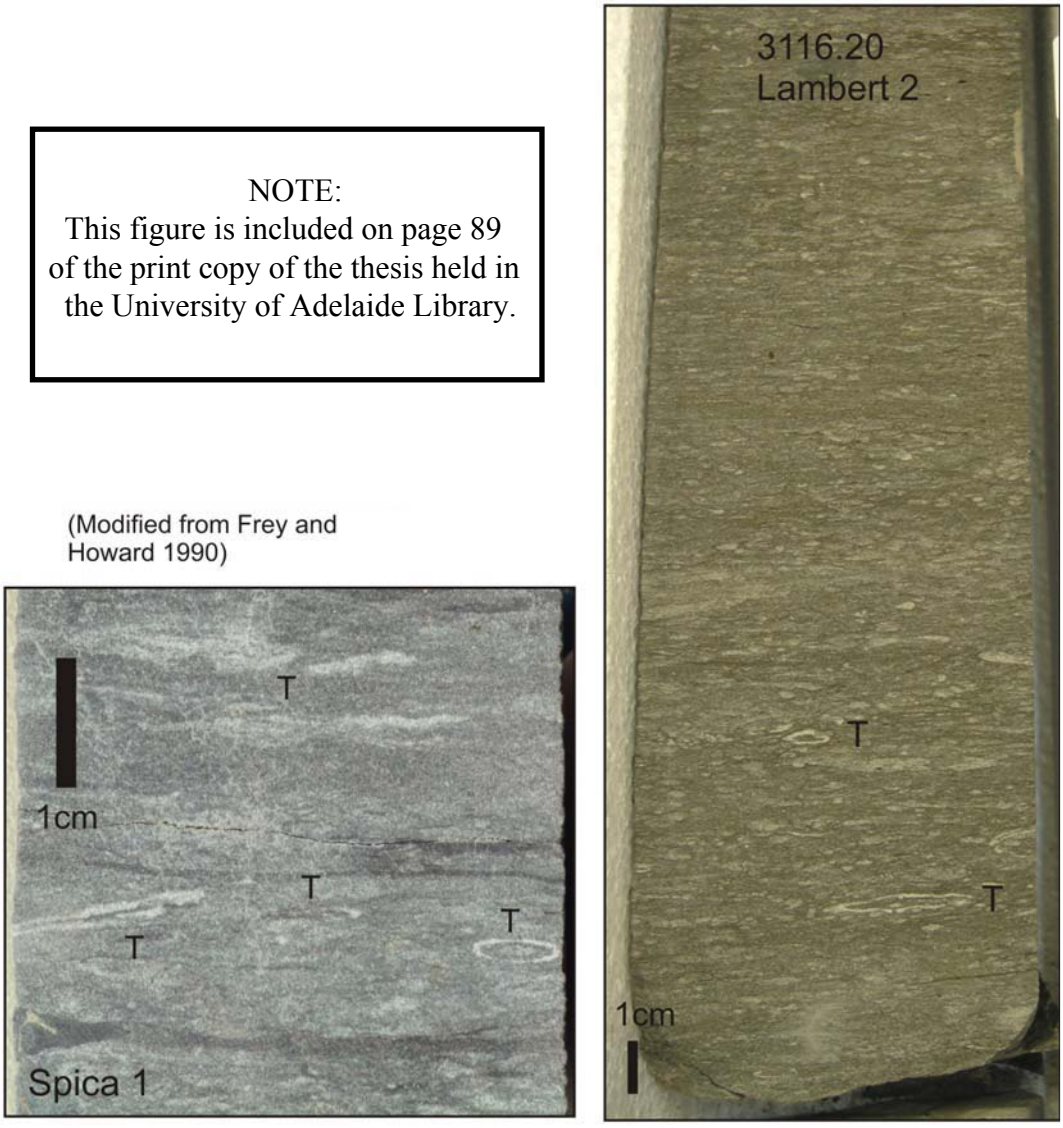

Figure 5-34: *Terebellina* ichnofacies In Lambert-2 and Spica-1. It is recognisable by sub-cylindrical, straight to gently curved inclined burrows which have a thick distinct wall lining of bonded fine-grained sandstone (Frey and Howard, 1990).

NOTE:
This figure is included on page 90 of the print copy of the thesis held in the University of Adelaide Library.

P. Montanus (Modified from Frey and Howard 1990)

NOTE:
This figure is included on page 90 of the print copy of the thesis held in the University of Adelaide Library.

P. Beverleyensis (Modified from Frey and Howard 1990)

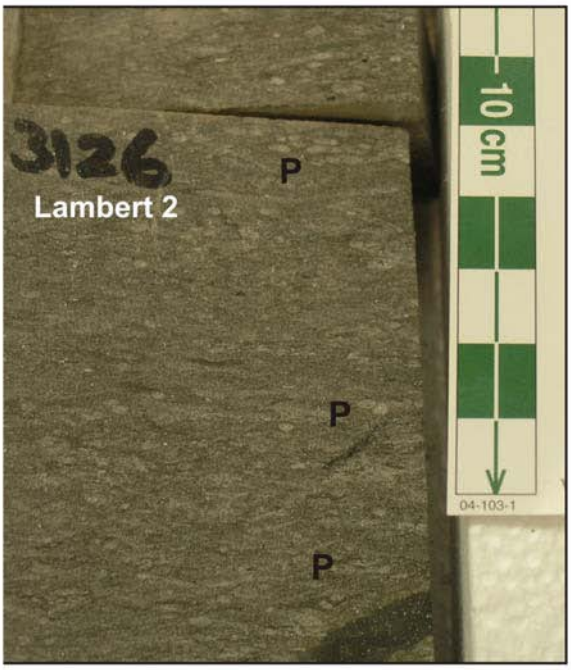

Figure 5-35: Examples of *Planolites* from Lambert-2 and Cossack-1. They are identified by unlined straight, typically smooth walled burrows which are circular to elliptical in cross section. Filling differs in lithology from host rock. It represents the feeding burrow of a deposit feeding organism and is found in almost all environments from freshwater to deep marine. Straight, non-bifurcated silty sandstone-filled burrows exist in siltstone. Burrows can be single or grouped.

NOTE:
This figure is included on page 91 of the print copy of the thesis held in the University of Adelaide Library.

(Modified from Frey and Howard 1990)

Figure 5-36: *Chondrites* populations from Lambert-2, Exeter-5ST1 and Mutineer-1B. They are represented by a complex root-like burrow system of branching feeding tunnels of uniform diameter. In core, they appear as an array of tiny elliptical dots. They represent a complicated deposit-feeding organism. *Chondrites* range in modern environments from very shallow water to over 3000 metres water depth (Ekdale and Berger, 1978). This trace fossil can be indicative of interstitial anoxic conditions (Savrda and Bottjer, 1991).

NOTE:
This figure is included on page 92 of the print copy of the thesis held in the University of Adelaide Library.

Adapted from Crimes (1973)

Figure 5-37: *Helminthoida* (regular meandering) and *Helminthopsis* (irregular meandering) from Lambert-2 and Spica-1. They are represented by smooth walled burrows that don't branch, interpenetrate or cut across another. In cross-section, they are generally horizontal. In core, they appear as either dark spots or dark lines (longitudinal). They represent grazing traces of worm-like organisms. They are common with distal *Cruziana* ichnofacies and proximal *Zoophycos* ichnofacies on a marine shelf setting (Pemberton *et al.,* 2001).

NOTE:
This figure is included on page 93 of the print copy of the thesis held in the University of Adelaide Library.

Adapted from Crimes (1973)

Figure 5-38: *Zoophycos* traces from Cossack-1, Lambert-2 and Spica-1. This trace is represented by a circular to lobate sheet-like spreite which can be flat, curved, inclined or wound in a screw fashion. It is the grazing trace of a deposit-feeding organism and is associated with distal *Cruziana* and *Zoophycos* ichnofacies in fully marine, offshore shelf settings (Pemberton *et al.,* 2001).

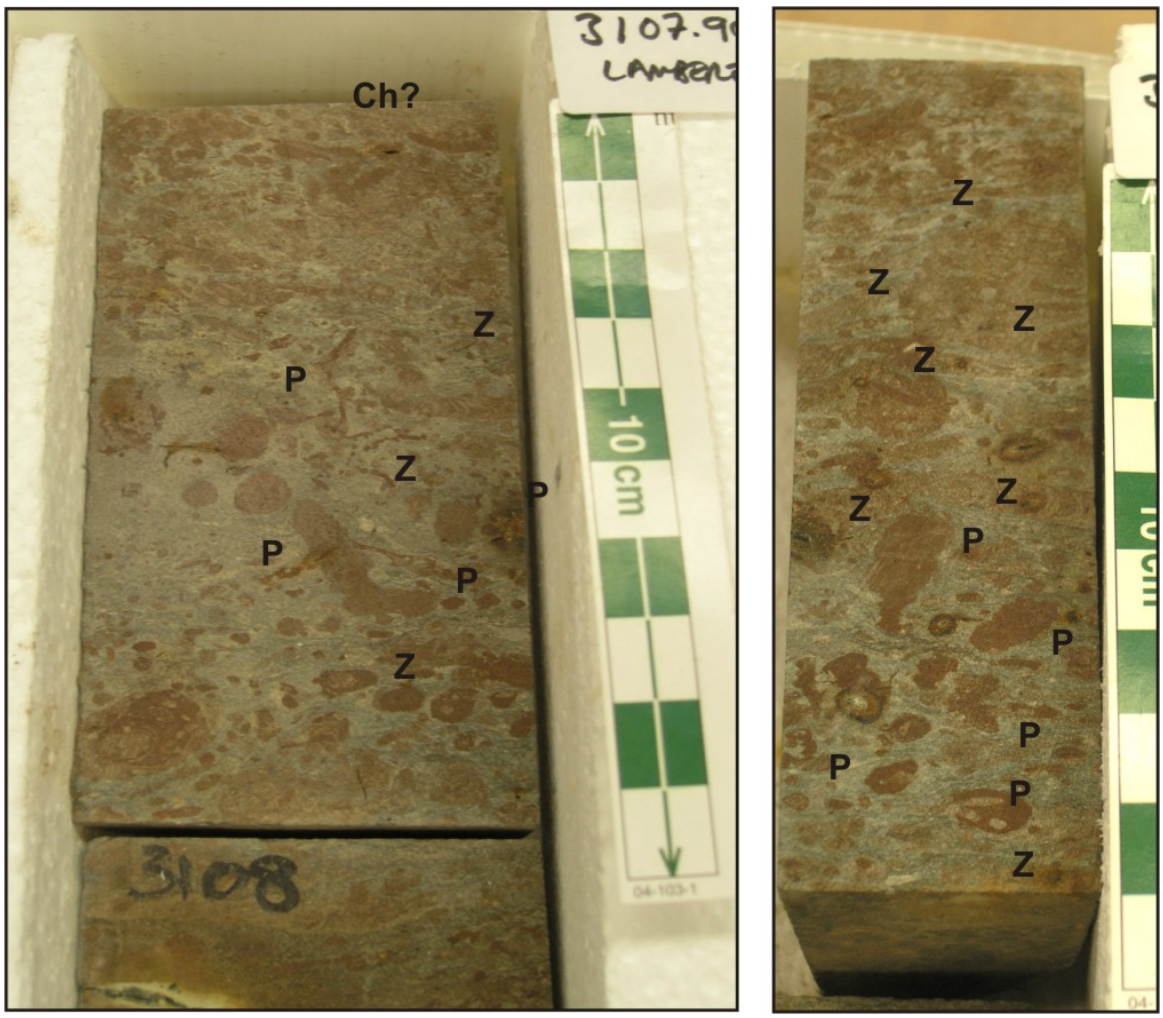

Figure 5-39: Example from Lambert-2 of preserved burrow successions cemented by early siderite.

5.3.5.2 Interpretation

Bioturbated heterolithic intervals, unlike the sand-dominated stratification of Lithofacies D, represent the stratified units formed through traction within a low density waning flow event that are deposited within distal settings where significant periods of time allowed organisms to thrive in the sediment. In rare cases, laminated unbioturbated heterolithic deposits exist above a thick bedded sandstone unit. They grade vertically into bioturbated heterolithics. These unbioturbated units have been deposited in rapid succession by multiple sandy low density turbidity currents (Figure 5-40). Bioturbation is most common within mudstone-dominated units of low density turbidity events as they contain the greatest food content and are the most stable environment.

Marine ichnofacies are not intended to be palaeobathometers (Frey *et al.,* 1990). This is due to the fact that location of certain ichnofacies are not controlled solely by water depth or distance from shore but by a combination of dynamic factors that include substrate consistency, hydraulic energy, rates of deposition, turbidity, oxygen and salinity levels, toxic substances, the quality and quantity of available food (Frey *et al.,* 1990). Ekdale (1988) further concluded that the occurrence of a particular ichnogenus doesn't automatically indicate the presence of a certain ichnofacies, that environmental

shifts of certain trace fossils can occur over time and that the nine standard ichnofacies have a broad environmental significance that may include but certainly extends beyond bathymetry.

The existence of certain ichnogenera can be used within the Angel Formation to infer the varying levels of oxygenation within the basin waters at the time of deposition. The existence of *Chondrites* and *Zoophycos* could represent an oxygen-poor setting where unoxidised organic matter is abundant for deposit-feeding organisms to feed on. *Helminthoida*, on the other hand, is common in organic-rich aerobic conditions. This information, combined with palynology, could be a useful indicator of increasing water depth for a particular period of deposition. One caveat with this approach is that tiering within the sediment can take place.

Figure 5-40: Interbedded heterolithics with little recognisable bioturbation. Each sandstone unit less than 1 centimetre thick represents the distal deposition of a sand-dominated low density turbiditic flow event. The unit grades vertically into a more bioturbated succession with identified *Planolites*.

5.3.6 Structureless to Laminated Siltstone and Mudstone (Lithofacies F)

5.3.6.1 Description

This lithofacies is easily identifiable as it comprises mudstones with a lack of visible bioturbation (Figure 5-41). Pyritic growths are common within these intervals ranging in size up to 5 centimetres wide. Siderite cements zones or bands up to 30 centimetres thick are recognisable within the core. Bioturbation is non-existent to uncommon (less than 5%). Thin mudstones commonly underlie homogenous sandstone successions (Figure 5-42).

5.3.6.2 Interpretation

Laminated and unstructured intervals of siltstones represent the combination of silt- and clay-dominated low density turbidites interbedded with hemiplegic fallout. Thick units are found to dominate the youngest succession of sediment representing transgression and overall deepening of the entire depositional system. The thin mudstones that overlie bioturbated heterolithics and underlie homogenous sandstones can be interpreted to represent small flooding or abandonment events (Figure 5-42).

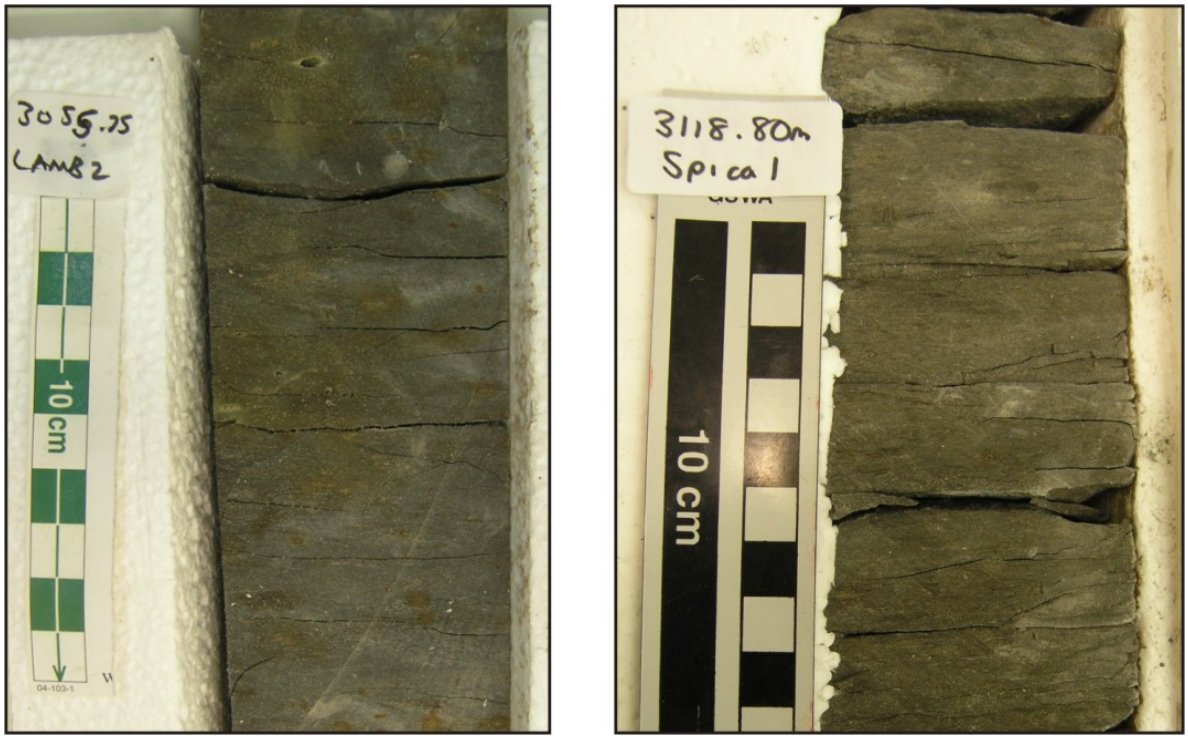

Figure 5-41: Unstructured to laminated claystone of Lithofacies F from Lambert-2 (left) and Spica-1 (right).

Figure 5-42: Thin mudstone units overlying bioturbated heterolithic and unstructured claystone intervals. They are commonly overlain by homogenous sandstone intervals of Lithofacies A and B. Erosive striations can be seen along the basal sandstone contact in Mutineer-1B. The thin mudstones can be interpreted to have been deposited during maximum flood conditions.

5.3.7 Ptygmatic Injectites (Lithofacies G)

5.3.7.1 Description

Ptygmatically folded injectites are commonly recognised within heterolithic and claystone intervals. They crosscut bedding and range up to 3 centimetres thick. They have been identified in Angel-4, Egret-2 (Figure 5-43 and 5-45), Lambert-2 (Figure 5-44 and 5-46), Exeter-5ST1 (Figure 5-44), Mutineer-1B, Mutineer-3, Spica-1 (Figure 5-43), Cossack-1, Wanaea-2A (Figure 5-46), Wanaea-3, and Wanaea-5. Injected intervals are often identified as being strongly cemented and microscopically cleaner than undeformed surrounding sandstones.

Concentrated populations of ptygmatically folded injectites have been identified and classified as "injection nests" by this study. They represent zones of intense injection (Figures 5-45 and 5-46) and have been identified in Egret-2 (3281.4 to 3283.4 metres), Lambert-2 (3136.0 to 3136.6 metres), Wanaea-2A (2918.25 to 2919.25m) and Exeter-5ST1 (3387.8 to 3388.3m).

5.3.7.2 Interpretation

Ptygmatic injectites develop during an early stage of burial beneath the subsurface. They represent injection features that are compacted and described as ptygmatic by Parize *et al.,* (2007). They are the product of fluidisation which is a direct result of fluid overpressurisation within the subsurface (Jolly and Lonergan, 2002; Duranti and Hurst, 2004). Fluidisation within subsurface sandstone bodies could be interpreted to be due to either dynamic loading exerted on the sandstone body by new flow events, overpressure or tectonic activity. Fluidisation of sediment occurs when the strength of the sediment is overcome by moving interstitial fluids buoying a particle of sediment (Maltman and Bolton, 2003). Once fluidised, the sediment will follow a fluid pressure gradient (Maltman and Bolton, 2003) and, combined with excessively high in-situ pore pressure, inject into heterolithic, claystone and sandstone intervals. Well-sorted and rounded medium to coarse-grained clastics with good permeability are more susceptible to the process of fluidisation with sediment loading (Jolly and Lonergan, 2002).

The ptygmatic nature of the injectites suggests injection prior to significant burial and compaction. The lack of in-situ hydrocarbon within the ptygmatic injectites demonstrates that injection activity and cementation occurred prior to the charging of the reservoir (Jonk *et al.,* 2005).

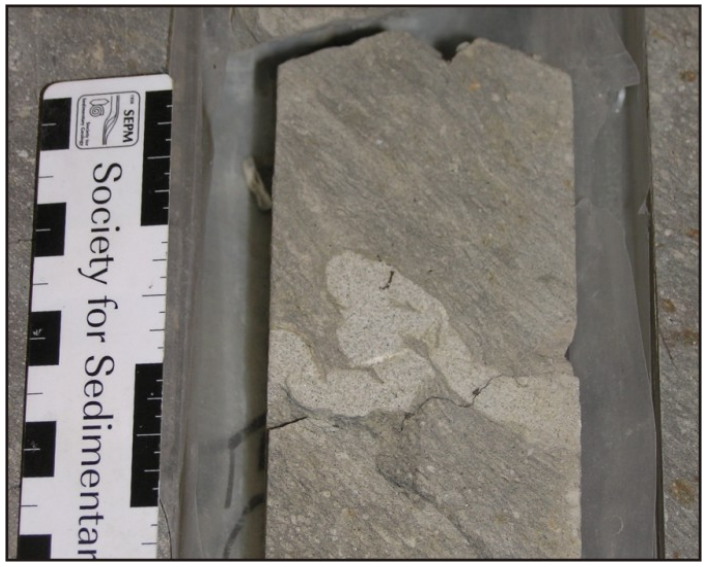

Figure 5-43: Small-scale ptygmatically folded injection features 1 centimetre thick and strongly cemented. Example from Spica-1 (left) and Egret-2 (top).

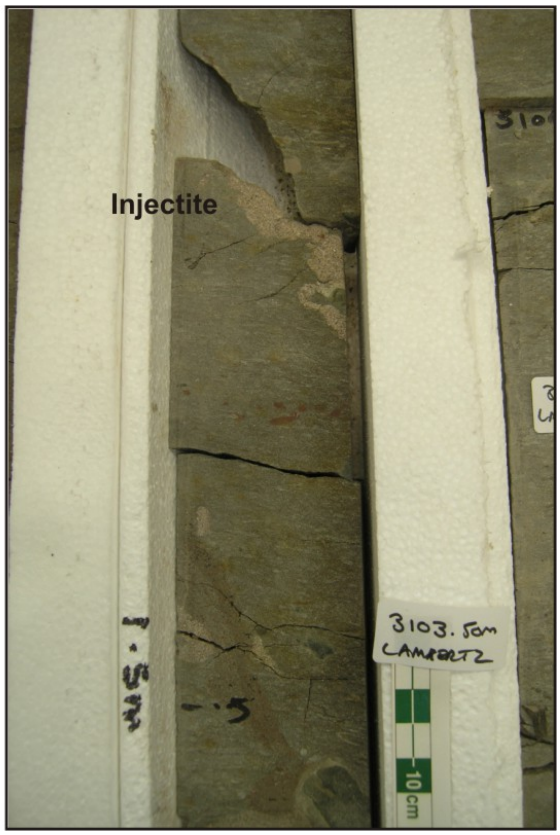

Figure 5-44: Ptygmatically folded injection features can be closely situated to depositional sandstones (Exeter-5ST1 left) or vertically distal from depositional sandstones (Lambert-2 right).

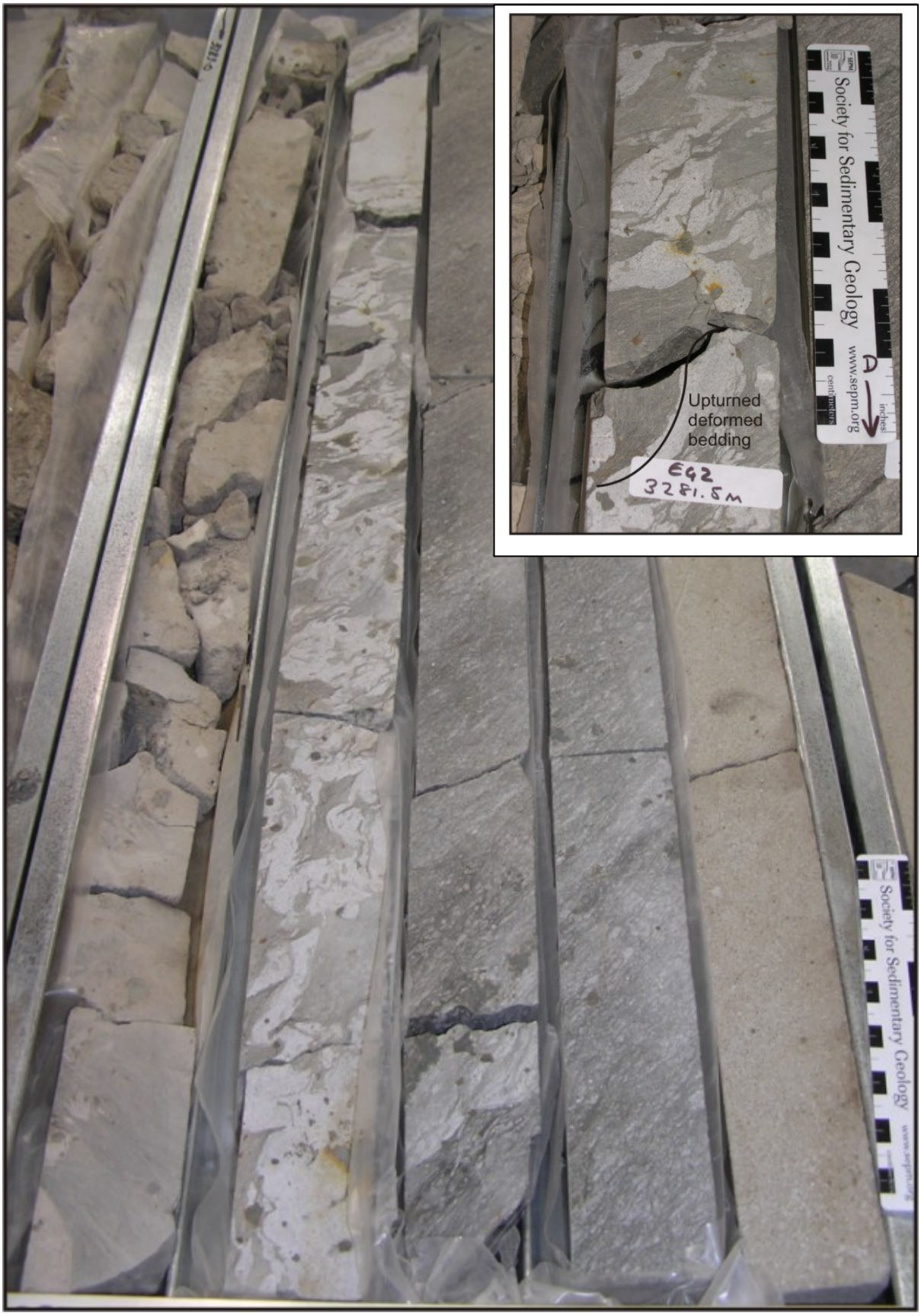

Figure 5-45: Injection nests (as named in this study) from Egret-2. The differing colouration exists between the unstructured host sandstones and the injected intervals in Egret-2 due to residual hydrocarbon in the host sandstone. This zone is approximately 80 centimetres thick.

Figure 5-46: Injection nests (as named in this study) from Lambert-2 (left) and Wanaea-2A (right). These units could be differently interpreted to be products of linked debrites (refer Facies H and K).

5.3.8 Deformed and Sheared Mudstone Breccia (Lithofacies H)

5.3.8.1 Description

Intervals of matrix-supported rounded to sheared claystone and heterolithic clasts are commonly identified within core. Individual clasts range in size from 1 to over 10 centimetres wide and can appear either rounded or sheared. They often display hair-like extensions (Figure 5-47). The clasts can exhibit internal preservation of primary bioturbation and heterolithic stratification.

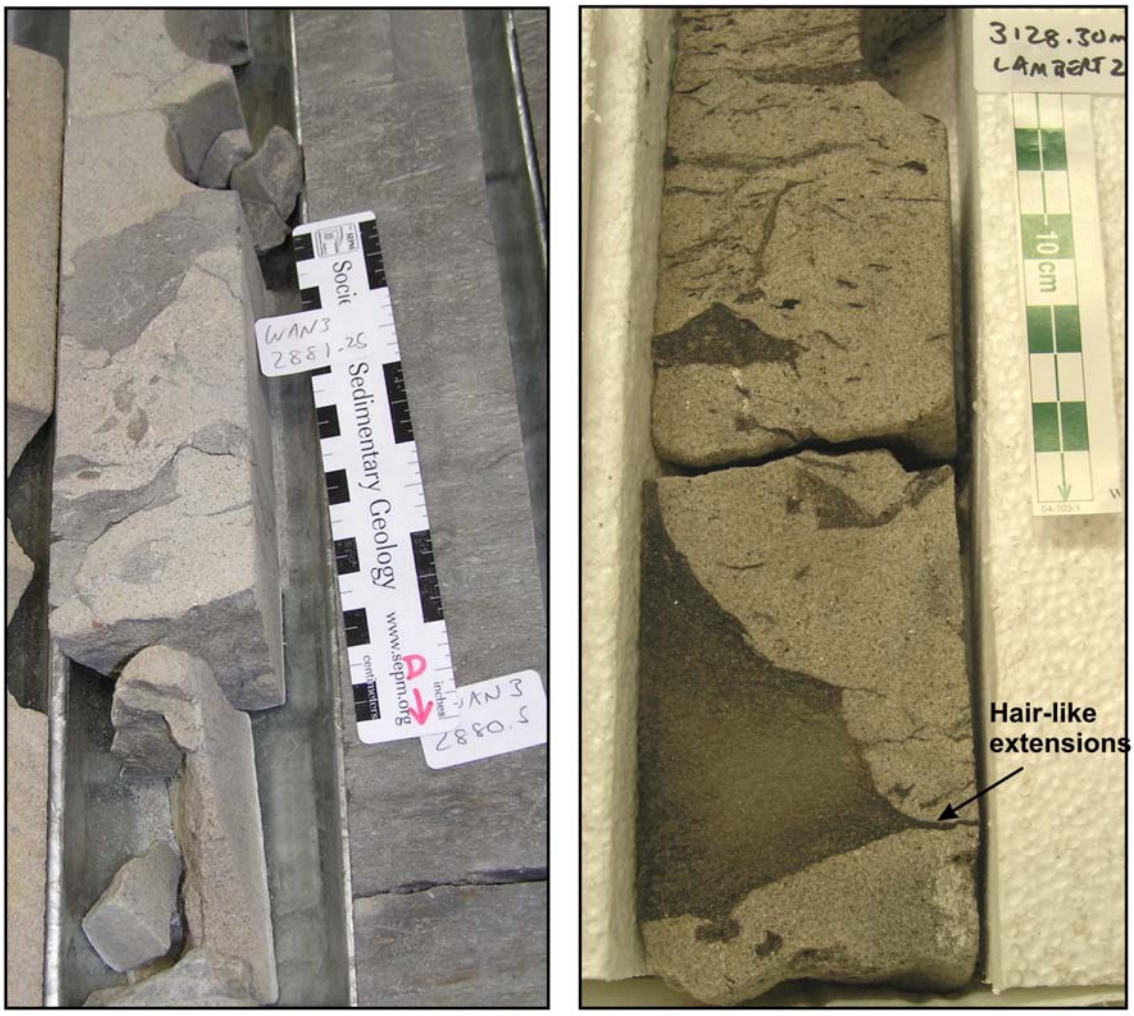

Figure 5-47: Sheared and deformed breccia from Lambert-2 and Wanaea-2A. All three examples are present within the topmost section of their host sandstone bed.

5.3.8.2 Interpretation

These clasts are interpreted to be formed through either:

- injection processes of sandstone invading a heterolithic or siltstone-dominated succession, or;
- the formation and deposition of linked debrites.

Intense injection of sandstone can result in the creation of injectite breccia. The injection breccia can commonly sink into the underlying fluidised sandstone, forming rip-down clasts (Chough and Chun, 1988; Johansson & Stow, 1995) (Figure 5-48).

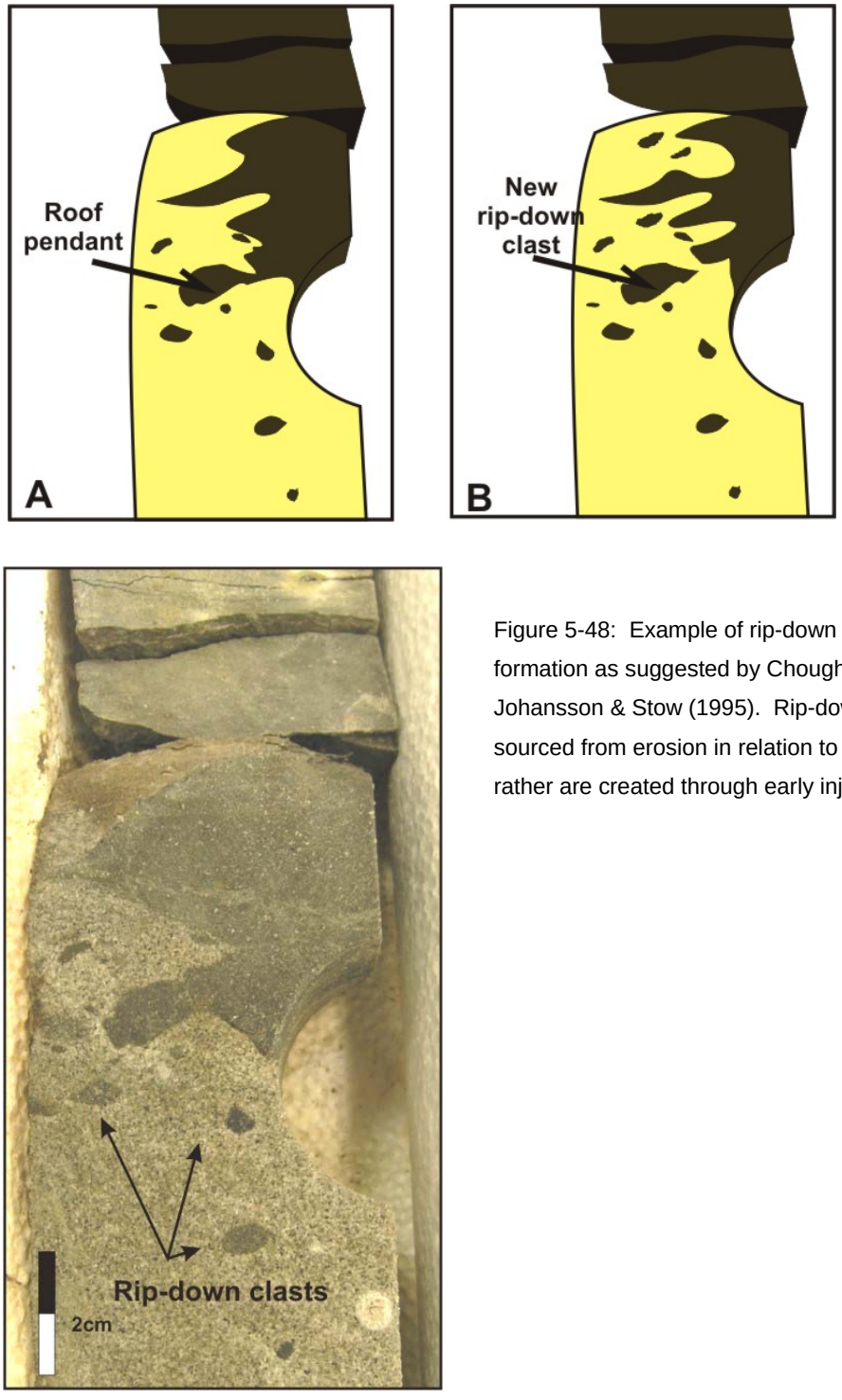

Figure 5-48: Example of rip-down clasts and their formation as suggested by Chough and Chun (1988) and Johansson & Stow (1995). Rip-down floating clasts are not sourced from erosion in relation to the flow event, but rather are created through early injection processes.

Contorted and sheared successions that overlie unstructured and dewatered sandstone units could also be interpreted to be products of linked debrites (Haughton *et al*., 2003; Talling *et al.,* 2004; Haughton *et al*., 2009). Linked debrites form through the bulking of a lagging tail behind sand-dominated turbidity currents. Clasts are incorporated either at the source during the failure process, or are acquired through up-slope basal erosion. They are reworked, hydraulically segregated and

concentrated towards the rear of the main flow body to form a trailing fluidized debrite (Haughton, 2001). The zone is strongly fluidised through rapidly expelling water from underlying rapidly deposited sandstone. These units are commonly deposited on top of or downslope from the main sandstone body through a reduction in shear due to the linked debrite riding a “carpet” of water that is simultaneously expelling from the underlying sandy body. Units representing this theory have been identified in fan fringe sand-dominated successions of the Magnus-Penguin and Miller-Kingfisher fan systems of the northern North Sea (Haughton *et al.,* 2003) (Figure 5-49).

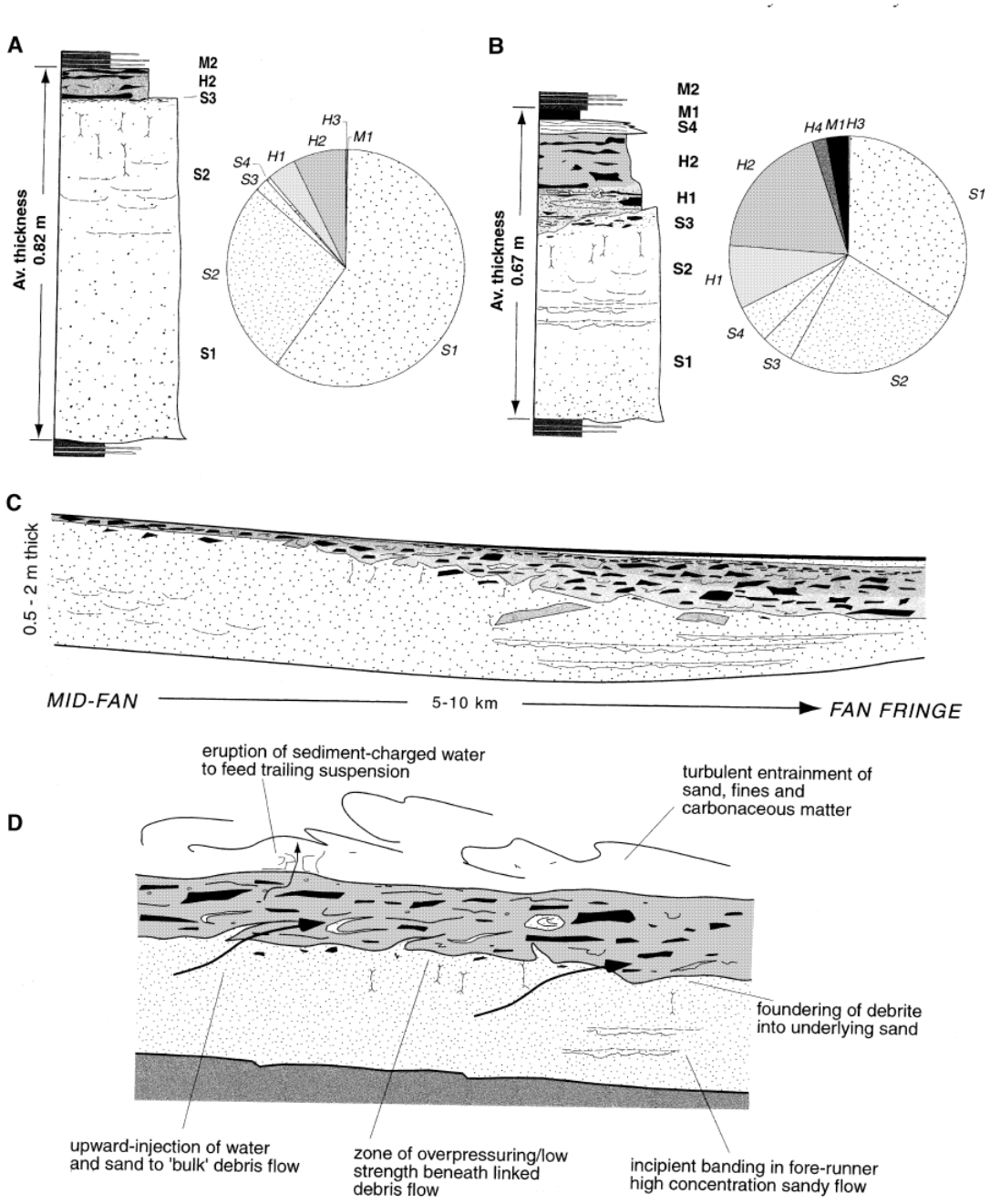

Figure 5-49: Facies, lateral trends and geometries of linked debrites interpreted by Haughton *et al* (2003) for the Magnus-Penguin and Miller-Kingfisher fans in the North Sea. Image C highlights the down-fan transition of these deposits. Image D represents the processes accountable for the origin of linked debrites and their associated sand beds (Haughton *et al*., 2003).

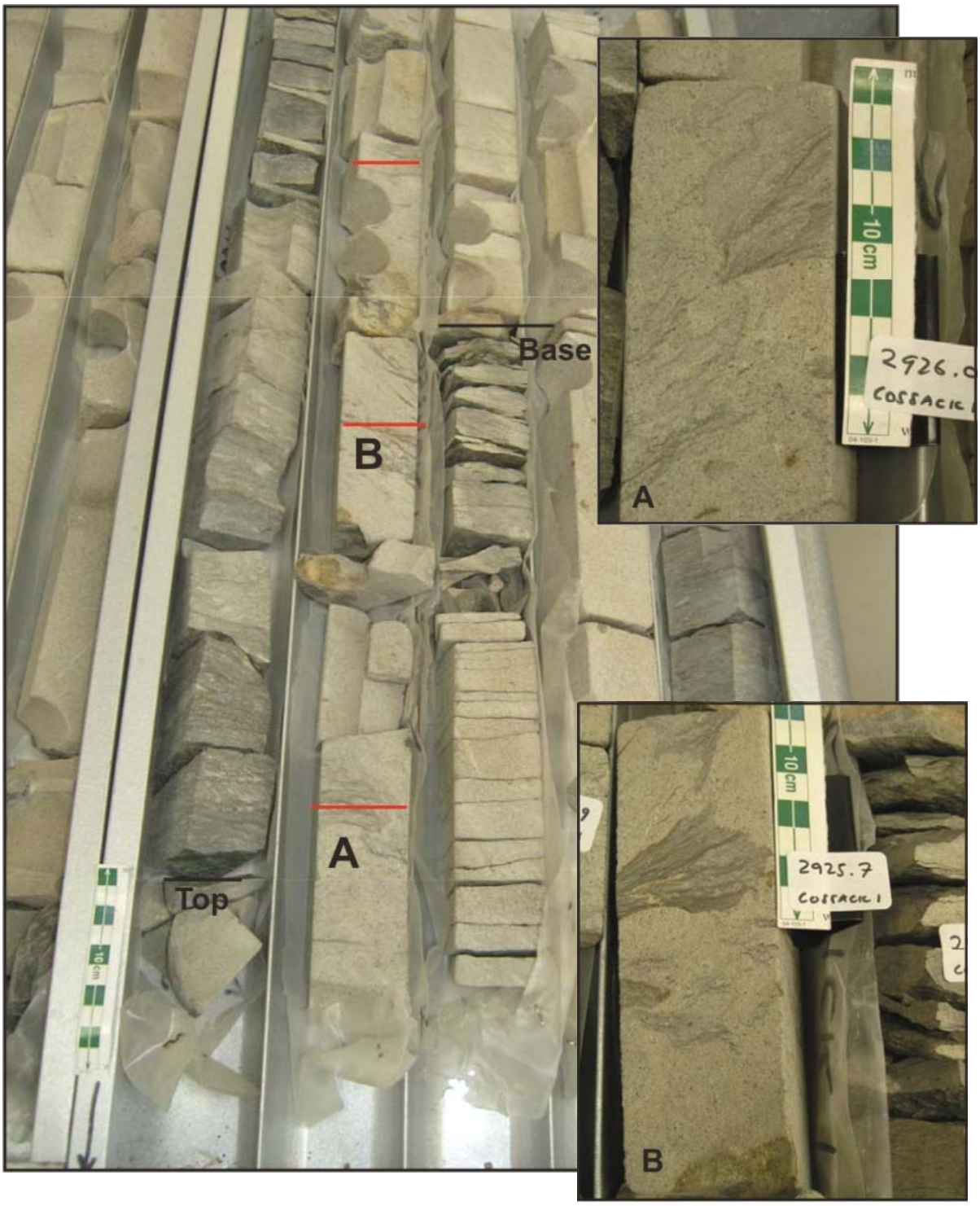

Figure 5-50: Sandstone units separated by clasts in Cossack-1. This succession could be interpreted as either the product of fluidisation or it could represent a succession of hybrid flows events with associated linked debrites. Note the angularity and hair-like extensions on the clasts.

5.3.9 Discordant sandstone bodies in sandstones and heterolithics (Lithofacies I)

5.3.9.1 Description

This lithofacies comprises discordant sandstone bodies that exist within sandstone or heterolithic units. They are generally wide, smooth-sided, sub-vertical in orientation and are lined with concentrated fine-grained materials (Figure 5-51). They were recognised in Spica-1 and Exeter-5ST1. The discordant sandstone bodies in Spica-1 (3129.20m and 3129m) are approximately 3 to 4 centimetres wide and exist within a sandstone unit (Figure 5-51). The bodies identified in Exeter-5ST1 rest within a heterolithic unit that was overlying the source sandstone. It resulted in a significant pull-up effect on the bedding (Figure 5-52).

5.3.9.2 Interpretation

Sandstone pillars form through a strong movement of pore fluid which destroys primary depositional features and transports grains and fines to produce sub-vertical pillar features. The linings are considered to be filter residue formed through water absorption driven by differential pore pressure between the pillar structure and the host sandstone (Figure 5-51).

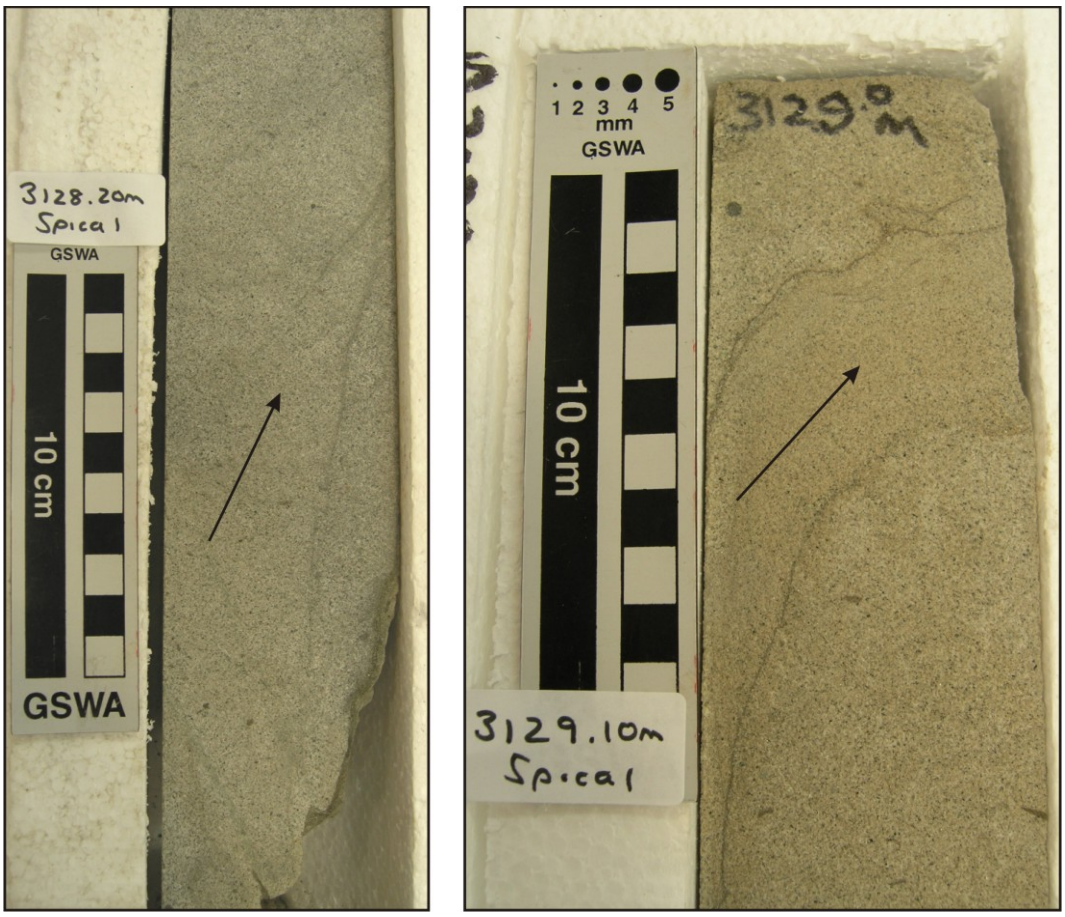

Figure 5-51: Sandstone-filled post-depositional pillar features within sandstone as identified within Spica-1. The linings visible in the pillars are concentrated fines that are filtered against the pillar wall as water and pressure is absorbed by the host sandstone due to differential pore pressures.

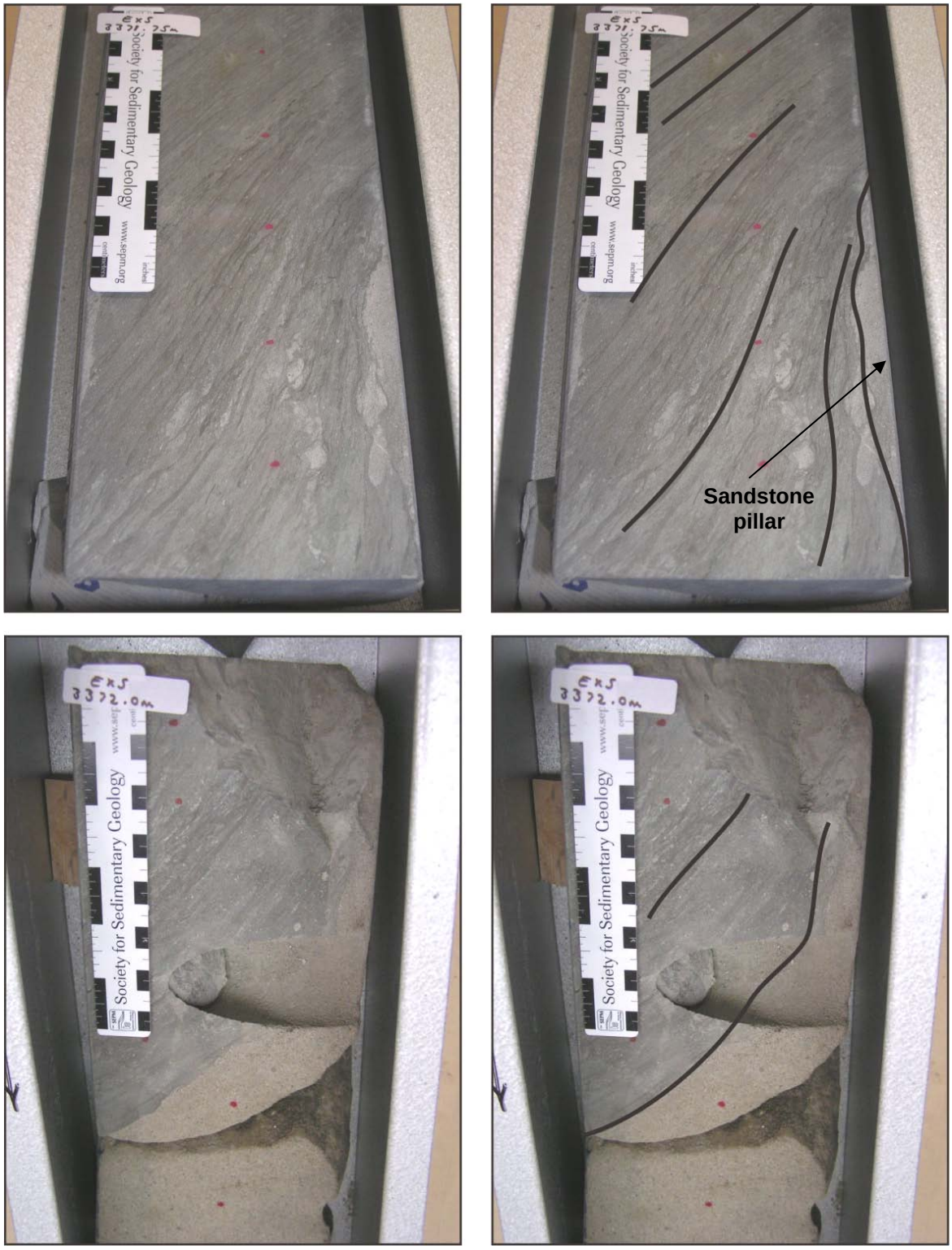

Figure 5-52: Sandstone-filled post-depositional pillar features injected into heterolithics as identified in Exeter-5ST1. The injection activity resulted in the dramatic pull-up of the heterolithic bedding.

5.3.10 Discordant sandstone bodies in mudstones (Lithofacies J)

5.3.10.1 Description

Sharp-sided structureless sandstones are recognised within siltstone- and mud-dominated sedimentary units. They form units ranging from several centimetres to over 30 centimetres thick. They display both upper and basal disconcordant bedding and contain unstructured and highly cemented sandstone. Individual matrix grains appear more tightly packed than primarily deposited sandstones. They are identified within Wanaea-2A (2882 to 2893 metres) (Figure 5-53) and Lambert-2 (3104 to 3106m) (Figure 5-54).

5.3.10.2 Interpretation

They are interpreted as clastic dykes and sills that represent later-stage intrusive injectite features. They differ from Lithofacies I as they are interpreted to have occurred with deep burial when sediments were more lithified and compacted. Dykes identified in Wanaea-2A are interpreted to have propagated along polygonal fault systems that developed within the overlying seal. Visible fault-related slickenslides were recognised in core (Figure 5-53). Dykes within Lambert-2 contain highly angular injection breccia which formed through the collapse of sediment from the walls of the injection feature (Figure 5-54).

Figure 5-53: Sandstone dykes identified in Wanaea-2A displaying structureless cemented sandstones and disconcordant bedding contacts. The injected sandstones used polygonal fault systems to propagate. Note the preserved slickenslides located at the top right.

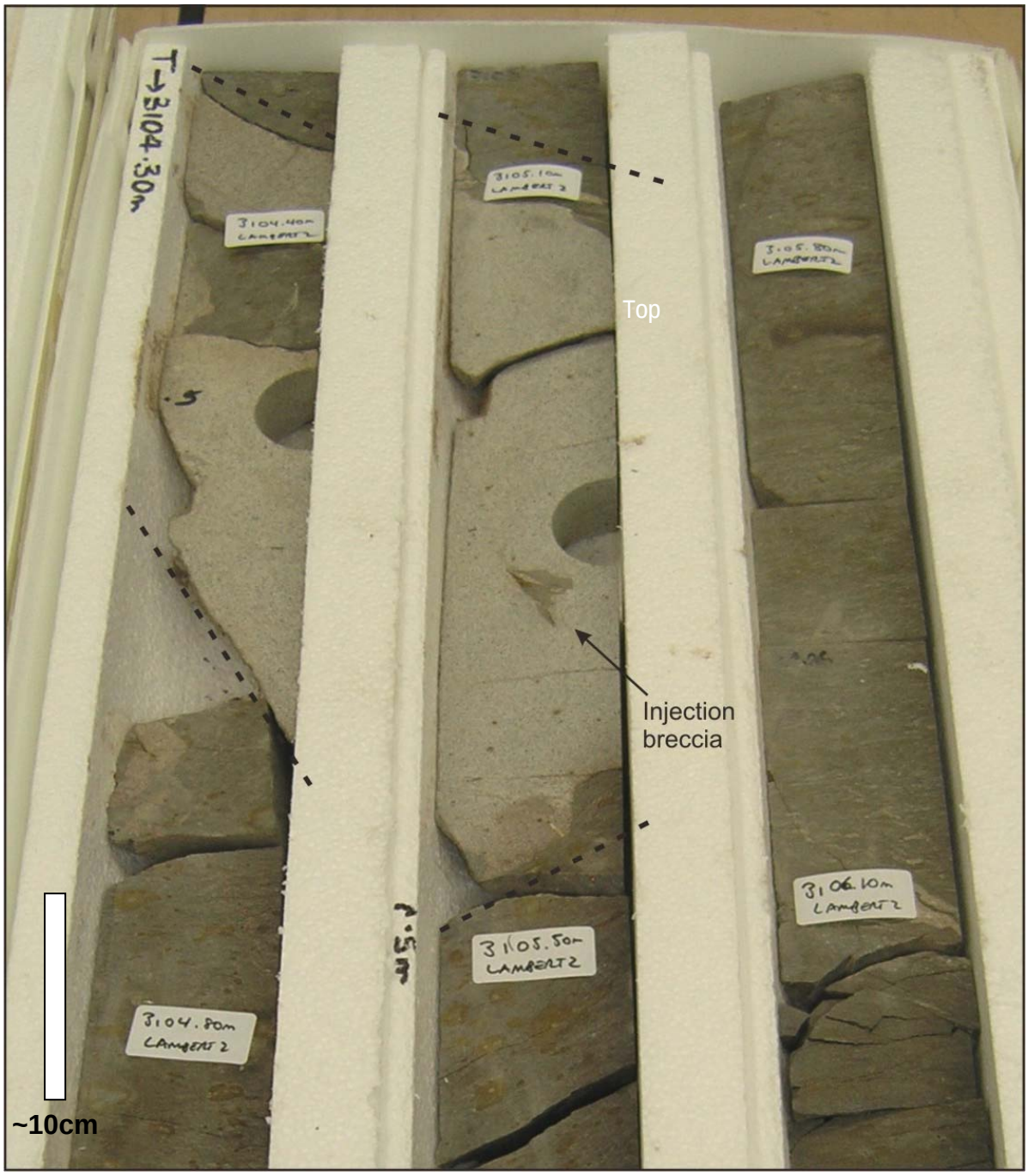

Figure 5-54: Sandstone dykes recognised in Lambert-2. They display sharp discordant boundaries, highly cemented featureless sandstone and angular injection breccia.

5.3.11 Contorted Sandstone (Lithofacies K)

5.3.11.1 Description

Contorted and sheared sandstone packages with chaotically orientated and sheared beds are occasionally identified either overlying homogenous sandstones (Lithofacies A) or dish and pipe structured sandstones (Lithofacies B). These contorted beds comprise dark argillaceous-rich sandstones which commonly display clean sandy patches, carbonaceous material, contorted rafts of folded and laminated sandstone and patches comprising of a 'starry night' texture due to the presence of sporadic quartz grains dispersed within a clay-rich matrix. The units range up to 1 metre thick in Spica-1 (Figure 5-55), Lambert-2 (Figure 5-56), Exeter-5ST1 and Egret-2 (Figure 5-57).

5.3.11.2 Interpretation

These units can be interpreted as:

i. the product of small-scale mass flow processes that occurred within unconsolidated sediment, or;
ii. banded and sheared deposits from either slurried hybrid flow events or linked debrites.

Active slumping can result in the formation of sheared and folded strata. 'Starry night' texture could be interpreted to be produced through the concentration of argillaceous fines within the deformed zone due to small slump-related injection processes (Figure 5-55). Clasts within these contorted intervals appear sheared and compressed and can display hair-like extensions similar to those identified in Facies H. Sheared folded clasts can also be identified within more homogeneous sandstones (Figure 5-57).

These intervals can also be interpreted as deposits from hybrid flow events. These deposits lack the large clasts seen in Facies H and they appear to comprise sheared banded beds of lighter and darker sandstones. They could be interpreted to represent transitional or "slurry" flow events. These events can underlie linked debrites in a typical five part hybrid event bed as discussed by Haughton *et al* (2009). It is also possible that these beds are linked debrite beds which lack rounded clasts as seen in Facies H. These varieties of linked debrites have been noted in the Miller and Magnus fans of the North Sea where clasts are elongated and lie parallel to bedding (Haughton *et al.,* 2009)

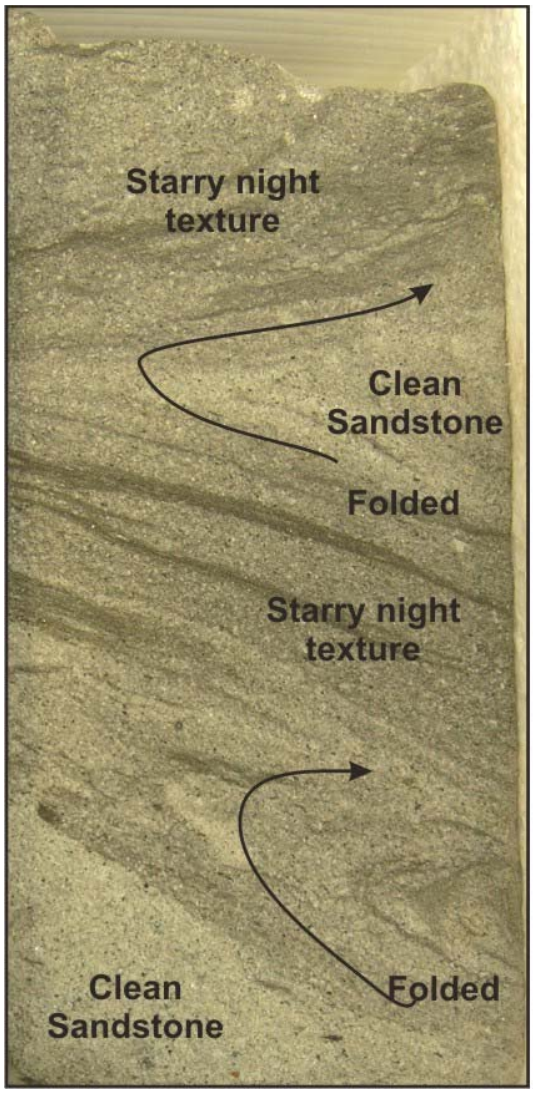

Figure 5-55: Shear and folding of laminated sediments from Spica-1. Note the 'starry night' texture and hair-like extensions.

Figure 5-56: Examples of fluidized and contorted sediments from Lambert-2 and Spica-1. On the left, fluidised and contorted sandstone identified in Lambert-2. Sheared and folded zones along with the basal contact are visibly not conformable with bedding. 'Starry night' texture and irregular patches of darker, more clay and pyrite rich units are interbedded with cleaner sandy patches.

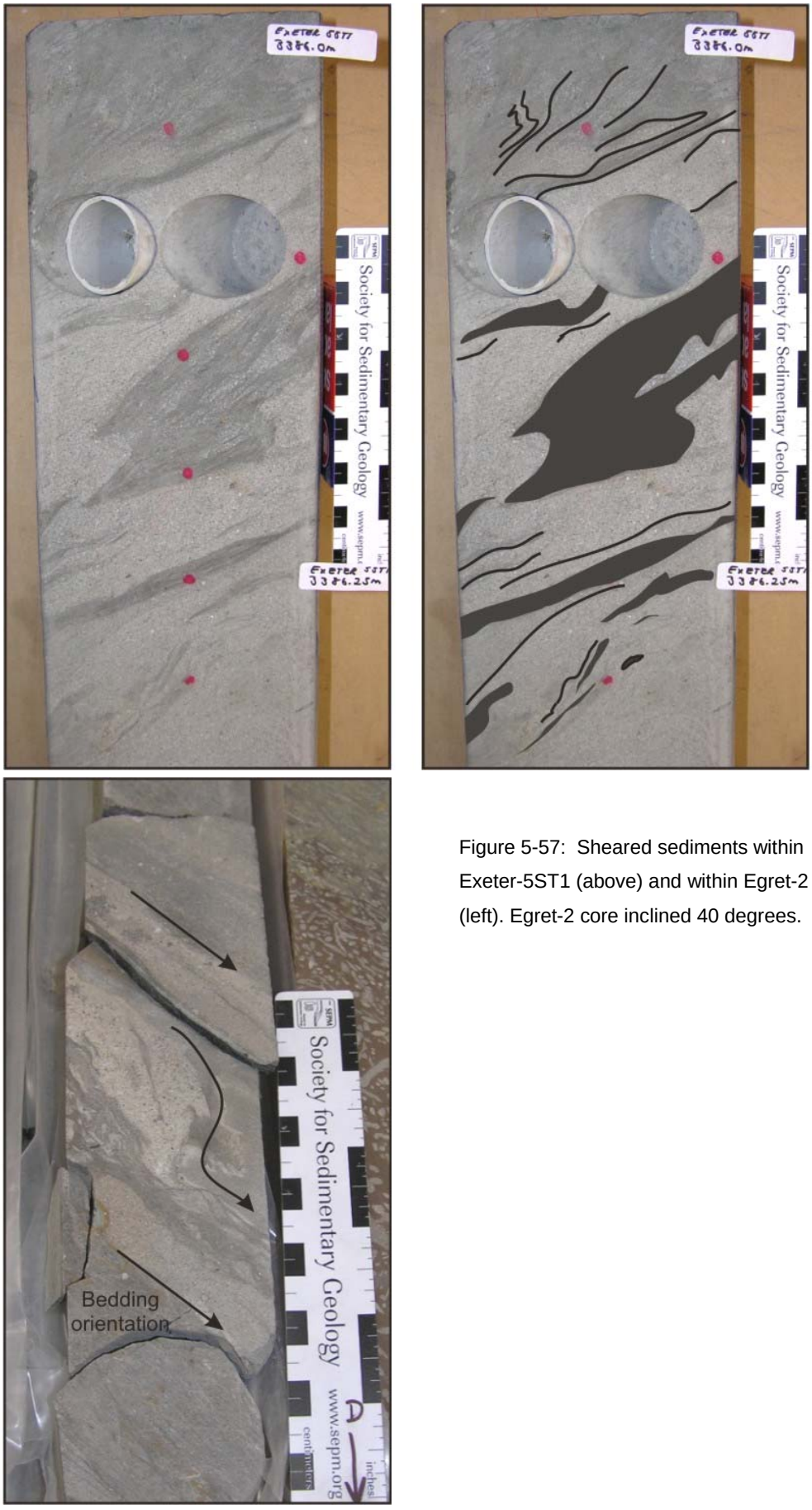

Figure 5-57: Sheared sediments within Exeter-5ST1 (above) and within Egret-2 (left). Egret-2 core inclined 40 degrees.

5.4 Summary

Logging of 547 metres of cored successions has revealed that the Tithonian successions of the Angel sandstone contain eleven lithofacies classifications which were created through either or both primary “depositional” and/or secondary “deformational” processes. In the following chapter, these eleven core lithofacies are grouped onto lithofacies associations which represent particular architectural elements. Further deliberation into the appropriate process model responsible for the Angel sandstone along with a full discussion into the varieties, models and implications of injectite features on reservoir architecture can be found in Sections 9.1 and 9.5 respectively.